COLLAGEN XI IMPACT ON STRUCTURE AND FUNCTION OF THE

VERTEBRATE INNER EAR IN A ZEBRAFISH MODEL

by

Makenna Hardy

A dissertation

submitted in partial fulfillment

of the requirements for the degree of

Doctor of Philosophy in Biomolecular Sciences

Boise State University

August 2021

BOISE STATE UNIVERSITY GRADUATE COLLEGE

DEFENSE COMMITTEE AND FINAL READING APPROVALS

of the thesis submitted by

Makenna Hardy

Thesis Title: Collagen XI Impact on Structure and Function of the Vertebrate Inner Ear in a Zebrafish Model

Date of Final Oral Examination: 30 June 2021

The following individuals read and discussed the thesis submitted by student Makenna Hardy, and they evaluated her presentation and response to questions during the final oral examination. They found that the student passed the final oral examination.

Julia T. Oxford, Ph.D.	Chair, Supervisory Committee
Matthew Ferguson, Ph.D.	Member, Supervisory Committee
Brad Morrison, Ph.D.	Member, Supervisory Committee
Allan Albig, Ph.D.	Member, Supervisory Committee

The final reading approval of the thesis was granted by Julia T. Oxford, Ph.D., Chair of the Supervisory Committee. The thesis was approved by the Graduate College.

DEDICATION

I would like to dedicate this work to my family. Thank you, Mom and Dad, for showing me at a young age that I could accomplish anything. Also, thank you to my sisters, Brittan and Henley, for listening to my science rants. Thank you to my friend and advocate, Dr. Karen Rudolph. Also, I would like to dedicate this to my dogs: Millie, Keeta, Niyla, Poppy, and Oliver; you always were my biggest fans.

ACKNOWLEDGEMENTS

ABSTRACT

The ear is essential to maintaining balance and hearing; both of which can be linked to one another and significantly impact a person's quality of life. Although aging and damage are more common reasons for hearing loss, congenital ear defects still have a considerable impact on our population. The function of the ear can be affected by structural deformities to the ear and its components which results in hearing loss. Mutations and single nucleotide polymorphisms in the gene encoding Collagen XI alpha one chain (COL11A1) protein can play a role in hearing and balance dysfunction in humans as seen in disorders such as Stickler Type 2 and Marshall Syndrome, and nonsyndromic hearing loss deafness autosomal dominant 37 (DFNA37). Due to its transparency, external fertilization, the zebrafish model system was used to create a COL11A1 zebrafish counterpart (Col11a1a) knockdown and knockout genetic model. This research highlights the importance of Col11a1a in the development and structure of the inner ear as a whole including the hair cells, kinocilia, and otolith formation. Studying the development and structural changes of the inner ear can provide insight into hearing loss and potential interventions.

TABLE OF CONTENTS

LIST OF TABLES

LIST OF FIGURES

LIST OF ABBREVIATIONS

Abbreviations of genes and proteins follow standard convention. Human gene names are italicized and in all capital letters, and human proteins are in all capital letters. Zebrafish genes are italicized and in all lowercase letters, and zebrafish proteins are not italicized with only the first letter capitalized. Mouse genes are italicized with the first letter capitalized, and mouse proteins are presented in all capital letters.

ADAMTS2	ADAM (A Disintegrin And Metalloproteinases) Metallopeptidase with Thrombospondin Type 1 Motif 2
AMO	Antisense morpholino oligonucleotide
ATOH1	Atonal BHLH Transcription Factor 1
BMP-1	Bone Morphogenetic Protein-1
BMP7	Bone Morphogenesis Protein 7
Ca^+	Calcium ion
cho	Chondrodystrophic
chr	Chromosome
COL11	Collagen type XI
COL11A1	Collagen XI alpha one chain
COL11A2	Collagen type XI alpha 2 chain
COL2A1	Collagen type II alpha one
COL9A1	Collagen type IX alpha one

COL9A2	Collagen type IX alpha two
Cpp or cpp	Carboxy propeptide
CRISPR	Clustered regularly interspaced short palindromic repeats
C-tp or ctp	Carboxy telopeptide
DAPI	4',6-diamidino-2-phenylindole
DFNA37	Deafness autosomal dominant 37
dig	Digoxigenin
dpf	Days post-fertilization
ECM	Extracellular matrix
EDTA	Ethylenediaminetetraacetic acid
ELISA	Enzyme-linked Immunosorbent Assay
FDR	False Discovery Rate
HET	Heterozygous
hpf	Hours post-fertilization
IACUC	Institutional Animal Care and Use Committee
IF	Immunofluorescence
ISH	*In situ* hybridization
K^+	Potassium ion
kbp	Kilobase pair
kDa	Kilodalton
KO	Knockout
LC-MS/MS	Liquid Chromatography with tandem mass spectrometry
LNS	Laminin-neurexin-sex hormone binding protein

mA	Milliampere
mbar	Millibar
MET	Mechanoelectrical transducer
mh	Minor helix
MTH	Major Triple Helix
Na^+	Sodium ion
NH_4HCO_3	Ammonium bicarbonate
NIH	National Institute of Health
Npp or npp	Amino propeptide
NTD	Amino terminal domain
N-tp and ntp	Amino telopeptide
OMIM	Online Mendelian Inheritance in Man
PFA	Paraformaldehyde
psi	Pounds per square inch
PTU	1-phenyl-2-thiourea
RT-PCR	Reverse Transcriptase-Polymerase Chain Reaction
SDS	Sodium dodecyl sulfate
SEM	Scanning Electron Microscopy
SOX2	SRY (sex determining region Y)-box2
TTBS	Tween-20 Tris buffered saline
VR	Variable region
WT	Wildtype

CHAPTER ONE: ZEBRAFISH AS A MODEL FOR STUDIES OF HEARING AND

DEAFNESS CAUSED BY MUTATIONS IN GENES ENCODING

EXTRACELLULAR MATRIX PROTEINS

Introduction and Background

One in eight people who are twelve years or older in the United States is affected

by hearing loss and 35% of people will experience balance complications in their lifetime

[1–4]. The ear is essential to maintaining balance and hearing; both of which can be

linked to one another and significantly impact a person's quality of life. Most hearing

loss is largely seen in adults with 14% adults 20 to 69 years of age experiencing hearing

loss [5,6]. Much of this observed hearing loss is due to a type of high frequency hearing

linked to genetics but also a high correlation with aging [7].

Although aging and damage are more common reasons for hearing loss,

congenital ear defects still have a considerable impact on our population. The function of

the ear can be affected by structural deformities to the ear and its components which

results in hearing loss. Studying the development and structural changes of the inner ear

can provide insight into hearing loss and potential interventions. Further determining the

role of extracellular matrix proteins in the inner ear can provide a more thorough

understanding of overall molecular, cellular, anatomical, and physiological mechanisms

in hearing and balance.

The Human Inner Ear versus the Zebrafish Inner Ear

The human ear is a complex organ comprised of the outer, middle, and inner ear sections, as shown in **Figure 1**. The outer ear is the external structure, which is referred to as the pinna, which leads to the ear canal. The middle ear is supported by the mastoid bone and contains the tympanic membrane, also known as the eardrum. The ossicles known as malleus, incus, and stapes, form the sound conducting system. These bones conduct the vibration of sound from the air through the tympanic membrane to the fluid-filled inner ear through the oval window see **Figure 1** [8].

The middle ear leads to the inner ear which contains the vestibular and membranous labyrinths. The vestibular labyrinth includes the three semicircular canals consisting of the otolith organs: the saccule and the utricle see **Figure 1** [9]. The membranous labyrinth is where sound conduction turns into the action of hearing. The cochlea, a small snail shell-like bony structure with two and a half turns, contains this membranous labyrinth. This labyrinth is surrounded by perilymph fluid. The cochlea is comprised of 30,000 hair cells arranged in four rows on top of the basilar membrane see **Figure 1** [10]. Each hair cell has sensory hair bundles with rows of stereocilia in the subtectorial space below the tectorial membrane which are surrounded by endolymph fluid. The outer hair cells have stereocilia attached to the tectorial membrane while the other hair cells' stereocilia are generally free or loosely attached see **Figure 1** [8]. Each sensory hair bundle has rows of stereocilia made of actin along with one kinocilia long primary cilia composed of microtubulin. In the cochlea, no kinocilia are present in the hair cells, instead longer stereocilia act as similar to the kinocilia in non-cochlear hair cell patches. Together, these cilia help sense vibrations and conduct this signal down into the

hair cells where nerve impulses are sent to the brain to correspond a hearing signal. Dysfunction in these hair cells results in hearing and balance complications.

As previously stated, the cilia help sense vibrations and conduct this signal down into the hair cells thus resulting in nerve impulses relaying hearing to the brain. The endolymph the stereocilia are surrounded by is rich in potassium ions (K^+) but sparse in calcium ions (Ca^{2+}) and sodium ions (Na^+) [11–13]. Mechanoelectrical transducer (MET) channels are located near the tips of the stereocilia. MET channels are cation-selective transduction channels which allow K^+ and Ca^{2+} from the endolymph to enter the hair cell when the MET channels are open. When the shorter outer stereocilia are positively deflected towards the taller stereocilia, MET channels are opened causing hyperpolarization of the hair cells [11,13]. When the stereocilia are negatively deflected towards the shorter outer stereocilia, MET channels are closed causing depolarization of the hair cells [11,13,14]. Fluxes in ion concentration in the hair cells result in a graded receptor potential at the basilar membrane [12,13]. At the basilar membrane, the graded receptor potential results in synaptic dialogue with afferent nerve fibers resulting in a hearing signal in the central nervous system [12]. When the stereocilia are damaged or shortened the MET channels can become dysfunctional or damaged or the hair cell's structure can be damaged as well resulting in failure of mechanotransduction of sound [15].
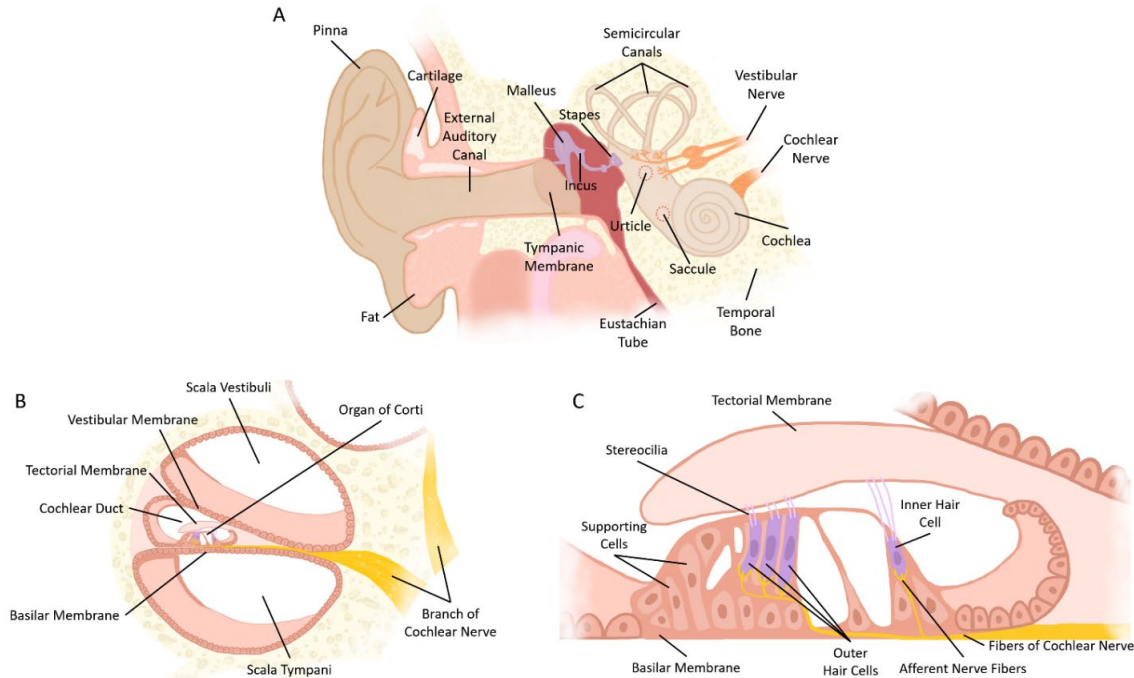
Figure 1.1.   Anatomy of the human inner ear.
A) Diagram of the outer, middle, and inner ear. Key locations are marked. B) Cross section of the cochlea revealing the three chambers including the Organ of Corti. C) Close-up of the Organ of Corti revealing the tectorial membrane, the basilar membrane, the supporting cells, and the outer and inner hair cells along with their stereocilia.

Studying the development and function of the inner ear using a zebrafish model for vertebrates is well documented in the literature [16–20]. The development of the inner ear and anatomy of zebrafish is similar to that of other vertebrate inner ears [21–23]. The development and structure of the zebrafish inner ear is analogous to and conserved in mammalians. Embryonic zebrafish do not contain the semicircular canals at first, but the maculae are observed in early embryonic development as early as 19 hours post fertilized (hpf) see **Figure 2 [18].**

Introduction and Background
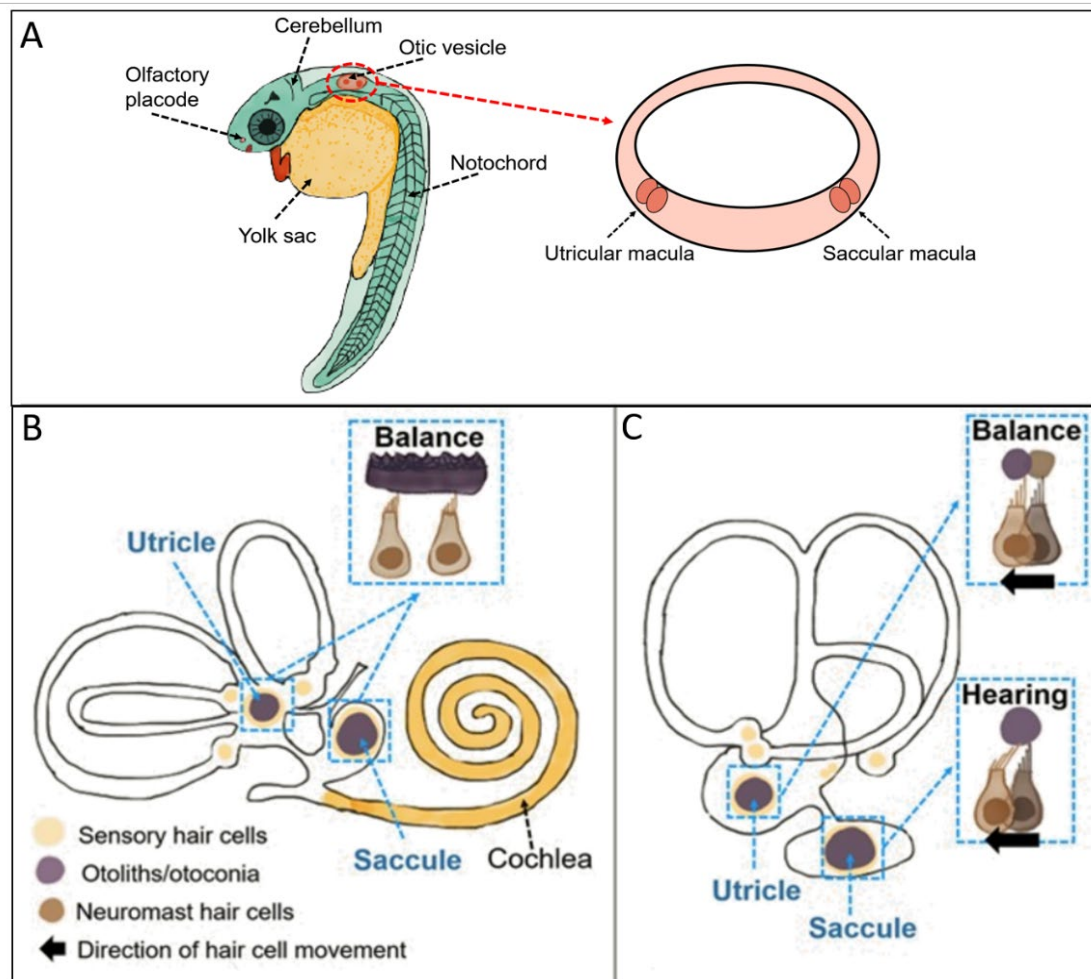
Figure 1.2.   Zebrafish embryo inner ear structure and function.
A) 24 hpf zebrafish embryo for reference. The otic vesicle is indicated by a red circle. A close-up of the otic vesicle is shown to the right. Both sensory patches are indicated: utricular macula and saccular macula. B) Anatomy of the human inner ear displaying the three semicircular canals, otocania, sensory hair cells, and cochlea are displayed. The otoconia are outlined in blue. Inset shows how balance is maintained. C) Anatomy of zebrafish inner ear displaying the three semicircular canals, otoliths, and sensory hair cells are displayed. The otoliths are outlined in blue. Inset shows how balance and hearing are maintained.

One in eight people who are twelve years or older in the United States is affected by hearing loss and 35% of people will experience balance complications in their lifetime [1–4]. The ear is essential to maintaining balance and hearing; both of which can be

linked to one another and significantly impact a person's quality of life. Most hearing loss is largely seen in adults with 14% adults 20 to 69 years of age experiencing hearing loss [5,6]. Much of this observed hearing loss is due to a type of high frequency hearing linked to genetics but also a high correlation with aging [7].

Although aging and damage are more common reasons for hearing loss, congenital ear defects still have a considerable impact on our population. The function of the ear can be affected by structural deformities to the ear and its components which results in hearing loss. Studying the development and structural changes of the inner ear can provide insight into hearing loss and potential interventions. Further determining the role of extracellular matrix proteins in the inner ear can provide a more thorough understanding of overall molecular, cellular, anatomical, and physiological mechanisms in hearing and balance.

The Human Inner Ear versus the Zebrafish Inner Ear

The human ear is a complex organ comprised of the outer, middle, and inner ear sections, as shown in **Figure 1**. The outer ear is the external structure, which is referred to as the pinna, which leads to the ear canal. The middle ear is supported by the mastoid bone and contains the tympanic membrane, also known as the eardrum. The ossicles known as malleus, incus, and stapes, form the sound conducting system. These bones conduct the vibration of sound from the Similar to humans, the zebrafish inner ear contains three semicircular canals lined with sensory hair cells (**Figure 2**).

While these structures are not visually identical to what is shown in the human inner ear anatomy, the cristae and maculae structure and function are highly similar to what is seen in mammals including humans [24]. Both humans and zebrafish have three

cristae lined with sensory hair cells in the semicircular canals and two maculae within the utricle and the saccule (**Figure 2B-2C**). Similarly, the formation of the semicircular canal is conserved throughout vertebrates from zebrafish to humans. In zebrafish the precursor to the inner ear, the otic vesicle, undergoes an epithelial thinning process early in development where the inter-sensory patch is thinned causing the segregation of sensory patches: utricular macula and saccular macula see **Figure 2A** [25]. This allows for innervation of the hair cells in the sensory patch which in turn allows the stereocilia and kinocilium to sense vibrations and changes in orientation and send that signal to the brain via the vestibulocochlear nerve see **Figure 2** [26].

Extracellular Matrix Molecules and the Inner Ear

Several research groups have explored the zebrafish inner ear over time, and numerous research groups have studied the inner ear development in mice. Many research groups have recently initiated studies using the zebrafish model to study ear development, and many of the same genes found to be important in the mechanism of hearing in mice have recently been reported as also having important roles in zebrafish [27–40]. Zebrafish have become increasingly popular for inner ear studies due to several advantages over higher vertebrates including mice [41–44]. Zebrafish are preferred for their optical clarity, their fast development, and the ease of genetic manipulation [41,43,44]. In hearing studies, zebrafish are preferred for their easily accessible hair cells as well as easily observable live otic development [41,43]. The inner ear development of zebrafish has been well-documented and easily seen in larval (3 days post fertilized) fish [43,44]. Several of these molecules include extracellular matrix (ECM) molecules. The ECM has been shown to be involved in the formation of the inner ear [30,45]. The

folding within the otic placode that results in the otic pit, later to become the otic vesicle, is the result of an increased secretion of ECM [45].

Several of the ECM molecules are involved in sensory hair cell development (Table 1). One of the transcription factors that regulates ECM molecule expression, the Yamanaka factor SOX2 (SRY (sex determining region Y)-box2) is expressed along floor of the otic vesicle and in the hair cells. *SOX2* expression is required for initial otic neuronal specification including formation of hair cells and supporting cells [46–48]. SOX2 works with ATOH1 (atonal BHLH transcription factor 1) to maintain sensory-neural boundaries in order to induce hair cell development [48–51]. Expressed in the epithelium of the otic vesicle, BMP7 (bone morphogenetic protein 7) regulates ATOH1 while promoting prosensory domain specification into nonsensory and supporting cells around the hair cells [52,53]. Not only do ECM molecules interact with one another, they also interact with the collagen network that supports structures during development.

Collagens make up the primary structural component of connective tissues. An alpha chain of collagen contains repeats of glycine, proline, and hydroxyproline. These repeats are important in the formation of trimeric collagen triplehelices which contain three alpha chains [54]. There are several groups of collagens based on the structure and supramolecular organization. The collagens we observe in the neural circuit, and more specifically the inner ear, collagen type I, II, III, IV, V, IX, and XI, are all fibrillar or fibril-associated (type IX) collagens see **Table 1** [54]. The major fibrillar collagens, collagen type I, II, and III have well-documented expression in the inner ear; specifically collagen II has been observed in the tectorial membrane and in the basilar membrane of

humans and other model systems such as the mouse. The minor fibrillar collagens,

collagen type V and XI, have less or very little known about them.

Table 1.1.   ECM molecules and their functions in the inner ear.

Molecule	Location	Function
SOX2	Hair cells, floor of the otic vesicle	Required for formation of hair cells and supporting cells, otic neurogenesis both neuron and sensory epithelia development
ATOH1	Hair cells, cochlea	Along with SOX2 help maintain sensory-neural boundary and is required for hair cell formation, important in hair cell differentiation in the cochlea
BMP7	Epithelium of otic vesicle	Regulates ATOH1, necessary for specification of nonsensory and supporting cells from the prosensory domain
COL1	Middle ear, inner ear, cochlea	Important for transforming sound to mechanical stimulation
COL2	Tectorial membrane, cochlea	Important for transforming sound to mechanical stimulation
COL3	Middle ear, inner ear, cochlea	Important for transforming sound to mechanical stimulation
COL4	Basilar membrane, cochlea	Important in the active tuning of the basilar and tectorial membrane to allow frequency discrimination and amplification of auditory signals
COL5	Tectorial membrane, basilar membrane, cochlea	Function and structure of tectorial membrane
COL9	Tectorial membrane, cartilage middle and inner ear	Function and structure of tectorial membrane
COL11A2	Cartilage middle and inner ear, tectorial membrane, cochlea	Affects the membranous labyrinth and the central nervous system,
COL11A1	Inner ear, tectorial membrane, cochlea	Affects the membranous labyrinth and the central nervous system,

For example, very little is known about Type XI collagen in the inner ear. Type

XI collagen, a minor fibrillar collagen, is known to be important in the regulation of

collagen fibril diameter and the maintenance of tissue integrity [55]. Disruption of

collagen type XI expression interrupts the organization and complexity of proper

functioning mature collagen networks. Collagen type XI alpha 2 chain (*COL11A2*) gene

expression has been reported in the fluid of the inner ear. Deletion of COL11A2 causes a

decrease in the density of collagen fibers, but also resulted in an increase in auditory

thresholds due to mechanical anisotropy of the tectorial membrane [56]. These results indicate that the mechanical integrity of the tectorial membrane is dependent on the proper organization of collagen radial fibers and the maintenance of the mechanical integrity of the tectorial membrane is vital to proper hearing.

Collagen XI Alpha One

The structure and formation of a type XI collagen fiber is displayed in **Figure 3**.Collagen type XI (COL11) is a minor fibrillar collagen made up of three alpha chains: α1(XI), α2(XI), and α3(XI). These alpha chains join at the carboxyl propeptide to form a triple helical molecule [57]. Cleavage of the carboxyl propeptide occurs first followed by the amino propeptide [57]. Collagen type XI alpha 1 chain (COL11A1) possesses a globular amino propeptide domain that is retained for a longer duration after synthesis and secretion than amino propeptides of other collagens see **Figure 3** [58]. The collagen type XI molecule can be post-translationally modified by further proteolytic cleavage. This includes removal of the COL11A1 amino propeptide domain or cleavage removing the amino propeptide domain along with the alternatively spliced region, or more extensive processing to remove the minor triple helix, leaving the mature collagen molecule with the amino telopeptide intact (**Figure 3E**). COL11A1 is alternatively spliced to generate a family of splice forms (**Figure 3F**).

Collagen type XI alpha 1 chain (*Col11a1*) gene expression has been reported in the nucleus pulposus of the intervertebral disc, the vitreous humor of the mammalian eye, skeletal muscle, brain tissue, tendons, heart valves, skin, the tectorial membrane of the inner ear, intestinal epithelial, and smooth muscle of the intestine and endochondral bones [59–62].
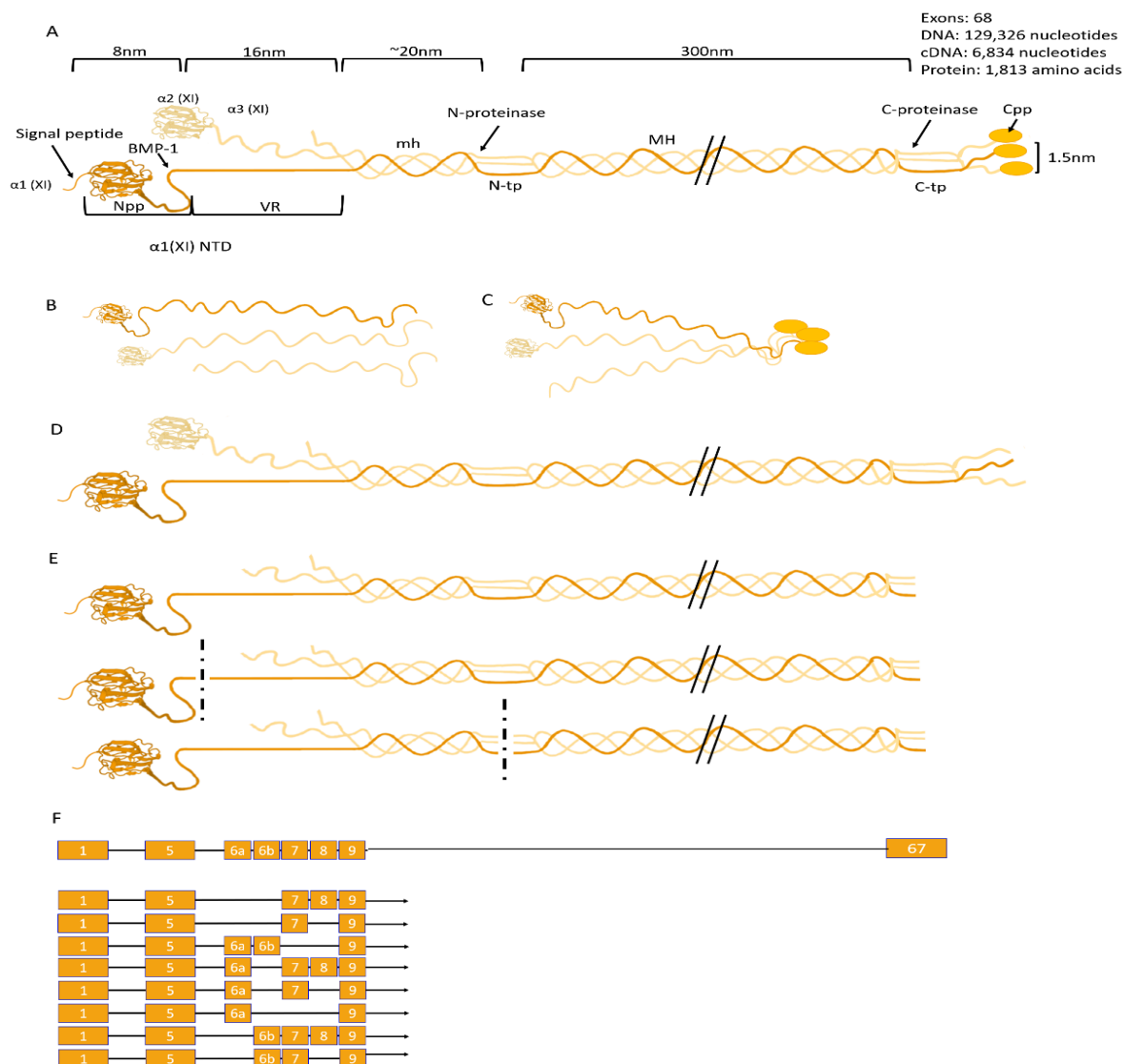
Figure 1.3.   Model of Collagen type XI.

A) Full Collagen type XI molecule. Structural regions are indicated such as the signal peptide, the amino and carboxy terminal propeptides, the amino and carboxy telopeptide, the variable region, the minor helix, and the major triple helix. Relative size and dimensions are shown above the molecular model. B) Three alpha chains: α1(XI), α2(XI), and α3(XI). C) Triple helical molecule formation from the C-terminus towards the N-terminus. D) Fully assembled triple helical molecule. E) Potential cleavage events indicated by a dotted line. (1) Carboxy propeptide removed, (2) With the amino propeptide removed at the BMP-1 cleavage site (35 kDa), (3) At the ADAMTS2 cleavage site within the amino telopeptide resulting in the major triple helix and a fragment containing the amino propeptide and variable region (100kDa). F) Exon structure of the molecule. Alternative splicing of isoforms is shown. amino terminal domain (NTD); amino propeptide domain (Npp); variable region (VR); minor helix (mh); amino telopeptide (N-tp); major triple helix (MH); carboxy telopeptide (C-tp); carboxy propeptide (Cpp).

According to previous literature, COL11A1 is only associated with the inner ear through hearing impairment associated with two diseases: Stickler syndrome and Marshall syndrome, which both can be caused by a mutation in COL11A1. Interestingly, COL11A1 mutations have also been discovered in nonsyndromic hearing loss deafness autosomal dominant 37 (DFNA37).

As previously mentioned, Marshall syndrome and Stickler syndrome are both genetically inherited disorders that are caused by mutations in COL11A1. Both of these diseases are chondrodysplasias characterized by midfacial hypoplasia, myopia, skeletal defects, and auditory deficits [63]. The phenotypes of these two diseases are very similar, but they have some unique characteristics that keep them from being merged into one disorder. Marshall syndrome is caused by one mutation in the COL11A1 gene and this gene is also identified as the locus of this syndrome. Some characteristics more common to Marshall than Stickler syndrome include short stature, cranial ossification abnormalities, and more pronounced facial dysmorphic features [63]. However, Stickler syndrome can also be caused by mutations in COL2A1, COL11A1, COL11A2, COL9A1, and COL9A2. Type II Stickler syndrome is caused by mutations specifically in COL11A1. Type II Stickler syndrome patients commonly have a hearing impairment. Balance problems are also reported in some patients with Stickler syndrome; however, it is not common among all patients [64].

Nonsyndromic deafness has been identified associated with the deafness, autosomal dominant 37 (DFNA37) locus [65,66]. *COL11A1* is located at the DFNA37 locus, and heterozygous variants in COL11A1 are responsible for this nonsyndromic deafness [65]. DFNA37 nonsyndromic hearing loss has been shown to occur as both

after the development of speech and language (postlingual) and before the development of speech and language (prelingual) [66,67]. Postlingual autosomal dominant nonsydromic hearing loss DFNA37 has been shown to result from a mutation in the COL11A1 gene that changes an A to a C within a splice consensus site, leading to changes in the splicing within the amino propeptide domain (c.652-2A>C) [66]. Prelingual autosomal dominant nonsyndromic hearing loss DFNA37 has been shown to result from disruption of the normal splicing process and mutations such as c.652-1G>C and c.4338+2T>C [67]. While mutations within the splice acceptor and donor consensus sites (c.652-1G>C, c.652-2A>C) are observed with different splicing outcomes, they both affect the intron 4 canonical splice site effectiveness [67]. In summary, this new information confirms that *COL11A1* mutations can be a cause of nonsyndromic deafness in addition to the well-established syndromes.

While Stickler syndrome type II, Marshall syndrome, and DFNA37 are the main diseases caused by mutations in COL11A1, other mutations also have been shown to cause other syndromic and nonsyndromic hearing loss disorders see Figure 4 [68]. A search of the Deafness Variation Database from the Molecular Otolaryngology and Renal Research Laboratories at the University of Iowa [69] revealed over 13,000 COL11A1 mutations resulting in hearing loss. Many of these mutations had an unidentified or benign result. Therefore, these mutations usually do not have an impact on health or development of an individual and thus these mutations are not often observed to be the cause of a disorder.

Approximately 60 genetic mutations in COL11A1 are classified as pathogenic or likely pathogenic in relation to hearing loss see **Figure 4** [68]. Many of these mutations

are high-impact mutations which tend to be more conserved compared to lower predicted impacts and thus often seen in diseases [70]. These COL11A1 high-impact and likely pathogenic mutations are often characteristic of significant syndromic and nonsyndromic diseases. **Figure 4** displays the 62 high impact, likely pathogenic mutations in COL11A1 resulting in syndromic and nonsyndromic hearing loss. Many of these mutations result in syndromic hearing loss such as Stickler syndrome and Marshall syndrome. However, other syndromic disorders with hearing loss as a symptom are displayed; many occur after the alternative splice zone of COL11A1 (**Figure 4**). Four mutations resulting in nonsyndromic hearing loss are also displayed. Three of these (c.560C>T, c.652-1G>C, c.652-2A>C) are in the amino propeptide domain of COL11A1 while one (c.4338+2T>C) lays in intron 57 within the major triple helix domain (**Figure 4**).
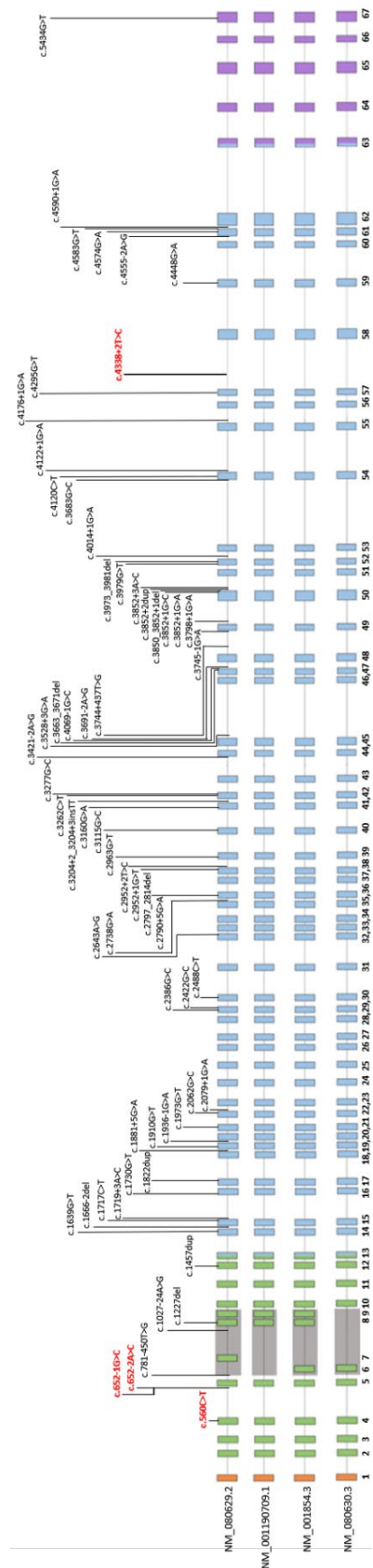
Figure 1.4. Genetic mutations in COL11A1 resulting in a hearing loss phenotype.

Mutations leading to nonsyndromic and syndromic hearing loss are indicated along the relative exons and introns in COL11A1. Exons are numbered 1-67 at the bottom of the figure. Isoforms of alternatively spliced molecules are listed to the left.

Summary

Collagen is fundamental to proper development within the embryonic stages. While collagen type XI is a minor fibrillar collagen, its expression is seen throughout development and in its absence, development cannot proceed properly. Mutations in COL11A1 cause Marshall and Stickler syndrome, which both display hearing deficit symptoms. Based on a recent literature review, COL11A1 has been briefly identified in the ear of fish and mice [71–75]. *Col11a1* expression has been mostly observed in the cochlear duct and tectorial membrane of embryonic mice [72] and in the Col11a1 knockout *cho/cho* mouse model characterized by underdevelopment of the organ of Corti in the cochlea leading to hearing impairment [71,75]. In fish, *col11a1* expression has been observed within the channel catfish swimbladder revealing involvement in sensory reception of sound [73]. This expression in the inner ear is still sparsely described and understood. Further knowledge is important in diagnosing and treating the hearing problems seen in Stickler and Marshall syndrome. Understanding the function of COL11A1 in the ear may lead to better diagnoses and treatment of ear and hearing disorders.

References

1.   Sampson, J.; Thompson, H. Youth Hearing Impairment. *Nursing* **2017**, *47*, 52–56, doi:10.1097/01.NURSE.0000512877.14257.cb.

2.   Lü, J.; Huang, Z.; Yang, T.; Li, Y.; Mei, L.; Xiang, M.; Chai, Y.; Li, X.; Li, L.; Yao, G.; et al. Screening for Delayed-Onset Hearing Loss in Preschool Children Who Previously Passed the Newborn Hearing Screening. *International Journal of Pediatric Otorhinolaryngology* **2011**, *75*, 1045–1049, doi:10.1016/j.ijporl.2011.05.022.

3.   Skarzynski, P.H.; Wlodarczyk, A.W.; Kochanek, K.; Pilka, A.; Jedrzejczak, W.W.; Olszewski, L.; Bruski, L.; Niedzielski, A.; Skarzynski, H. Central Auditory Processing Disorder (CAPD) Tests in a School-Age Hearing Screening Programme – Analysis of 76,429 Children. *Annals of Agricultural and Environmental Medicine* **2015**, *22*, 90–95, doi:10.5604/12321966.1141375.

4.   Golz, A.; Angel-Yeger, B.; Parush, S. Evaluation of Balance Disturbances in Children with Middle Ear Effusion. *International Journal of Pediatric Otorhinolaryngology* **1998**, *43*, 21–26, doi:10.1016/S0165-5876(97)00150-X.

5.   Smith, P.F. Is Hippocampal Neurogenesis Modulated by the Sensation of Self-Motion Encoded by the Vestibular System? *Neuroscience and Biobehavioral Reviews* **2017**, *83*, 489–495, doi:10.1016/j.neubiorev.2017.09.013.

6.   Hoffman, H.J.; Dobie, R.A.; Losonczy, K.G.; Themann, C.L.; Flamme, G.A. Declining Prevalence of Hearing Loss in US Adults Aged 20 to 69 Years. *JAMA Otolaryngology - Head and Neck Surgery* **2017**, *143*, 274–285, doi:10.1001/jamaoto.2016.3527.

7.   Staecker, H.; Zheng, Q.Y.; van de Water, T.R. Oxidative Stress in Aging in the C57B16/J Mouse Cochlea. *Acta Oto-Laryngologica* **2001**, *121*, 666–672, doi:10.1080/00016480152583593.

8.   Alberti, P.W. The Anatomy and Physiology of the Ear and Hearing. *Occupational exposure to noise: evaluation, prevention and control* **2001**, 53–62.

18

9.   Agrup, C.; Gleeson, M.; Rudge, P. The Inner Ear and the Neurologist1. *Journal of Neurology, Neurosurgery and Psychiatry* **2007**, *78*, 114–122, doi:10.1136/jnnp.2006.092064.

10.   Pan, L.; Zhang, M. Structures of Usher Syndrome 1 Proteins and Their Complexes. *Physiology* 2012, *27*, 25–42.

11.   Fettiplace, R. Hair Cell Transduction, Tuning, and Synaptic Transmission in the Mammalian Cochlea. *Comprehensive Physiology* **2017**, *7*, 1197–1227, doi:10.1002/cphy.c160049.

12.   Mammano, F.; Bortolozzi, M.; Ortolano, S.; Anselmi, F. Ca2+ Signaling in the Inner Ear. *Physiology* **2007**, *22*, 131–144, doi:10.1152/physiol.00040.2006.

13.   Qiu, X.; Müller, U. Mechanically Gated Ion Channels in Mammalian Hair Cells. *Frontiers in Cellular Neuroscience* 2018, *12*.

14.   Dierich, M.; Altoè, A.; Koppelmann, J.; Evers, S.; Renigunta, V.; Schäfer, M.K.; Naumann, R.; Verhulst, S.; Oliver, D.; Leitner, M.G. Optimized Tuning of Auditory Inner Hair Cells to Encode Complex Sound through Synergistic Activity of Six Independent K+ Current Entities. *Cell Reports* **2020**, *32*, doi:10.1016/j.celrep.2020.107869.

15.   Wagner, E.L.; Shin, J.B. Mechanisms of Hair Cell Damage and Repair. *Trends in Neurosciences* 2019, *42*, 414–424.

16.   Lu, Z.; Desmidt, A.A. Early Development of Hearing in Zebrafish. *JARO - Journal of the Association for Research in Otolaryngology* **2013**, *14*, 509–521, doi:10.1007/s10162-013-0386-z.

17.   Yao, Q.; Desmidt, A.A.; Tekin, M.; Liu, X.; Lu, Z. Hearing Assessment in Zebrafish during the First Week Postfertilization. *Zebrafish* **2016**, *13*, 79–86, doi:10.1089/zeb.2015.1166.

18.   Whitfield, T.T.; Riley, B.B.; Chiang, M.-Y.; Phillips, B. Development of the Zebrafish Inner Ear. *Developmental Dynamics* **2002**, *223*, 427–458, doi:10.1002/dvdy.10073.

19. Vona, B.; Doll, J.; Hofrichter, M.A.H.; Haaf, T.; Varshney, G.K. Small Fish, Big Prospects: Using Zebrafish to Unravel the Mechanisms of Hereditary Hearing Loss. *Hearing Research* 2020, *397*, 107906.

20. Leitner, M.G. Zebrafish in Auditory Research: Are Fish Better than Mice? *Journal of Physiology* **2014**, *592*, 4611–4612, doi:10.1113/jphysiol.2014.280438.

21. Ou, H.C.; Santos, F.; Raible, D.W.; Simon, J.A.; Rubel, E.W. Drug Screening for Hearing Loss: Using the Zebrafish Lateral Line to Screen for Drugs That Prevent and Cause Hearing Loss. **2010**, doi:10.1016/j.drudis.2010.01.001.

22. Whitfield, T.T. Zebrafish as a Model for Hearing and Deafness. *Journal of Neurobiology* **2002**, *53*, 157–171, doi:10.1002/neu.10123.

23. Shen, Y.C.; Jeyabalan, A.K.; Wu, K.L.; Hunker, K.L.; Kohrman, D.C.; Thompson, D.L.; Liu, D.; Barald, K.F. The Transmembrane Inner Ear (Tmie) Gene Contributes to Vestibular and Lateral Line Development and Function in the Zebrafish (Danio Rerio). *Developmental Dynamics* **2008**, *237*, 941–952, doi:10.1002/dvdy.21486.

24. Bever, M.M.; Fekete, D.M. Atlas of the Developing Inner Ear in Zebrafish. *Developmental Dynamics* **2002**, *223*, 536–543, doi:10.1002/dvdy.10062.

25. Alsina, B.; Whitfield, T.T. Sculpting the Labyrinth: Morphogenesis of the Developing Inner Ear. *Seminars in Cell and Developmental Biology* **2017**, *65*, 47–59, doi:10.1016/j.semcdb.2016.09.015.

26. Ma, E.Y.; Raible, D.W. Signaling Pathways Regulating Zebrafish Lateral Line Development. *Current Biology* **2009**, *19*, R381–R386, doi:10.1016/j.cub.2009.03.057.

27. Stepanyan, R.; Frolenkov, G.I. Fast Adaptation and Ca 2+ Sensitivity of the Mechanotransducer Require Myosin-XVa in Inner but Not Outer Cochlear Hair Cells. *Journal of Neuroscience* **2009**, *29*, 4023–4034, doi:10.1523/JNEUROSCI.4566-08.2009.

20

28. He, Y.; Tang, D.; Li, W.; Chai, R.; Li, H. Histone Deacetylase 1 Is Required for the Development of the Zebrafish Inner Ear. *Nature Publishing Group* **2016**, 1–16, doi:10.1038/srep16535.

29. Newman, D.L.; Fisher, L.M.; Ohmen, J.; Parody, R.; Fong, C.T.; Frisina, S.T.; Mapes, F.; Eddins, D.A.; Frisina, R.D.; Frisina, R.D.; et al. GRM7 Variants Associated with Age-Related Hearing Loss Based on Auditory Perception. *Hearing Research* **2012**, *294*, 125–132, doi:10.1016/j.heares.2012.08.016.

30. Legan, P.K.; Richardson, G.P. Extracellular Matrix and Cell Adhesion Molecules in the Developing Inner Ear. *Seminars in Cell and Developmental Biology* **1997**, *8*, 217–224, doi:10.1006/scdb.1997.0145.

31. Gao, X.; Yuan, Y.; Lin, Q.; Xu, J.; Wang, W.; Qiao, Y.; Kang, D.; Bai, D.; Xin, F.; Huang, S.; et al. Mutation of IFNLR1 , an Interferon Lambda Receptor 1 , Is Associated with Autosomal-Dominant Non- Syndromic Hearing Loss. **2018**, 298–306, doi:10.1136/jmedgenet-2017-104954.

32. Chen, K.; Jiang, D. MicroRNA-194 Regulates the Development and Differentiation of Sensory Patches and Statoacoustic Ganglion of Inner Ear by Fgf4. **2018**, 1712–1723, doi:10.12659/MSM.906277.

33. Mulvaney, J.F.; Thompkins, C.; Noda, T.; Nishimura, K.; Sun, W.W.; Lin, S.Y.; Coffin, A.; Dabdoub, A. Kremen1 Regulates Mechanosensory Hair Cell Development in the Mammalian Cochlea and the Zebrafish Lateral Line. *Scientific Reports* **2016**, *6*, doi:10.1038/srep31668.

34. Li, X.; Song, G.; Zhao, Y.; Zhao, F.; Liu, C.; Liu, D.; Li, Q.; Cui, Z. Claudin7b Is Required for the Formation and Function of Inner Ear in Zebrafish. *Journal of Cellular Physiology* **2018**, *233*, 3195–3206, doi:10.1002/jcp.26162.

35. Delmaghani, S.; Aghaie, A.; Bouyacoub, Y.; el Hachmi, H.; Bonnet, C.; Riahi, Z.; Chardenoux, S.; Perfettini, I.; Hardelin, J.P.; Houmeida, A.; et al. Mutations in CDC14A, Encoding a Protein Phosphatase Involved in Hair Cell Ciliogenesis, Cause Autosomal-Recessive Severe to Profound Deafness. *American Journal of Human Genetics* **2016**, *98*, 1266–1270, doi:10.1016/j.ajhg.2016.04.015.

36.   Lin, S.; Vollrath, M.A.; Mangosing, S.; Shen, J.; Cardenas, E.; Corey, D.P. The Zebrafish Pinball Wizard Gene Encodes WRB , a Tail-Anchored-Protein Receptor Essential for Inner-Ear Hair Cells and Retinal Photoreceptors. **2016**, *4*, 895–914, doi:10.1113/JP271437.

37.   Didangelos, A.; Yin, X.; Mandal, K.; Baumert, M.; Jahangiri, M.; Mayr, M. Proteomics Characterization of Extracellular Space Components in the Human Aorta. *Molecular and Cellular Proteomics* **2010**, *9*, 2048–2062, doi:10.1074/mcp.M110.001693.

38.   Wright, K.D.; Rogers, A.A.M.; Zhang, J.; Shim, K. Cooperative and Independent Functions of FGF and Wnt Signaling during Early Inner Ear Development. *BMC Developmental Biology* **2015**, 1–15, doi:10.1186/s12861-015-0083-8.

39.   Zallocchi, M.; Delimont, D.; Meehan, D.T.; Cosgrove, D. Regulated Vesicular Trafficking of Specific PCDH15 and VLGR1 Variants in Auditory Hair Cells. *Journal of Neuroscience* **2012**, *32*, 13841–13859, doi:10.1523/JNEUROSCI.1242-12.2012.

40.   Chen, J.; Ingham, N.; Kelly, J.; Jadeja, S.; Goulding, D.; Pass, J.; Mahajan, V.B.; Tsang, S.H.; Nijnik, A.; Jackson, I.J.; et al. Spinster Homolog 2 (Spns2) Deficiency Causes Early Onset Progressive Hearing Loss. **2014**, *10*, doi:10.1371/journal.pgen.1004688.

41.   Sheets, L.; Holmgren, M.; Kindt, K.S. How Zebrafish Can Drive the Future of Genetic-Based Hearing and Balance Research. *JARO - Journal of the Association for Research in Otolaryngology* 2021, *22*, 215–235.

42.   Singleman, C.; Holtzman, N.G. Growth and Maturation in the Zebrafish, Danio Rerio: A Staging Tool for Teaching and Research. *Zebrafish* **2014**, *11*, 396–406, doi:10.1089/zeb.2014.0976.

43.   Leitner, M.G. Zebrafish in Auditory Research: Are Fish Better than Mice? *Journal of Physiology* **2014**, *592*, 4611–4612, doi:10.1113/jphysiol.2014.280438.

44. Pickett, S.B.; Raible, D.W. Water Waves to Sound Waves: Using Zebrafish to Explore Hair Cell Biology. *JARO - Journal of the Association for Research in Otolaryngology* 2019, *20*, 1.

45. Gerchman, E.; Hilfer, S.R.; Brown, J.W. Involvement of Extracellular Matrix in the Formation of the Inner Ear. *Developmental Dynamics* **1995**, *202*, 421–432, doi:10.1002/aja.1002020411.

46. Steevens, A.R.; Glatzer, J.C.; Kellogg, C.C.; Low, W.C.; Santi, P.A.; Kiernan, A.E. SOX2 Is Required for Inner Ear Growth and Cochlear Nonsensory Formation before Sensory Development. *Development (Cambridge)* **2019**, *146*, doi:10.1242/dev.170522.

47. Steevens, A.R.; Sookiasian, D.L.; Glatzer, J.C.; Kiernan, A.E. SOX2 Is Required for Inner Ear Neurogenesis. *Scientific Reports* **2017**, *7*, doi:10.1038/s41598-017-04315-2.

48. Gou, Y.; Guo, J.; Maulding, K.; Riley, B.B. Sox2 and Sox3 Cooperate to Regulate Otic / Epibranchial Placode Induction in Zebra Fi Sh. *Developmental Biology* **2018**, *435*, 84–95, doi:10.1016/j.ydbio.2018.01.011.

49. Zhong, C.; Fu, Y.; Pan, W.; Yu, J.; Wang, J. Atoh1 and Other Related Key Regulators in the Development of Auditory Sensory Epithelium in the Mammalian Inner Ear: Function and Interplay. *Developmental Biology* **2019**, *446*, 133–141, doi:10.1016/j.ydbio.2018.12.025.

50. Hongmiao, R.; Wei, L.; Bing, H.; Xiong, D.; Jihao, R. Atoh1: Landscape for Inner Ear Cell Regeneration. *Current Gene Therapy* **2014**, *14*, 101–111, doi:10.2174/1566523214666140310143407.

51. Mulvaney, J.; Dabdoub, A. Atoh1, an Essential Transcription Factor in Neurogenesis and Intestinal and Inner Ear Development: Function, Regulation, and Context Dependency. *JARO - Journal of the Association for Research in Otolaryngology* **2012**, *13*, 281–293, doi:10.1007/s10162-012-0317-4.

52. Mann, Z.F.; Thiede, B.R.; Chang, W.; Shin, J.B.; May-Simera, H.L.; Lovett, M.; Corwin, J.T.; Kelley, M.W. A Gradient of Bmp7 Specifies the Tonotopic Axis in the Developing Inner Ear. *Nature Communications* **2014**, *5*, 1–16, doi:10.1038/ncomms4839.

53. Kamaid, A.; Neves, J.; Giráldez, F. Id Gene Regulation and Function in the Prosensory Domains of the Chicken Inner Ear: A Link between Bmp Signaling and Atoh1. *Journal of Neuroscience* **2010**, *30*, 11426–11434, doi:10.1523/JNEUROSCI.2570-10.2010.

54. Meyer Zum Gottesberge, A.M.; Gross, O.; Becker-Lendzian, U.; Massing, T.; Vogel, W.F. Inner Ear Defects and Hearing Loss in Mice Lacking the Collagen Receptor DDR1. *Laboratory Investigation* **2008**, *88*, 27–37, doi:10.1038/labinvest.3700692.

55. Vaughan-Thomas, A.; Young, R.D.; Phillips, A.C.; Duance, V.C. Characterization of Type XI Collagen-Glycosaminoglycan Interactions*. *THE JOURNAL OF BIOLOGICAL CHEMISTRY* **2001**, *276*, 5303–5309, doi:10.1074/jbc.M008764200.

56. Masaki, K.; Gu, J.W.; Ghaffari, R.; Chan, G.; Smith, R.J.H.; Freeman, D.M.; Aranyosi, A.J. Col11a2 Deletion Reveals the Molecular Basis for Tectorial Membrane Mechanical Anisotropy. *Biophysical Journal* **2009**, *96*, 4717–4724, doi:10.1016/j.bpj.2009.02.056.

57. Exposito, J.Y.; Valcourt, U.; Cluzel, C.; Lethias, C. The Fibrillar Collagen Family. *International Journal of Molecular Sciences* **2010**, *11*, 407–426, doi:10.3390/ijms11020407.

58. Fallahi, A.; Kroll, B.; Warner, L.R.; Oxford, R.J.; Irwin, K.M.; Mercer, L.M.; Shadle, S.E.; Oxford, J.T. Structural Model of the Amino Propeptide of Collagen XI A1 Chain with Similarity to the LNS Domains. *Protein Science* **2009**, *14*, 1526–1537, doi:10.1110/ps.051363105.

59. Hardy, M.J.; Reeck, J.C.; Fang, M.; Adams, J.S.; Oxford, J.T. Col11a1a Expression Is Required for Zebrafish Development. *Journal of Developmental Biology* **2020**, *8*, doi:10.3390/JDB8030016.

60. Mendler, M.; Eich-Bender, S.G.; Vaughan, L.; Winterhalter, K.H.; Bruckner, P. Cartilage Contains Mixed Fibrils of Collagen Types II, IX, and XI. *The Journal of cell biology* **1989**, *108*, 191–197, doi:10.1083/jcb.108.1.191.

61. Nah, H.D.; Barembaum, M.; Upholt, W.B. The Chicken A1(XI) Collagen Gene Is Widely Expressed in Embryonic Tissues. *Journal of Biological Chemistry* **1992**, *267*, 22581–22586.

62. Mayne, R.; Brewton, R.G.; Mayne, P.M.; Baker, J.R. Isolation and Characterization of the Chains of Type V/Type XI Collagen Present in Bovine Vitreous. *Journal of Biological Chemistry* **1993**, *268*, 9381–9386.

63. Annunen, S.; Körkkö, J.; Czarny, M.; Warman, M.L.; Brunner, H.G.; Kääriäinen, H.; Mulliken, J.B.; Tranebjærg, L.; Brooks, D.G.; Cox, G.F.; et al. Splicing Mutations of 54-Bp Exons in the COL11A1 Gene Cause Marshall Syndrome, but Other Mutations Cause Overlapping Marshall/Stickler Phenotypes. *American Journal of Human Genetics* **1999**, *65*, 974–983, doi:10.1086/302585.

64. Acke, F.R.; Swinnen, F.K.; Malfait, F.; Dhooge, I.J. Auditory Phenotype in Stickler Syndrome : Results of Audiometric Analysis in 20 Patients. **2016**, *185*, 3025–3034, doi:10.1007/s00405-016-3896-6.

65. Booth, K.T.; Askew, J.W.; Talebizadeh, Z.; Huygen, P.L.M.; Eudy, J.; Kenyon, J.; Hoover, D.; Hildebrand, M.S.; Smith, K.R.; Bahlo, M.; et al. Splice-Altering Variant in COL11A1 as a Cause of Nonsyndromic Hearing Loss DFNA37. *Genetics in Medicine* **2019**, *21*, 948–954, doi:10.1038/s41436-018-0285-0.

66. Čopíková, J.; Paděrová, J.; Románková, V.; Havlovicová, M.; Balaščáková, M.; Zelinová, M.; Vejvalková, Š.; Simandlová, M.; Štěpánková, J.; Hořínová, V.; et al. Expanding the Phenotype Spectrum Associated with Pathogenic Variants in the COL2A1 and COL11A1 Genes. *Annals of Human Genetics* **2020**, *84*, 380–392, doi:10.1111/ahg.12386.

67. Rad, A.; Schade-Mann, T.; Gamerdinger, P.; Yanus, G.A.; Schulte, B.; Müller, M.; Imyanitov, E.N.; Biskup, S.; Löwenheim, H.; Tropitzsch, A.; et al. Aberrant COL11A1 Splicing Causes Prelingual Autosomal Dominant Nonsyndromic Hearing Loss in the DFNA37 Locus. *Human Mutation* **2021**, *42*, 25–30, doi:10.1002/humu.24136.

68. Azaiez, H.; Booth, K.T.; Ephraim, S.S.; Crone, B.; Black-Ziegelbein, E.A.; Marini, R.J.; Shearer, A.E.; Sloan-Heggen, C.M.; Kolbe, D.; Casavant, T.; et al. Genomic Landscape and Mutational Signatures of Deafness-Associated Genes. *American Journal of Human Genetics* **2018**, *103*, 484–497, doi:10.1016/j.ajhg.2018.08.006.

69. Deafness Variation Database Available online: https://deafnessvariationdatabase.org/references (accessed on 24 May 2021).

70. Svetlichnyy, D.; Imrichova, H.; Fiers, M.; Kalender Atak, Z.; Aerts, S. Identification of High-Impact Cis-Regulatory Mutations Using Transcription Factor Specific Random Forest Models. *PLoS Computational Biology* **2015**, *11*, 1004590, doi:10.1371/journal.pcbi.1004590.

71. Chatterjee, S.; Lufkin, T. The Sound of Silence: Mouse Models for Hearing Loss. *Genetics Research International* **2011**, *2011*, doi:10.4061/2011/416450.

72. Shpargel, K.B.; Makishima, T.; Griffith, A.J. Col11a1 and Col11a2 MRNA Expression in the Developing Mouse Cochlea: Implications for the Correlation of Hearing Loss Phenotype with Mutant Type XI Collagen Genotype. *Acta Oto-Laryngologica* **2004**, *124*, 242–248, doi:10.1080/00016480410016162.

73. Yang, Y.; Wang, X.; Liu, Y.; Fu, Q.; Tian, C.; Wu, C.; Shi, H.; Yuan, Z.; Tan, S.; Liu, S.; et al. Transcriptome Analysis Reveals Enrichment of Genes Associated with Auditory System in Swimbladder of Channel Catfish. *Comparative Biochemistry and Physiology - Part D: Genomics and Proteomics* **2018**, *27*, 30–39, doi:10.1016/j.cbd.2018.04.004.

74. Yao, Q.; Wang, L.; Mittal, R.; Yan, D.; Richmond, M.T.; Denyer, S.; Requena, T.; Liu, K.; Varshney, G.K.; Lu, Z.; et al. Transcriptomic Analyses of Inner Ear Sensory Epithelia in Zebrafish. *Anatomical Record* **2020**, *303*, 527–543, doi:10.1002/ar.24331.

75. YAMADA, H.C.Y.; YOO, T.J. Ultrastructural Changes of Cochlea in Mice with Hereditary Chondrodysplasia (Cho/Cho). *Annals of the New York Academy of Sciences* **1991**, *630*, 259–261, doi:10.1111/j.1749-6632.1991.tb19598.x.

CHAPTER TWO: COL11A1A EXPRESSION IS REQUIRED FOR ZEBRAFISH DEVELOPMENT

Makenna J. Hardy [1,2], Jonathon C. Reeck [1,2,†], Ming Fang [1,3,‡], Jason S. Adams [1,3,4], and Julia Thom Oxford [1,2,3,5,*]

[1] Biomolecular Research Center; Boise State University, Boise, ID, 83725 USA

[2] Biomolecular Sciences Graduate Program; Boise State University, Boise, ID 83725 USA

[3] Department of Biological Sciences, Boise State University, Boise ID 83725 USA

[4] Department of Physiology and Developmental Biology, Brigham Young University, Provo, UT 84602 USA

[5] Center of Biomedical Research Excellence in Matrix Biology, Boise State University, Boise, ID 83725 USA

* Correspondence: joxford@boisestate.edu; Tel.: +01-208-426-2395 (J.O.)

† Current Address: Beigene Pharmaceuticals

‡ Current Address: Facible, Inc.

Abstract

The autosomal dominant chondrodystrophies, the Stickler type 2 and Marshall syndromes, are characterized by facial abnormalities, vision deficits, hearing loss, and articular joint issues resulting from mutations in COL11A1. Zebrafish carry two copies of the Col11a1 gene, designated Col11a1a and Col11a1b. Col11a1a is located on zebrafish chromosome 24 and Col11a1b is located on zebrafish chromosome 2. Expression patterns are distinct for Col11a1a and Col11a1b and Col11a1a is most similar to COL11A1 that is responsible for human autosomal chondrodystrophies and the gene responsible for changes in the chondrodystrophic mouse model cho/cho. We investigated the function of Col11a1a in craniofacial and axial skeletal development in zebrafish using a knockdown approach. Knockdown revealed abnormalities in Meckel's cartilage, the otoliths, and overall body length. Similar phenotypes were observed using a CRISPR/Cas9 gene-editing approach, although the CRISPR/Cas9 effect was more severe compared to the transient effect of the antisense morpholino oligonucleotide treatment. The results of this study provide evidence that the zebrafish gene for Col11a1a is required for normal development and has similar functions to the mammalian COL11A1 gene. Due to its transparency, external fertilization, the Col11a1a knockdown, and knockout zebrafish model systems can, therefore, contribute to filling the gap in knowledge about early events during vertebrate skeletal development that are not as tenable in mammalian model systems and help us understand Col11a1-related early developmental events.

Keywords: collagen; *Col11a1*; alternative splicing; minor fibrillar collagen; zebrafish; Stickler Type 2 Syndrome, Marshall Syndrome, Fibrochondrogenesis

1. Introduction

The molecular mechanisms directing developmental patterning and gene expression at early stages in vertebrate development are conserved in many respects between zebrafish and humans, with cartilage forming the majority of the vertebrate embryonic skeleton in early development, relying on mesenchymal cell proliferation and condensation [1,2]. Chondroprogenitor proliferation and terminal differentiation lead to the formation of precisely sized and shaped skeletal elements [3]. Cartilage defects during this process can lead to chondrodystrophies that may include abnormal bone formation, joint dysfunction, and early-onset osteoarthritis [4]. In addition to skeletal symptoms, chondrodystrophies such as Stickler syndrome also includes hearing loss, and the zebrafish model system may provide insight into the mechanism that links the skeletal phenomena to hearing loss, resulting from mutations in the Col11a1 gene. The development of the zebrafish ear is similar to other vertebrates [5,6] and zebrafish has served as a model system for the study of ear development [6–8]. Cartilage-related defects associated with collagen type XI have been identified in several vertebrate species including mice, humans, dogs, and zebrafish [9–13]. In mice, a Col11a1 mutation causing a hereditary recessive chondrodysplasia (cho/cho) has provided key insight into the role of Col11a1 in the formation of cartilaginous structures. Cho/cho mice display severe hearing impairment due to underdevelopment of the organ of Corti in the cochlea [14] and chondrodysplasia of the limbs, palate, ribs, mandible, and trachea [15], all of which are present as transient or permanent cartilaginous structures in the developing mouse embryo. Human mutations in COL11A1 result in similar abnormalities that constitute the Marshall and Stickler syndromes. These syndromes are similar, characterized by varying

degrees of craniofacial abnormalities, such as cleft palate, myopia, retinal detachment, deafness, dental anomalies, and early-onset arthritis [16–20]. Collagen is the most abundant protein in connective tissue and plays an integral part in most vertebrate tissues [21]. Disturbances in cartilage collagen composition and distribution during development results in alterations in the skeletal structure that contribute to an increased risk of disease [22]. Specifically, disruption in the expression of collagen type II and XI negatively impacts the organization and complexity needed for proper functioning mature cartilage [23]. Collagen type XI belongs to the fibrillar class of collagens [24] and polymerizes with collagen type II and IX to produce heterotypic collagen fibrils [25] found in fetal and adult cartilage [26]. Col11a1 gene expression is reported widely beyond cartilage, to include the nucleus pulposus of the intervertebral disc, the developing notochord, the vitreous humour of the mammalian eye, skeletal muscle, brain tissue, tendons, heart valves, skin, the tectorial membrane of the inner ear, intestinal epithelia and smooth muscle of the intestine, the calvaria, and endochondral bones [26–28]. In our previous study, we identified zebrafish orthologues of the minor fibrillar collagen genes and analyzed the exons included within the specific splice forms. We characterized the temporal and spatial expression patterns of the Col11a1a splice-forms in the developing zebrafish embryo and found these splice forms to be prevalent in the ear, notochord, and Meckel's cartilage. In this study, we designed antisense morpholino oligonucleotides (AMOs) that effectively block translational initiation as well as intron/exon splicing of exon 6a within the alternatively spliced variable region. The results that we present here from this knockdown technique using AMOs further substantiate the identification of the homologous zebrafish genes as orthologues of COL11A1. The result of the exclusion of

exon 6a also resulted in malformations in the otoliths in the ear, of the notochord, and of Meckel's cartilage. Finally, results of the AMO knockdowns were compared to CRISPR/Cas9-mediated gene editing of Col11a1a to confirm our findings. These investigations of zebrafish orthologues of COL11A1 increase our understanding of the function of Col11a1 and help to establish zebrafish as a biological model for the study of collagen type XI in vertebrate development and disease.

The molecular mechanisms directing developmental patterning and gene expression at early stages in vertebrate development are conserved in many respects between zebrafish and humans. Cartilage forms the majority of the vertebrate embryonic skeleton in early development. The formation of cartilage involves mesenchymal cell proliferation and condensation. Chondroprogenitor proliferation and terminal differentiation lead to less-densely packed regularly shaped and arranged cells vital to the formation of precise size and shape skeletal elements [1]. Cartilage defects during this process can lead to abnormal bone formation, joint dysfunction, and early-onset osteoarthritis [2].

Stickler syndrome includes hearing loss, and the zebrafish model system may provide insight into the mechanism of hearing loss, which results from mutations in the *Col11a1* gene. The development of the zebrafish ear is similar to other vertebrates in many ways [3,4]. Zebrafish do not possess a cochlea and there is not a middle or outer ear system as seen in humans [5].

Cartilage-related defects associated with collagen type XI have been identified in several vertebrate species including mice, humans, dogs, and zebrafish [6–10]. In mouse, a *Col11a1* mutation causing a hereditary recessive chondrodysplasia (*cho/cho*) has

provided key insight into the role of Col11a1 in the formation of cartilaginous structures. *Cho/cho* mice display severe hearing-impairment due to underdevelopment of the organ of Corti in the cochlea [11] and chondrodysplasia of the limbs, ribs, mandible, and trachea [12], all of which are present as transient or permanent cartilaginous structures in the developing mouse embryo. Human mutations in *COL11A1* result in similar abnormalities that constitute Marshall and Stickler syndromes. These syndromes are similar, characterized by varying degrees of craniofacial abnormalities, cleft palate, myopia, retinal detachment, deafness, dental anomalies, and early onset arthritis [13].

Collagen is the most abundant protein in connective tissue and plays an integral part in most vertebrate tissues. Once development has occurred, collagen architecture cannot be restored if injury or degeneration of the mature cartilage occurs [14]. Disturbance in collagen composition and distribution during development results in alterations of the skeletal structure that contributes to an increased risk of disease. Specifically, disruption in the expression of collagen type II and XI negatively impacts the organization and complexity needed for proper functioning matured cartilage [15].

Collagen type XI belongs to the fibrillar class of collagens [16] and polymerizes with collagen type II and IX to produce heterotypic collagen fibrils [17], found in fetal and adult cartilage [18]. *Col11a1* gene expression is reported widely beyond cartilage, to include nucleus pulposus of the intervertebral disc, the developing notochord, the vitreous of the mammalian eye, skeletal muscle, brain, tendons, heart valves, skin tectorial membrane of the inner ear, intestinal epithelia and smooth muscle of the intestine, calvaria and endochondral bones [18–20].

In our previous study, we identified zebrafish orthologues of the minor fibrillar collagen genes and analyzed the exons included within the specific splice forms and the temporal and spatial expression patterns of the col11a1a splice forms were characterized in the developing zebrafish embryo and found to be prevalent in the ear, notochord, and Meckel's cartilage, among others.

In this study, we designed antisense morpholino oligonucleotides (AMOs) that effectively block translational initiation as well as intron/exon splicing within the alternatively spliced variable region. The results that we present here from knockdown using AMOs further substantiate the identification of the homologous zebrafish genes as orthologues of *COL11A1*. The result of the exclusion of specific exons of the alternatively spliced variable region also resulted in malformations of the otoliths in the ear, notochord, and Meckel's cartilage. Finally, results of the AMO knockdowns were compared to CRISPR/Cas9 mediated gene editing of *Col11a1a* to confirm findings.

Investigation of zebrafish orthologues of *COL11A1* increases our understanding of the function of Col11a1 and helps to establish the zebrafish as a biological model for the study of collagen type XI in vertebrate development and disease.

2. Materials and Methods

2.1. Fish Maintenance, Care, and Staging

Ab/Ab Danio rerio embryos were obtained from Zebrafish International Resource Center (ZIRC) (Eugene, OR, USA). Juvenile and adult zebrafish were housed in an Aquatic Habitat (Apopka, FL, USA) system with regulated temperature and light cycle. Fertilized eggs were maintained in a smaller tank with a temperature of 28.5 ∘C, 20 to 25 embryos per 100 mL. Zebrafish were euthanized with 300 mg/mL ethyl 3-aminobenzoate

methane sulfonate salt (MS-222) (Sigma Aldrich, St. Louis, MO, USA), by treating for

5–10 min until the opercular movement stopped, as approved by the Boise State

University Institutional Animal Care and Use Committee (AC18-014 and AC18-015).

Embryos were staged before euthanization or experimentation to determine age in hours

or days post-fertilization (hpf and dpf) at 28.5 °C using a Zeiss Stemi 2000-C dissecting

microscope (Carl Zeiss MicroImaging, Inc., Thornwood, NY, USA).

2.2. PCR

Zebrafish RNA was isolated at specific developmental stages (4 h, 10 h, 24 h, 48

h, 72 h, 3.5 d, 4.5 d, and 6.5 d) and used to generate cDNAs using Retroscript (Ambion,

Austin, TX, USA). cDNA was used as a template in PCR reactions with primers flanking

the variable region of the Col11a1a chain. Ten picomoles of each primer and 2 µL of

cDNA were added to 22 µL of PCR master mix generated by adding water to Ready-To-

Go PCR Beads (Amersham Biosciences, Piscataway, NJ, USA). The final reaction (25

µL) contained 1.5 U Taq DNA Polymerase, 10 mM Tris-HCl, pH 9.0 at room

temperature, 50 mM KCl, 1.5 mM MgCl2, 200 µM of each dNTP as well as bovine

serum albumin (BSA). Each reaction was then incubated as follows: 95 °C for 5 min, (95

°C for 1 min, 55.5 °C for 1 min, 72 °C for 1 min) × 30 cycles, and 72 °C for 10 min. PCR

products were separated by size by electrophoresis on a 2% agarose gel (Nusieve 3:1) in

Tris Acetate EDTA (TAE) buffer and stained with ethidium bromide. Bands were

visualized using a Kodak ID Image Station (Eastman Kodak Company, Rochester, NY,

USA) trans-illuminator.

2.3. Cloning and Riboprobe Synthesis

Excised PCR products were purified using the Ultrafree-DA Centrifugal purification system (Millipore/Amicon, Bellerica, MA, USA) and sequenced by the Idaho State University Molecular Research Core Facility (Pocatello, ID, USA). Purified products were ligated into the PCRII vector (Invitrogen, Carlsbad, CA, USA) overnight at 14 °C. The ligation product was transformed into chemically competent TOP10 Escherichia coli cells (Invitrogen, Carlsbad, CA, USA). Sequence analysis was performed by the Idaho State University Molecular Research Core Facility (Pocatello, ID, USA).

Five micrograms of riboprobe-containing plasmids were linearized using 5U Hind III with 10× BSA in 20 µL total volume. Plasmid digest fragments were subsequently purified by phenol/chloroform extraction. One-tenth volume of 8 M LiCl was added to each reaction followed by the addition of 2.5 volumes of 100% ethanol. One microgram of linearized/purified plasmid was used as a template to synthesize antisense, digoxigenin-labeled probe using DIG RNA Labeling (Roche Applied Science, Indianapolis, IN, USA). A control probe was synthesized using pSPT18-neo empty plasmid. Riboprobe synthesis products were purified using P-30 Bio Spin columns (BioRad Laboratories, Hercules, CA, USA). Probe reactions were then diluted to a working concentration with hybridization buffer for in situ hybridization assays.

2.4. In Situ Hybridization

Zebrafish embryos were fixed in 4% paraformaldehyde in phosphate buffer (PBS) containing 8% sucrose and 0.3 µM CaCl2. Embryos were dehydrated, rehydrated,

washed and hybridized as previously described [29]. Embryos were washed and fixed in

2% formalin in PBST overnight at 4 ∘C, and stored in 75% glycerol at 4 ∘C.

2.5. Antisense Morpholino Oligonucleotide Injection

Antisense morpholino oligonucleotides (AMOs) were designed to knockdown the

protein expression of Col11a1a, Col11a1b, or alter specific isoforms of Col11a1a (Gene

Tools, LLC Philomath, OR). AMOs directed to the translational start site in exon 1 of

Col11a1a (chr24) consisted of the sequence 5' -

GGGACCACCTTGGCCTCTCCATGGT-3', and Col11a1b (chr2) exon 1 consisted of

the sequence 5' -ACCACCTTTCCTTATCCTTATCCAT-3' to block initiation of

protein synthesis. AMOs used to block the inclusion of specific exons within the variable

region were as follows:

exon 6A 5' -GTTGTGTACTGCACATAGGGAGAGG-3';

exon 6B 5' -GTTTCACTCTCTGGAAAAAGGTTAT-3';

exon 8 5' -CATGGCCTTATTACACCCAAAGCAA-3'.

A control AMO 5' -CCTCTTACCTCAGTTACAATTTATA-3' directed to the

gene encoding β-globin of a human patient with thalassemia was used as a negative

control, as this sequence should not be present in the experimental samples (Gene Tools

#18633993). AMOs were injected into the yolk of one- to two-cell embryos using an

Eppendorf Femtotip II microinjection needle and an injection pressure of 3.5 psi for 0.1 s

with a compensation pressure of 0.22 psi (Eppendorf, Hamburg, Germany). The

effectiveness of splice blocking AMOs was confirmed by RT-PCR (see Supplementary

Materials). The skeletal effects of the Col11a1 AMOs were detected by analysis of

morphants directly or by using Alcian blue staining of the injected zebrafish at specific

time points and compared to time-matched untreated zebrafish and those treated with the control AMO.

2.6. CRISPR/Cas9 Gene Editing

A CRISPR/Cas9 gene-editing approach was used to introduce a premature stop codon in Col11a1a. Target sequences were designed as described by Gagnon and colleagues [30]. The target sequences were identified through the CHOPCHOP webtool (https://chopchop.rc.fas.harvard.edu/). The six best targets were selected and were used to create six different guide sequences shown in Table 1. Guide sequence e201 resulted in a premature stop codon within exon 2 and was used for Col11a1a CRISPR/Cas9 mutant generation.

Table 2.1.   CRISPR/Cas9 gene editing.

Name	Target	Guide Sequence[1]	Forward Primer	Reverse Primer
E101	Exon 1	ATTTAGGTGACACTATA**GGCCAAGGTGGTCCCCAATG**GTTTTAGAGCTAGAAATAGCAAG	GGCACTTTTGGGATTGTAGAAG	CATCTCCTCTTAGAAAGCCCCT
E201	Exon 2	ATTTAGGTGACACTATA**AAGAGCATCACAGCCAGACG**GTTTTAGAGCTAGAAATAGCAAG	CTGCTGACATTTTGCATGTCTT	CATTTAAACGCAGCTGAACGTA
E301	Exon 3	ATTTAGGTGACACTATA**AGGCGTCCAGCAGCTGGGCG**GTTTTAGAGCTAGAAATAGCAAG	GTAAGAAGAAGCTGACCAAGCC	CCCGTTTATTTCTACCTCATGC
E401	Exon 4	ATTTAGGTGACACTATA**TGGCACCAGGATCCTGGATG**GTTTTAGAGCTAGAAATAGCAAG	GTAAGAAGAAGCTGACCAAGCC	CCCGTTTATTTCTACCTCATGC
E501	Exon 5	ATTTAGGTGACACTATA**GCCTGCAGTGTGTCCTTGTG**GTTTTAGAGCTAGAAATAGCAAG	GCTCTGTTTTTGGTCTCCTCAG	AGACGTCCAGAAGCGTTTAGTC
E2701	Exon 27	ATTTAGGTGACACTATA**GGTGTCCGTGGTCTAAAGGG**GTTTTAGAGCTAGAAATAGCAAG	TTCACTGTTGTCATTTTCAGGG	ACGTGTGACGATTTCTCCATTA

[1] Bold nucleotides indicate the coding sequence with the guide sequences.

2.7. Statistical Analysis

One-way ANOVA was used with randomized blocking. *p*-values of <0.05 were considered statistically significant. Measurements were analyzed using SAS/STAT software, v. 9.1 (SAS System, Cambridge, MA: Cytel Software Corporation, 2007).

3. Results

The *Danio rerio Col11a1a* gene is located on chromosome 24 (chr24) and the *Col11a1b* gene is located on chromosome 2 (chr2). Exon 1 of both *Col11a1a* and *Col11a1b* encodes the translational start site and the signal peptide, as is true for the other minor fibrillar collagen genes. Exons 2 through 5 of *Col11a1a* and *Col11a1b* encode the relatively large amino propeptide (Npp), which is also conserved for α1(XI), α2(XI), α1(V) and α3(V) alpha chains. Sequence comparison demonstrated the high degree of sequence conservation between humans and zebrafish, as shown in **Figure 1**. The degree of identity was used to identify the homologs of human genes within the zebrafish model system. **Figure 1** demonstrates that the percent amino acid sequence identity varies among specific regions of the corresponding protein and that the most closely related zebrafish gene is that located on zebrafish chromosome 24, *Col11a1a*.

Within the npp of the amino-terminal domain, the position of four cysteines is strictly conserved, as are stretches of amino acids predicted to adopt β-strand secondary structure. Originally predicted to adopt an Ig domain fold by analysis of primary sequence [31], it has been further demonstrated that this domain is a homolog of the amino-terminal domain of thrombospondin 1 and 2 and the LNS family, so named for laminin, neurexin, and sex-hormone binding protein [32,33,34,35]. The predicted amino propeptide domain of *Col11a1a* and *Col11a1b* of zebrafish also shares sequence

homology with the N-terminal domains of FACIT collagens types IX, XII, XIV, and XIX [36,37,38,39,40,41] as well as collagens type XXVIIa and XXVIIb. Divalent cation binding sites and sites of interactions with sulfated glycosaminoglycans are present in many of the LNS domains and appear to be conserved within the zebrafish genes.

Amino acid sequence identity relative to *H. sapiens* COL11A1

	npp	VR	mh	ntp	MTH	ctp	cpp
H. sapien COL11A1	npp	VR	mh	ntp	MTH	ctp	cpp
D. rerio Chr24: Col11a1a	76%		81%		87%		80%
D. rerio Chr21: Col5a1	75%		74%		82%		73%
D. rerio Chr2: Col11a1b	71%		73%		75%		71%
D. rerio Chr19: Col11a2	63%		72%		78%		57%
D. rerio Chr 3: Col5a3	57%		72%		75%		52%

Figure 2.1. **Amino acid sequence identity between *Homo sapien* and *Danio rerio* genes.**
Amino propeptide (npp), variable region (VR), minor helix (mh), amino telopeptide (ntp), major triple helix (MTH), carboxyl telopeptide (ctp), and carboxyl propeptide (cpp). Percentages shown indicate identity between human *COL11A1* and the zebrafish gene. Homology is observed within the npp, mh and ntp, MTH, and the ctp and cpp domains, while the degree of identity is very low for the VR. Amino acid sequence identity for other minor fibrillar collagens is shown in comparison to human *COL11A1*. The *D. rerio* chromosome 2 *Col11a1* locus identity corresponds to *Col11a1b.*

In addition to the highly conserved Npp domain, within the *Col11a1a* and *Col11a1b* amino-terminal domains in zebrafish there are predicted amino acid sequences that are poorly conserved among paralogues α1(XI), α2(XI), α1(V), and α3(V) chains, and also poorly conserved among the orthologues of any one of the minor fibrillar collagens compared across species. This region is referred to as the variable region (VR) [41,42,43,44]. In zebrafish *Col11a1a* but not *Col11a1b*, the α1(XI) mRNA exists as a set of splice forms arising by the mechanism of alternative splicing [45,46]. Alternative splicing in the analogous region has also been reported for the orthologues in other

vertebrate species for *Col11a1* as well as for genes encoding the α2(XI) chain. Interestingly, no alternative splicing has been reported for the alpha chains of the type V collagens. However, zebrafish may represent an exception to this rule [29,47].

We have analyzed the zebrafish intron–exon structure of the *Col11a1a* gene, comparing it to other vertebrates, and have found that a similar genomic structure exists. The *Col11a1a* on chromosome 24 gene comprises 130 kbp of genomic DNA, compared to 150 kbp in humans, with 67 exons compared to 68 exons in humans. The protein length is predicted to be slightly longer than in humans—1866 amino acids compared to 1852 amino acids. The amino acid sequence identity between zebrafish and humans, estimated by global alignment was found to be 76%, with regions of higher sequence identity in the carboxyl telopeptide and carboxyl propeptide (80%), the major triple helix (87%), and the minor helix and amino telopeptide region (81%) identity. Amino acid sequence identity for specific regions is shown in comparison to human *COL11A1* in **Figure 1**.

Col11a1a (chr24) was expressed during development, as shown in **Figure 2**. *Col11a1a* (chr 24) mRNA was not detectable at 4 hpf, but it was apparent at 10 hpf, during the segmentation phase of development. Expression levels were consistent through 72 hpf see **Figure 2A-B**. *Col11a1b* (chr2) mRNA expression was detectable at 4 Error! Reference source not found.hpf through the 72 hpf time point see **Figure 2A**. GAPDH is shown as an internal control housekeeping gene for each time point.
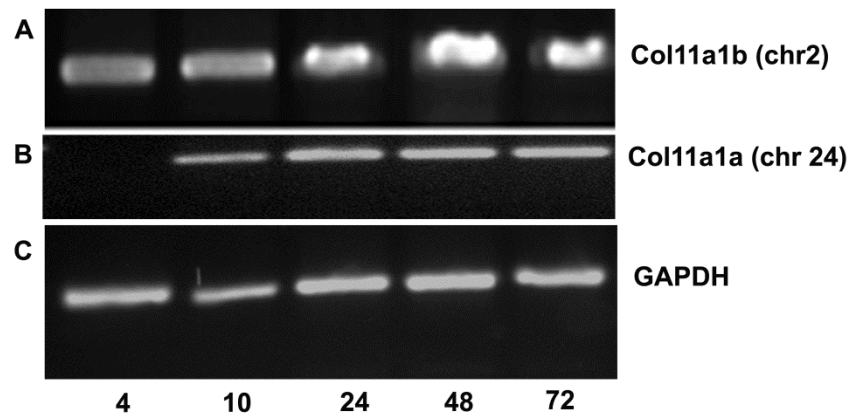
Figure 2.2.   RT-PCR indicates that *Col11a1a* (chr24) is expressed between 10 and 72 hpf and *Col11a1b* (chr2) is expressed at 4 hpf through 72 hpf. (A) Using primers to amplify a 470 bp fragment, *Col11a1b* (*chr2*) mRNA was detected in embryos and larval fish. Time post-fertilization is indicated at the bottom of gels as 4, 10, 24, 48, and 72 hpf. (B) *Col11a1a* (chr24) was detected at 10 hpf through 72 hpf. (C) *GAPDH* was included as housekeeping gene control.

Exons 6a through 8 of the variable region of Col11a1a were analyzed to evaluate

the intron–exon boundaries across the variable region. To determine the pattern of

alternative splicing that took place within this region of the zebrafish mRNA, RT-PCR

was carried out using primers that would distinguish between the different possible

splicing outcomes. Results indicated changes due to alternative splicing of

the Col11a1a mRNA between 10 hpf and 6.5 dpf, as shown in Figure 3.
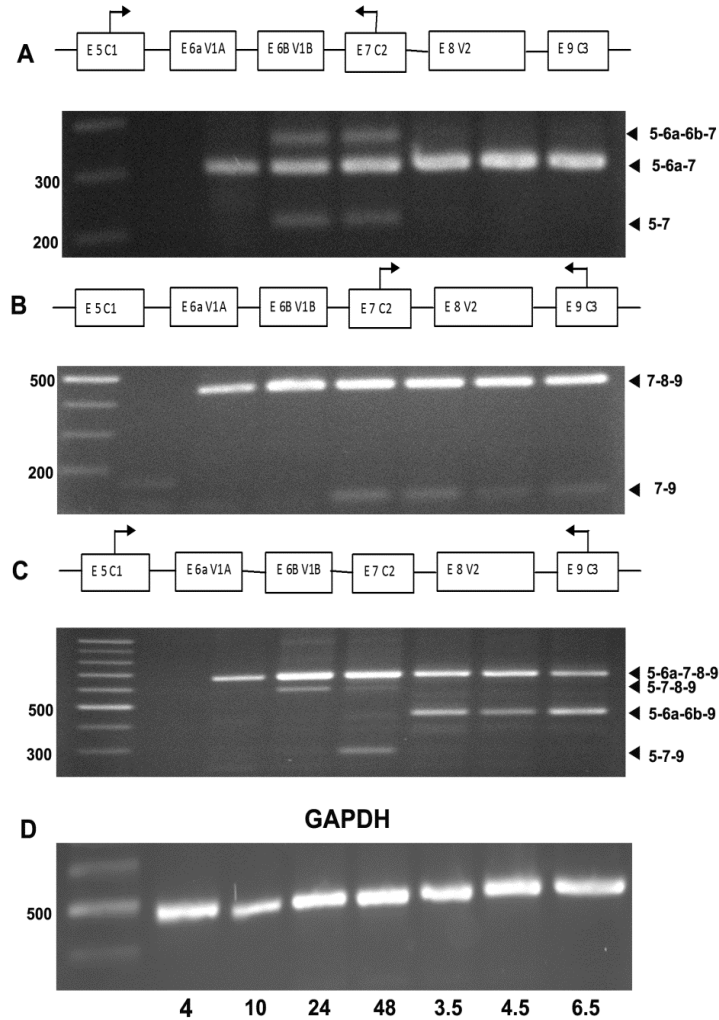
Figure 2.3. **RT-PCR demonstrates alternative splicing patterns in the expression of *Col11a1a* isoforms.**

(A) PCR primers hybridizing to sequences within exons 5 and 7 were used to investigate the inclusion and exclusion of exons 6a and 6b overtime during development. Expression was detected as early as 10 hpf and continued throughout development to the last time point queried in this study, which was 6.5 dpf. (B) PCR primers hybridizing to sequences within exon 7 and 9 were used to investigate the inclusion and exclusion of exon 8 overtime during development. Exon 8 was included in the most predominant form of Col11a1a at all time points investigated. However, exon 8 was skipped in some forms of Col11a1a, joining exon 7 directly to exon 9, as shown by the PCR band migrating below 200 kilobases. (C) PCR primers hybridizing to sequences within exons 5 and 9 were used to investigate the complexity of splice form expression across the variable region of Col11a1a in zebrafish. The predominant splice form included exons 6a and 8, in agreement with observations shown in panels A and B. Alternative patterns of expression were observed to exclude exons 6a and 6b but include exon 8 at 24 hpf. Additionally, exclusion of exons 6a, 6b, and 8 resulted in the expression of the splice form comprising exons 5-7-9 migrating at approximately 300 kilobases at 48 hpf. (D) GAPDH was included as housekeeping gene control to confirm RNA content in samples representing distinct time points in development. The identity of the PCR product was verified by DNA sequencing.

Alternative splicing of the *Col11a1a* (chr 24) mRNA in zebrafish generated similar splice variants to those previously been described for humans, rats, mice, and chicken with a few notable exceptions. The splice variant that includes exon 6a, 7, and 8 but excludes exons 6b ($\alpha1^{6a-7-8}$(XI)) was observed in zebrafish at the earliest time points. Additionally, splice variants $\alpha1^{7}$(XI), $\alpha1^{6a-7}$(XI), and $\alpha1^{7-8}$(XI) were also confirmed in zebrafish. Interestingly, the splice variant $\alpha1^{6a-6b}$(XI), was observed in zebrafish at 3.5, 4.5 and 6.5 days post-fertilization (dpf). This is noteworthy because exon 7 was thought to be constitutively expressed in all vertebrates, and exons 6a and 6b were previously thought to be either included or excluded in a mutually exclusive manner based on data from other species. This observation warrants further investigation, not only in the zebrafish system but also in humans and other vertebrate organisms. The most predominant form observed was $\alpha1^{6a-7-8}$(XI), which is also the predominant form found in mesenchymal stem cells in other vertebrates previously shown by our laboratory [48].

The spatial expression of *Col11a1a* and *Col11a1b* was determined by in situ hybridization, as shown in **Figure 4**. Using probes directed to exons 6a-7-8-9 for *Col11a1a* (chr 24) and exons 6-7-8-9 for *Col11a1b* (chr2), expression was detected in early zebrafish embryos. Spatial expression varied with the developmental stage. At 10 hpf, *Col11a1a* (chr24) expression was present along the dorsal midline. At 24 hpf, expression was most pronounced in the notochord and in the hindbrain. At 60–72 hpf, expression was detected in the craniofacial structures. The overall expression pattern for *Col11a1a* (chr24) was similar to that determined for *Col11a2* (chr19), as both were expressed in notochord and developing cranial cartilages [29]. *Col11a1b* (chr2) was

observed in the somites at 20–24 hpf, similar to *Col5a1* [29]. *Col11a1b* (chr2) was

detected within the craniofacial region at 60–72 hpf similar to *Col11a1a* (**Figure 4**).
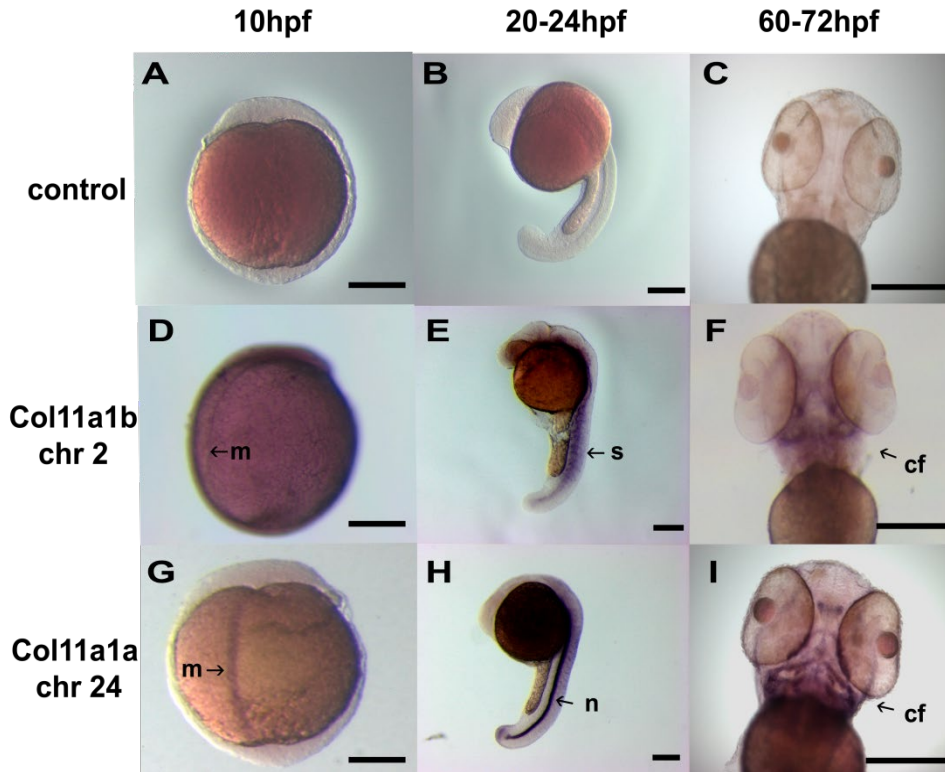
Figure 2.4. *In situ* hybridization of *Col11a1a* (chr 24) and *Col11a1b* (chr 2).
Wild-type embryos were treated with pSPT-18 control riboprobe (**A–
C**), *Col11a1b* (chr2) ex6-7-8-9 riboprobe (**D–F**), and *Col11a1a* (chr24) ex6a-7-8-9
(**G–I**). Embryos were observed at 10 hpf (**A,D,G**), 20–24 hpf (**B,E,H**), and 60–72 hpf
(**C,F,I**). Expression was limited to the embryonic midline (m) at 10 hpf. At 20–24 hpf,
expression was most pronounced in the notochord (n) for *Col11a1a* (chr24) and in the
somites (s) for *Col11a1b* (chr2). At 60–72 hpf, developing craniofacial structures
showed high levels of expression in addition to the notochord observed at 24 hpf seen
for *Col11a1a* (chr24). *Col11a1b* (chr2) was also apparent in the craniofacial (cf)
structures at 60–72 hpf in addition to the somites. Scale bars = 250 μm.
apparent in the craniofacial (cf) structures at 60–72 hpf in addition to the somites.
Scale bars = 250 μm.

An AMO-mediated knockdown strategy was used to investigate the role

of *Col11a1a* and *Col11a1b* in early development. Microinjection of 2 nL of a 0.5 mM

AMO targeting the translational start site of *Col11a1a* (Col11a1a-MOe1) was lethal in

57% of treated embryos compared to 26% lethality for treatment with the AMO targeting

the translational start site of *Col11a1b* (Col11a1b-MOe1) (**Table 2**). The knockdown of specific variants to explore the contribution of the variable region to survival was performed under the same conditions. AMOs targeting splice sites of exon 6a or exon 8 are shown in the **Supplementary Materials**.

Table 2.2.   Summary of lethal effect on reduced levels of *Col11a1b* and *Col11a1a* variants.

AMO	N	Lethality
Col11a1b-MOe1	54	14(26%)
Col11a1a-MOe1	87	50(57%)
Col11a1a-MOe6a	80	24(30%)
Col11a1a-MOe8	56	19(34%)
Std. AMO control	32	11(34%)

Comparing the efficiency of splice-modifying AMOs indicated that the exon 6a AMO was more effective than the exon 8 AMO. Therefore, we focused primarily on the splice-altering effect of skipping exon 6a, including the AMO targeting exon 8 for comparison. Lethality levels were similar to standard morpholino control, indicating that alternative isoforms may be able to compensate for each other in the case of *Col11a1a*. The AMO targeting exon 6b, Col11a1a-MOe6b, did not affect mRNA splicing.

Notochord deformities and a shortened overall body length were observed in morphants (**Table 3** and **Table 4**). Approximately 74% of Col11a1a-MOe1 morphants exhibited a severely curved notochord. A significantly shorter body length was observed in the remaining morphants when compared to the standard AMO control (2.81 ± 0.12 mm vs. 3.02 ± 0.17 mm; $p = 0.0031$). Col11a1b-MOe1 morphants exhibited a similar

trend, with 75% having a severely curved notochord and the remaining showing a significantly shortened body length than the standard AMO control (2.67 ± 0.16 mm; $p <$ 0.0001). Although AMOs directed toward splice sites of exons 6a and 8 did not alter viability, as shown in **Table 2**, they did have a significant effect on development and body plan. Morphants treated with the AMO preventing the inclusion of exon 6a (Col11a1a-MOe6a) showed a 93% prevalence of notochord deformity as well as a significantly shortened body length in measurable morphants (2.85 ± 0.12 mm; $p =$ 0.0284). By contrast, Col11a1a-MOe8 morphants showed the lowest prevalence of notochord deformities but still demonstrated a shortened body length (2.85 ± 0.18 mm; $p = 0.0123$).

Additionally, missing or extra otoliths, pericardial edema, and smaller Meckel's cartilage were observed in the *Col11a1a* and *Col11a1b* knockdown morphants (**Table 4**). To illustrate the change in body length and curvature observed due to treatment with AMOs that block protein translation by targeting the translational start site that exists with exon 1 for *Col11a1a*, representative examples are shown in **Figure 5**.

Table 2.3.   **Col11a1a knockdown results in a decrease in body length.**

AMO	Length (mm)	% Decrease
Col11a1b-MOe1	2.67 ± 0.16	-13.1%
Col11a1a-MOe1	2.81 ± 0.12	-7.5%
Col11a1a-MOe6a	2.85 ± 0.12	-6.0%
Col11a1a-MOe8	2.85 ± 0.18	-6.0%
Std. AMO control	3.02 ± 0.17	0

No effect was observed for MOe6b

Table 2.4. **Summary of Defects Observed under Reduced Levels of *Col11a1a* and *Col11a1b***

AMO	n	Missing or Extra Otoliths	Pericardial Edema	Curved Notochord	Smaller Meckel's
Col11a1b-MOe1	40	40(100%)	39 (98%)	30 (75%)	40(100%)
Col11a1a-MOe1	34	18(53%)	28(82%)	25(74%)	33(97%)
Col11a1a-MOe6a	44	30(68%)	42(95%)	41(93%)	44(100%)
Col11a1a-MOe8	18	0	0	1	18(100%)
Std. AMO control	32	0	0	0	0

No effect was observed for MOe6b

A similar phenotype was observed using the Col11a1b-MOe1, as shown in **Figure 5**.

Treatment with the AMO that blocks protein translation by targeting the translational

start site existing with exon 1 for *Col11a1b* resulted in the defects illustrated in **Figure 6**.

48
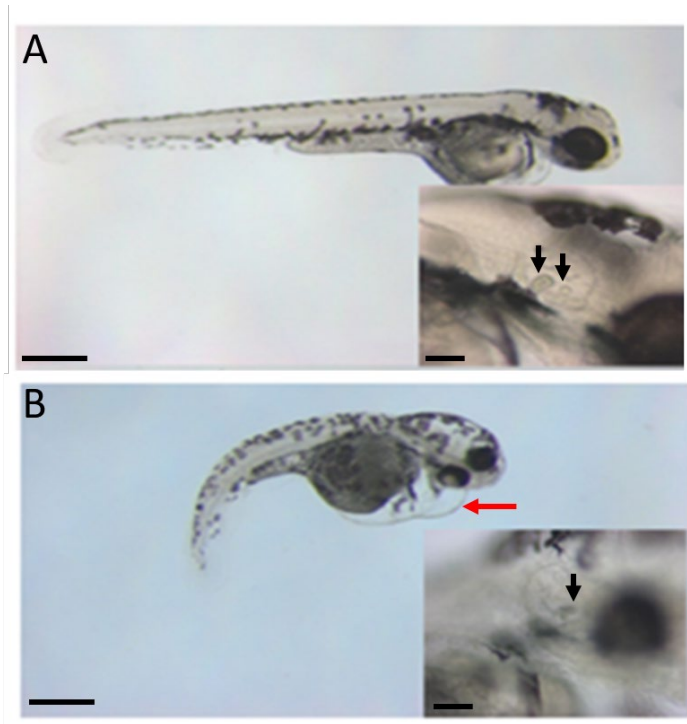
Figure 2.5.   Cardiac, body length, and curvature changes due to Col11a1b-MOe1 AMO knockdown.
(**A**) Control AMO injection, observed at 72 hpf. (**B**) Col11a1b-MOe1 AMO injection, observed at 72 hpf. Body length shortening, the curvature of the primary axis, and edema of the heart are apparent in zebrafish embryos treated with the transcriptional start site-specific AMO for *Col11a1b*. Otoliths are affected as indicated by arrows within the insets. Two arrows in A (inset) indicate the position of two otoliths in control zebrafish embryos. One arrow in B (inset) indicates the presence of only one otolith. Pericardial edema is indicated by the red arrow in B. Scale bar = 200 μm. Scale bars in inset represent 50 μm.

We investigated *Col11a1a* in more detail, focusing on the effect of splice-modifying AMOs. A reduction in Alcian blue staining was observed in the cartilage of Col11a1a-MOe1, Col11a1a-MOe6a, and Col11a1a-MOe8 morphants (**Figure 7**). A reduction in the size of Meckel's cartilage was observed. Otolith defects were observed that included a reduction in size, extra or missing otoliths.
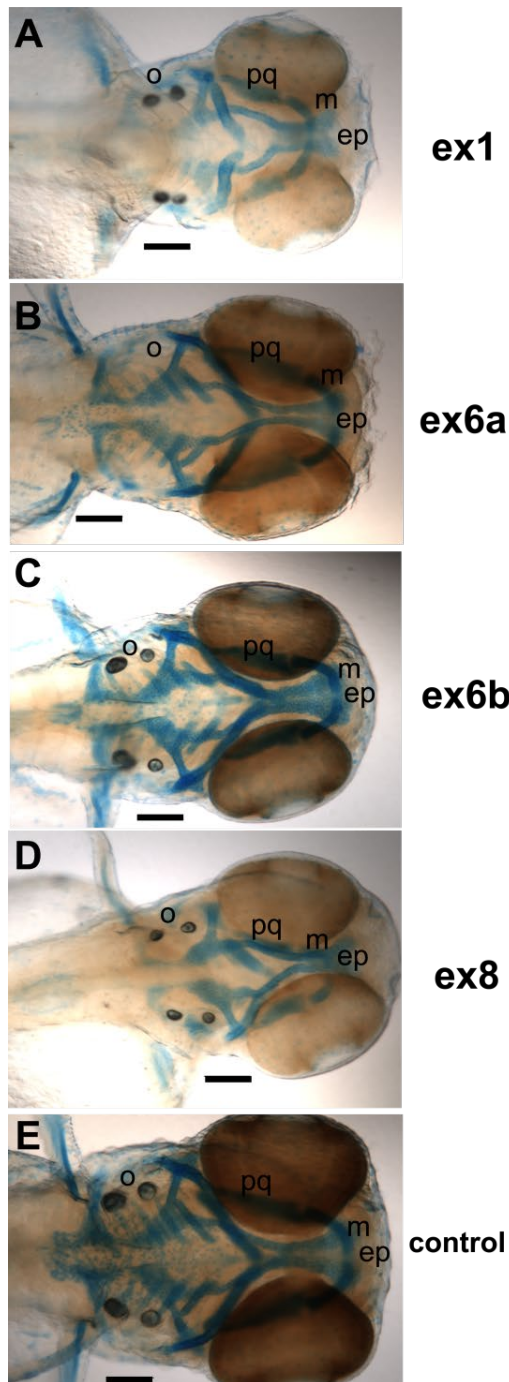
Figure 2.6.   Alcian blue staining of craniofacial cartilage in 72 hpf zebrafish morphants of *Col11a1a*.

A range of severity was observed among embryos of *Col11a1a* morphants. (A) Antisense morpholino oligonucleotide targeting the translational start site of Col11a1a-MOe1 morphants demonstrate reduced Alcian blue staining, disorganized cartilage, and shortened jaw. (B) Col11a1a-MOe6a morphants demonstrate reduced Alcian blue staining, shortened Meckel's cartilage, and an absence of otoliths. (C) Col11a1a-MOe6b show relatively little effect and are similar to the control zebrafish. (D) Col11a1a-MOe8 show reduced Alcian blue staining. (E) Standard AMO control. Abbreviations palatoquadrate (pq); Meckel's cartilage (m); ethmoid plate (ep); otolith (o). Scale bars = 200 µm.
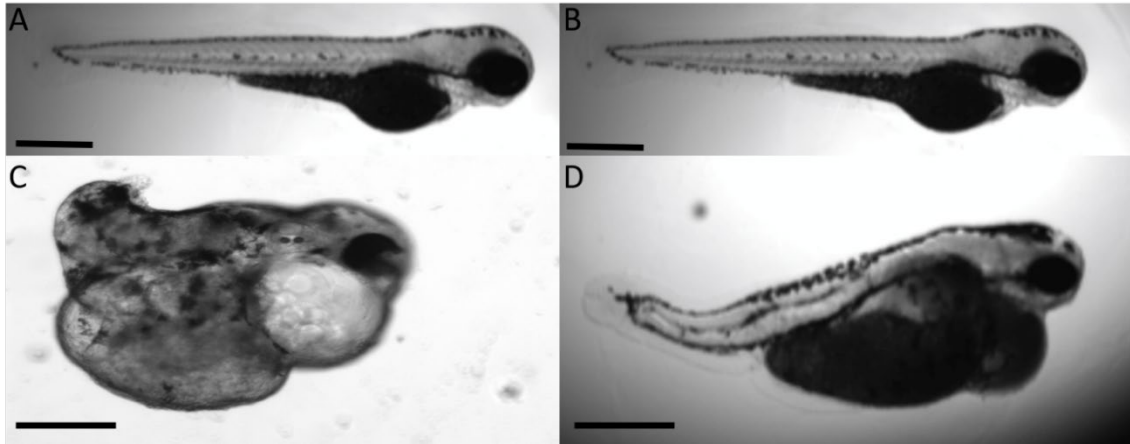
Figure 2.7. **CRISPR/Cas9-mediated homozygous and heterozygous knockout of Col11a1a shows a similar but more severe outcome compared to AMO knockdown.** (A) Wild-type 72 hpf embryo compared to (C) homozygous *Col11a1a* $^{-/-}$ knockout embryo at 72 hpf showing the severe effect of the complete absence of *Col11a1a* in early embryogenesis. Homozygous offspring were raised to adulthood and bred to wild type to generate heterozygous *Col11a1a*$^{-/+}$ offspring. (B) Wild-type 72 hpf embryo. (D) Heterozygous *Col11a1a* $^{-/+}$ embryo at 72 hpf. Scale bar = 200 μm.

Homozygous knockout embryos displayed severe phenotypes such as that shown in **Figure 8** and demonstrated a more severe lethality, as shown in **Table 5.** Heterozygous knockouts that resulted from crossing homozygous knockouts with a wild-type fish resulted in a lower level of lethality and a phenotype that was more similar to the AMO morphants. Representative homozygous and heterozygous offspring are shown in **Figure 8**.

Table 2.5. **Summary of lethality in CRISPR/Cas9 mutants**

CRISPR/Cas9	n	Lethality
Col11a1a -/-	303	299 (98 %)
Col11a1a +/-	299	152 (50 %)
Wildtype control	311	25(8 %)

4. Discussion

Mutations in the *COL11A1* gene have been identified as a cause for a range of human developmental defects resulting in facial abnormalities, eye defects, hearing loss, and articular joint defects. Zebrafish have been well established as a model for studying mammalian developmental processes and disorders resulting from genetic defects. Two chromosomal locations were investigated for *Col11a1a* and *Col11a1b* in zebrafish. Gene expression was detected throughout development. Alternative splicing was observed in the zebrafish gene *Col11a1a* but not *Col11a1b*. Knockdown of zebrafish gene expression and splice forms resulted in varying degrees abnormalities in the Meckel's cartilage, otoliths, notochord, and heart. Additionally, shortening of total body length and embryonic lethality was observed. These data provide evidence that the zebrafish genes for *Col11a1a* and *Col11a1b* are essential for normal development and that *Col11a1a* has similar characteristics as the human *COL11A1* gene.

The development of every organ system depends on a properly organized extracellular matrix. Extracellular matrix (ECM) assembly involves the dynamic interaction around structural macromolecules as well as between cells and ECM molecules. Biosynthetic or structural deficiencies of the components of the ECM are associated with a wide spectrum of birth defects that predispose individuals to symptoms ranging in severity from mild osteoarthritis to lethal chondrodysplasia with associated eye involvement and hearing loss [49,50], designated Stickler syndrome type 2 (OMIM #604841) or Marshall syndrome (OMIM #154780) [17].

Cloning of the zebrafish orthologues *Col11a1a* and *Col11a1b* with subsequent analysis of the various splice forms presented here form the basis on which further

studies of vertebrate type XI collagen function can be performed. This work also confirms the value of the zebrafish as a model for the study of the role of type XI collagen during vertebrate development.

In our studies, riboprobes localized to the structures that were affected during AMO-mediated knockdown. The zebrafish craniofacial structures are analogous to those that are affected in the *cho/cho* mice as well as the structure commonly affected by a mutation in the human *COL11A1* gene. These affected structures include a small jaw, changes to the ears that lead to hearing loss, and cleft palate [51]. In the *cho/cho* mouse, a model for chondrodysplasia, the result of a mutation in Col11a1 is dwarfism, with both chondrogenesis and endochondral ossification affected [52]. These data provide encouraging evidence that the functions of zebrafish *Col11a1a* and human *COL11A1* are conserved. If the zebrafish mutant generated in this study is an accurate model, mutants may also display cleft palate, smaller rib cage, and signs of osteoarthritis. Vison impairment and hearing loss would also be expected. Additionally, disturbed endochondral bone formation would possibly occur. Studies are now underway to investigate ear development and hearing, eye development and vision, and jaw formation with subsequent mineralization in our mutant zebrafish.

CRISPR/Cas9 gene editing was used to create a model system that expressed a lower level of *Col11a1a*. CRISPR/Cas9 has advantages over AMO knockdown because, unlike the transient effect of AMOs, the CRISPR/Cas9-mediated change is stable. Further, while AMOs are ideal for observing the effects very early in development, CRISPR/Cas9 may be useful for looking at the effect of genes that are expressed at later times in development.

Expression of the *Col11a1a* within the developing otic vesicle suggests that the zebrafish model will provide a means by which to study the further molecular and cellular basis of the hearing loss characteristic of the Marshall and Stickler syndromes.

The structural role of collagens in the formation of the ECM is well established. However, many ECM proteins also function as signaling molecules, directing the behavior of cells [53]. Interestingly, the craniofacial structures commonly affected by mutations in *Col11a1a* are derived from neural crest cells, including Meckel's cartilage, the otic vesicle, and otoliths [7]. Perhaps a lack of proper neural crest migration or differentiation, in addition to structural abnormalities, may be responsible for the phenotypes that characterize aberrant *Col11a1a* expression [54,55]. The ECM may serve as a scaffold on which neural crest cells migrate [56], and may facilitate the onset of migration of cells of neural crest origin during emigration [57]. ECM molecules may also influence cells by inhibiting or deflecting migrating neural crest cells, thus establishing a specific developmental pattern within the developing embryo [58]. Complex patterns of alternative splicing and splice form expression may be the key to unlocking the roles played by type XI collagen, minor fibrillar collagens, and other ECM proteins.

Supplementary Materials

The following are available online at **https://www.mdpi.com/2221-3759/8/3/16/s1**, Supplemental Figure S1. Col11a1a-MOe6a and Col11a1a-MOe8 alter splicing pattern at 48 hpf but recover by 72 hpf. Treatment with AMOs was performed at the one- to two-cell stage and splicing was monitored at 48 and 72 hpf. Lane 1: size markers; Lane 2: PCR product amplified using primers for exon 5 and 9 of *Col11a1a* (chr 24) from 48 hpf embryos after treatment with the control AMO showing that the most prevalent splice form consists of 6a-7-8-9 at 48 hpf. Lane 3: PCR products of amplification after treatment with Col11a1a-MOe6a, showing a decrease in the most prominent splice form and the appearance of new splice forms that exclude exon 6a. Lane 4: PCR products of amplification after treatment with Col11a1a-MOe8, showing appearance of new splice forms that exclude exon 8. Lanes 5, 6, and 7: control and treatment at the 72 hpf time point demonstrate the transient effect of AMO treatment, showing that the splice patterns of the treated samples match the control. Size markers are indicated in basepairs on the left, while identity of the PCR bands is indicated on the right, referring to exons included as a result of alternative splicing. The identity of PCR products was confirmed by DNA sequencing.

Author Contributions

The following contributions were made: Conceptualization, J.T.O., J.S.A., M.F., J.C.R., and M.J.H.; methodology, M.F., J.S.A., J.C.R., and M.J.H.; validation, M.F., J.C.R., and M.J.H.; formal analysis, J.T.O., J.S.A., M.F., J.C.R., and M.J.H.; investigation, J.T.O., J.S.A., M.F., J.C.R., and M.J.H.; resources, J.T.O.; writing—original draft, review and editing, M.J.H. and J.T.O.; visualization, J.S.A., M.F., J.C.R.,

and M.J.H.; supervision, J.T.O.; funding acquisition, J.T.O. All authors have read and agreed to the published version of the manuscript.

Conflicts of Interest

The authors declare no conflict of interest.

References

1. Goldring, M.B.; Tsuchimochi, K.; Ijiri, K. The control of chondrogenesis. *J. Cell. Biochem.* **2006**, *97*, 33–44. [**Google Scholar**] [**CrossRef**] [**PubMed**]

2. Hall, B.K.; Miyake, T. Divide, accumulate, differentiate: Cell condensation in skeletal development revisited. *Int. J. Dev. Biol.* **1995**, *39*, 881–893. [**Google Scholar**] [**PubMed**]

3. Glenister, T.W. An embryological view of cartilage. *J. Anat.* **1976**, *122*, 323–330. [**Google Scholar**]

4. Zylińska, B.; Silmanowicz, P.; Sobczyńska-Rak, A.; Jarosz, Ł.; Szponder, T. Treatment of articular cartilage defects: Focus on tissue engineering. *In Vivo* **2018**, *32*, 1289–1300. [**Google Scholar**] [**CrossRef**] [**PubMed**]

5. Riley, B.B.; Phillips, B.T. Ringing in the new ear: Resolution of cell interactions in otic development. *Dev. Biol.* **2003**, *261*, 289–312. [**Google Scholar**] [**CrossRef**]

6. Whitfield, T.T.; Riley, B.B.; Chiang, M.Y.; Phillips, B. Development of the zebrafish inner ear. *Dev. Dyn.* **2002**, *223*, 427–458. [**Google Scholar**] [**CrossRef**]

7. Whitfield, T.T.; Granato, M.; Van Eeden, F.J.M.; Schach, U.; Brand, M.; Furutani-Seiki, M.; Haffter, P.; Hammerschmidt, M.; Heisenberg, C.P.; Jiang, Y.J.; et al. Mutations affecting development of the zebrafish inner ear and lateral line. *Development* **1996**, *123*, 241–254. [**Google Scholar**]

8. Nicolson, T. The Genetics of Hearing and Balance in Zebrafish. *Annu. Rev. Genet.* **2005**, *39*, 9–22. [**Google Scholar**] [**CrossRef**]

9. Stickler, G.B.; Belau, P.G.; Farrell, F.J.; Jones, J.D.; Pugh, D.G.; Steinberg, A.G.; Ward, L.E. Hereditary progressive artho-opthalmopathy. *Mayo Clin. Proc.* **1965**, *40*, 433–455. [**Google Scholar**]

10. Yelick, P.C.; Schilling, T.F. Molecular dissection of craniofacial development using zebrafish. *Crit. Rev. Oral Biol. Med.* **2002**, *13*, 308–322. [**Google Scholar**] [**CrossRef**]

11. Mundlos, S.; Olsen, B.R. Heritable diseases of the skeleton. Part II: Molecular insights into skeletal development-matrix components and their homeostasis. *FASEB J.* **1997**, *11*, 227–233. [**Google Scholar**] [**CrossRef**] [**PubMed**]

12. Todhunter, R.J.; Garrison, S.J.; Jordan, J.; Hunter, L.; Castelhano, M.G.; Ash, K.; Meyers-Wallen, V.; Krotscheck, U.; Hayward, J.J.; Grenier, J. Gene expression in hip soft tissues in incipient canine hip dysplasia and osteoarthritis. *J. Orthop. Res.* **2019**, *37*, 313–324. [**Google Scholar**] [**CrossRef**]

13. Marshall, D. Ectodermal dysplasia. Report of kindred with ocular abnormalities and hearing defect. *Am. J. Ophthalmol.* **1958**, *45*, 143–156. [**Google Scholar**] [**CrossRef**]

14. Chatterjee, S.; Lufkin, T. The Sound of Silence: Mouse Models for Hearing Loss. *Genet. Res. Int.* **2011**, *2011*, 1–9. [**Google Scholar**] [**CrossRef**]

15. Seegmiller, R.; Fraser, F.C.; Sheldon, H. A new chondrodystrophic mutant in mice. Electron microscopy of normal and abnormal chondrogenesis. *J. Cell Biol.* **1971**, *48*, 580–593. [**Google Scholar**] [**CrossRef**] [**PubMed**]

16. Cremers, C.W.R.J.; Cornelius, W.R.J.; Smith, R. *Genetic Hearing Impairment: Its Clinical Presentations*; Karger: Basel, Switzerland, 2002; ISBN 9783805574495. [**Google Scholar**]

17. Griffith, A.J.; Sprunger, L.K.; Sirko-Osadsa, D.A.; Tiller, G.E.; Meisler, M.H.; Warman, M.L. Marshall syndrome associated with a splicing defect at the COL11A1 locus. *Am. J. Hum. Genet.* **1998**, *62*, 816–823. [**Google Scholar**] [**CrossRef**] [**PubMed**]

18. Szymko-Bennett, Y.M.; Kurima, K.; Olsen, B.; Seegmiller, R.; Griffith, A.J. Auditory function associated with Col11a1 haploinsufficiency in chondrodysplasia (cho) mice. *Hear. Res.* **2003**, *175*, 178–182. [**Google Scholar**] [**CrossRef**]

19. Hufnagel, S.B.; Weaver, K.N.; Hufnagel, R.B.; Bader, P.I.; Schorry, E.K.; Hopkin, R.J. A novel dominant *COL11A1* mutation resulting in a severe skeletal

dysplasia. *Am. J. Med. Genet. Part A* **2014**, *164*, 2607–2612. [**Google Scholar**] [**CrossRef**]

20. Acke, F.R.E.; Dhooge, I.J.M.; Malfait, F.; De Leenheer, E.M.R. Hearing impairment in Stickler syndrome: A systematic review. *Orphanet J. Rare Dis.* **2012**, *7*, 84. [**Google Scholar**] [**CrossRef**]

21. Shoulders, M.D.; Raines, R.T. Collagen Structure and Stability. *Annu. Rev. Biochem.* **2009**, *78*, 929–958. [**Google Scholar**] [**CrossRef**]

22. Eyre, D. Collagen of articular cartilage. *Arthritis Res.* **2002**, *4*, 30–35. [**Google Scholar**] [**CrossRef**]

23. Ahmed, S.; Nowlan, N.C. Initiation and emerging complexity of the collagen network during prenatal skeletal development. *Eur. Cells Mater.* **2020**, *39*, 136–155. [**Google Scholar**] [**CrossRef**] [**PubMed**]

24. Jacenko, O.; Olsen, B.; LuValle, P. Organization and regulation of collagen genes. In *Critical Reviews in Eukaryotic Gene Expression*; Stein, G.S., Stein, J., Lians, J.B., Eds.; CRC Press: Boca Raton, FL, USA, 1991; Volume 1, pp. 327–353. [**Google Scholar**]

25. Eyre, D.R.; Wu, J.J.; Fernandes, R.J.; Pietka, T.A.; Weis, M.A. Recent developments in cartilage research: Matrix biology of the collagen II/IX/XI heterofibril network. *Biochem. Soc. Trans.* **2002**, *30*, 893–899. [**Google Scholar**] [**CrossRef**]

26. Mendler, M.; Eich-Bender, S.G.; Vaughan, L.; Winterhalter, K.H.; Bruckner, P. Cartilage contains mixed fibrils of collagen types II, IX, and XI. *J. Cell Biol.* **1989**, *108*, 191–197. [**Google Scholar**] [**CrossRef**] [**PubMed**]

27. Nah, H.D.; Barembaum, M.; Upholt, W.B. The chicken α1(XI) collagen gene is widely expressed in embryonic tissues. *J. Biol. Chem.* **1992**, *267*, 22581–22586. [**Google Scholar**]

28. Mayne, R.; Brewton, R.G.; Mayne, P.M.; Baker, J.R. Isolation and characterization of the chains of type V/type XI collagen present in bovine vitreous. *J. Biol. Chem.* **1993**, *268*, 9381–9386. [**Google Scholar**] [**PubMed**]

29. Fang, M.; Adams, J.S.; McMahan, B.L.L.; Brown, R.J.R.J.; Oxford, J.T. The expression patterns of minor fibrillar collagens during development in zebrafish. *Gene Expr. Patterns* **2010**, *10*, 315–322. [**Google Scholar**] [**CrossRef**]

30. Gagnon, J.A.; Valen, E.; Thyme, S.B.; Huang, P.; Ahkmetova, L.; Pauli, A.; Montague, T.G.; Zimmerman, S.; Richter, C.; Schier, A.F. Efficient mutagenesis by Cas9 protein-mediated oligonucleotide insertion and large-scale assessment of single-guide RNAs. *PLoS ONE* **2014**, *9*, e98186. [**Google Scholar**] [**CrossRef**]

31. Moradi-Améli, M.; Deléage, G.; Geourgjon, C.; van der Rest, M. Common topology within a non-collagenous domain of several different collagen types. *Matrix Biol.* **1994**, *14*, 233–239. [**Google Scholar**] [**CrossRef**]

32. Tisi, D.; Talts, J.; Timpl, R.; Hohenester, E. Structure of the C-terminal laminin G-like domain pair of the laminin α2 chain harbouring binding sites for α-dystroglycan and heparin. *EMBO J.* **2009**, *19*, 1432–1440. [**Google Scholar**] [**CrossRef**]

33. Timpl, R.; Tisi, D.; Talts, J.F.; Andac, Z.; Sasaki, T.; Hohenester, E. Structure and function of laminin LG modules. *Matrix Biol.* **2000**, *19*, 309–317. [**Google Scholar**] [**CrossRef**]

34. Hohenester, E.; Tisi, D.; Talts, J.F.; Timpl, R. The crystal structure of a laminin G-like module reveals the molecular basis of α-dystroglycan binding to laminins, perlecan, and agrin. *Mol. Cell* **1999**, *4*, 783–792. [**Google Scholar**] [**CrossRef**]

35. Fallahi, A.; Kroll, B.; Warner, L.R.; Oxford, R.J.; Irwin, K.M.; Mercer, L.M.; Shadle, S.E.; Oxford, J.T. Structural model of the amino propeptide of collagen XI alpha1 chain with similarity to the LNS domains. *Protein Sci.* **2005**, *14*, 1526–1537. [**Google Scholar**] [**CrossRef**]

36. Wälchi, C.; Trueb, J.; Kessler, B.; Winterhalter, K.H.; Trueb, B. Complete primary structure of chicken collagen XIV. *Eur. J. Biochem.* **1993**, *212*, 483–490. [**Google Scholar**] [**CrossRef**] [**PubMed**]

37. Bork, P. The modular architecture of vertebrate collagens. *FEBS Lett.* **1992**, *307*, 49–54. [**Google Scholar**] [**CrossRef**]

38. Tillet, E.; Mann, K.; Nischt, R.; Pan, T.-C.; Chu, M.-L.; Timpl, R. Recombinant Analysis of Human α1(XVI) Collagen: Evidence for Processing of the N-Terminal Globular Domain. *Eur. J. Biochem.* **1995**, *228*, 160–168. [**Google Scholar**] [**CrossRef**] [**PubMed**]

39. Inoguchi, K.; Yoshioka, H.; Khaleduzzaman, M.; Ninomiya, Y. The mrna for α1(XIX) collagen chain, a new member of FACITs, contains a long unusual 3′ untranslated region and displays many unique splicing variants. *J. Biochem.* **1995**, *117*, 137–146. [**Google Scholar**] [**CrossRef**]

40. Van Der Rest, M.; Garrone, R. Collagen family of proteins. *FASEB J.* **1991**, *5*, 2814–2823. [**Google Scholar**] [**CrossRef**]

41. Fang, M.; Jacob, R.; McDougal, O.; Oxford, J.T. Minor fibrillar collagens, variable regions alternative splicing, intrinsic disorder, and tyrosine sulfation. *Protein Cell* **2012**, *3*, 419–433. [**Google Scholar**] [**CrossRef**]

42. Tsumaki, N.; Kimura, T. Differential expression of an acidic domain in the amino-terminal propeptide of mouse pro-α2(XI) collagen by complex alternative splicing. *J. Biol. Chem.* **1995**, *270*, 2372–2378. [**Google Scholar**] [**CrossRef**]

43. Yoshioka, H.; Ramirez, F. Pro-alpha 1(XI) collagen. Structure of the amino-terminal propeptide and expression of the gene in tumor cell lines. *J. Biol. Chem.* **1990**, *265*, 6423–6426. [**Google Scholar**] [**PubMed**]

44. Gregory, K.E.; Oxford, J.T.; Chen, Y.; Gambee, J.E.; Gygi, S.P.; Aebersold, R.; Neame, P.J.; Mechling, D.E.; Bächinger, H.P.; Morris, N.P. Structural organization of distinct domains within the non-collagenous N-terminal region of collagen type XI. *J. Biol. Chem.* **2000**, *275*, 11498–11506. [**Google Scholar**] [**CrossRef**] [**PubMed**]

45. Zhidkova, N.I.; Justice, S.K.; Mayne, R. Alternative mRNA processing occurs in the variable region of the pro- α1(XI) and pro-α2(XI) collagen chains. *J. Biol. Chem.* **1995**, *270*, 9486–9493. [**Google Scholar**] [**CrossRef**]

46. Oxford, J.T.; Doege, K.J.; Morris, N.P. Alternative exon splicing within the amino-terminal nontriple-helical domain of the rat pro-α1(XI) collagen chain

generates multiple forms of the mRNA transcript which exhibit tissue-dependent variation. *J. Biol. Chem.* **1995**, *270*, 9478–9485. [**Google Scholar**] [**CrossRef**] [**PubMed**]

47. Hoffman, G.G.; Branam, A.M.; Huang, G.; Pelegri, F.; Cole, W.G.; Wenstrup, R.M.; Greenspan, D.S. Characterization of the six zebrafish clade B fibrillar procollagen genes, with evidence for evolutionarily conserved alternative splicing within the pro-α1(V) C-propeptide. *Matrix Biol.* **2010**, *29*, 261–275. [**Google Scholar**] [**CrossRef**] [**PubMed**]

48. Davies, G.B.; Oxford, J.T.; Hausafus, L.C.; Smoody, B.F.; Morris, N.P. Temporal and spatial expression of alternative splice-forms of the alpha1(XI) collagen gene in fetal rat cartilage. *Dev. Dyn.* **1998**, *213*, 12–26. [**Google Scholar**] [**CrossRef**]

49. Richards, A.J.; Martin, S.; Nicholls, A.C.; Harrison, J.B.; Pope, F.M.; Burrows, N.P. A single base mutation in COL5A2 causes Ehlers-Danlos syndrome type II. *J. Med. Genet.* **1998**, *35*, 846–848. [**Google Scholar**] [**CrossRef**]

50. Annunen, S.; Körkkö, J.; Czarny, M.; Warman, M.L.; Brunner, H.G.; Kääriäinen, H.; Mulliken, J.B.; Tranebjærg, L.; Brooks, D.G.; Cox, G.F.; et al. Splicing Mutations of 54-bp Exons in the COL11A1 Gene Cause Marshall Syndrome, but Other Mutations Cause Overlapping Marshall/Stickler Phenotypes. *Am. J. Hum. Genet.* **1999**, *65*, 974–983. [**Google Scholar**] [**CrossRef**] [**PubMed**]

51. Robin, N.H.; Moran, R.T.; Ala-Kokko, L. *Gene Reviews: Stickler Syndrome*; University of Washington: Seattle, WA, USA, 2017. [**Google Scholar**]

52. Seegmiller, R.E.; Foster, C.; Burnham, J.L. Understanding chondrodysplasia (cho): A comprehensive review of cho as an animal model of birth defects, disorders, and molecular mechanisms. *Birth Defects Res.* **2019**, *111*, 237–247. [**Google Scholar**] [**CrossRef**]

53. Schilling, T.F.; Walker, C.; Kimmel, C.B. The chinless mutation and neural crest cell interactions in zebrafish jaw development. *Development* **1996**, *122*, 1417–1426. [**Google Scholar**]

62

54. Newgreen, D.F.; Erickson, C.A. The migration of neural crest cells. *Int. Rev. Cytol.* **1986**, *103*, 89–145. [**Google Scholar**] [**PubMed**]

55. Perris, R.; Krotoski, D.; Bronner-Fraser, M. Collagens in avian neural crest development: Distribution in vivo and migration-promoting ability in vitro. *Development* **1991**, *113*, 969–984. [**Google Scholar**] [**PubMed**]

56. Lallier, T.; Leblanc, G.; Artinger, K.B.; Bronner-Fraser, M. Cranial and trunk neural crest cells use different mechanisms for attachment to extracellular matrices. *Development* **1992**, *116*, 531–541. [**Google Scholar**] [**PubMed**]

57. Maxwell, G.D. Substrate dependence of cell migration from explanted neural tubes in vitro. *Cell Tissue Res.* **1976**, *172*, 325–330. [**Google Scholar**] [**CrossRef**]

58. Seufert, D.W.; Hanken, J.; Klymkowsky, M.W. Type II collagen distribution during cranial development in Xenopus laevis. *Anat. Embryol.* **1994**, *189*, 81–89. [**Google Scholar**] [**CrossRef**]

CHAPTER THREE: AUTHENTICATION OF A NOVEL ANTIBODY TO

ZEBRAFISH COLLAGEN TYPE XI ALPHA ONE CHAIN (COL11A1A)

Jonathon C. Reeck[†], Makenna J. Hardy[†], Xinzhu Pu, Cynthia Keller-Peck, Julia Thom Oxford

[†] Co-first authors; Jonathon C. Reeck and Makenna J. Hardy equally contributed to first authorship.

Jonathon C. Reeck, Department of Biological Sciences, Biomolecular Sciences Graduate Program, and Biomolecular Research Center, Boise State University, Boise, ID 83725, USA, Email: jonathonreeck@u.boisestate.edu

Makenna J. Hardy, Biomolecular Sciences Graduate Program, Biomolecular Research Center, Boise State University, Boise, ID 83725, USA, Email: makennahardy@u.boisestate.edu

Xinzhu Pu, Biomolecular Research Center, Boise State University, Boise, ID 83725, USA, Email: shinpu@boisestate.edu

Cynthia Keller-Peck, Biomolecular Research Center, Boise State University, Boise, ID 83725, USA, Email: ckpeck@boisestate.edu

Julia Thom Oxford, Department of Biological Sciences, Biomolecular Sciences Graduate Program, and Biomolecular Research Center, Boise State University, Boise, ID 83725, USA, Email: joxford@boisestate.edu, Corresponding author

Abstract

Objective: Extracellular matrix proteins play important roles in embryonic development and antibodies that specifically detect these proteins are essential to understanding their function. The zebrafish embryo is a popular model for vertebrate development but suffers from a dearth of authenticated antibody reagents for research. Here, we describe a novel antibody designed to detect the minor fibrillar collagen chain Col11a1a in zebrafish (AB strain).

Results: The Col11a1a antibody was raised in rabbit against a peptide comprising a unique sequence within the zebrafish Col11a1a gene product. The antibody was affinity-purified and characterized by ELISA. The antibody is effective for immunoblot and immunohistochemistry applications. Protein bands identified by immunoblot were confirmed by mass spectrometry and sensitivity to collagenase. Col11a1a knockout zebrafish were used to confirm specificity of the antibody. The Col11a1a antibody labeled cartilaginous structures within the developing jaw, consistent with previously characterized Coll11a1 antibodies in other species. Col11a1a within formalin-fixed paraffin-embedded zebrafish were recognized by the antibody. The antibodies and the approaches described here will help to address the lack of well-defined antibody reagents in zebrafish research.

Keywords: Collagen α1(XI), Col11a1a, Col11a1a, cartilage, vertebrate development, zebrafish, antibody authentication, immunoblot, immunofluorescence microscopy

Introduction

The extracellular matrix (ECM) plays a key role during embryonic development [1–5], and the minor fibrillar collagens play regulatory roles in collagen assembly and structural integrity of connective tissues [6–11]. While progress has been made on the documentation of ECM protein expression patterns within the developing embryo by *in situ* hybridization, such information does not always indicate the location of the resulting protein within tissue [6,8]. This is a particularly important limitation for secreted proteins of the ECM that have long half-lives, making specific antibodies essential reagents for ECM research.

Collagen type XI is a trimeric molecule consisting of α1, α2, and α3 chains. The α1(XI) and α2(XI) chains possess unique amino terminal domains (NTD) that contain an amino propeptide and a variable region, and can be retained at the surface of collagen fibrils for an extended period of time. Collagens persist in tissues for long periods of time [12,13], and undergo post transcriptional and post translational modifications such as alternative splicing of the primary transcript, proteolytic cleavage of the procollagen, and post translational modifications [14,15] that add to complexity. The development of novel and specific research tools such as antibodies are essential to accurately monitor tissue changes, both temporally and spatially [12,16].

The fibril structure of collagens creates a challenge for accessing epitopes for immunolocalization studies. Additionally, sequence conservation among all collagens increases the challenge associated with the design and development of novel and robust antibodies for research focused on the role of fibrillar collagens [17,18]. However, the NTD of minor fibrillar collagens offers attractive targets for specific protein recognition

[11,16,19,20]. The location and slow proteolytic processing make the NTD a suitable epitope target for antibody-based detection.

Zebrafish, a model vertebrate organism [21], offer the advantages of optical transparency and *ex utero* development [22]. One limitation, however, is the paucity of antibody reagents for zebrafish ECM proteins. Here we describe antigen selection and antibody development of a novel Col11a1a antibody. Antibody validation is a critical component of research as indicated by NIH guidelines to assure rigor and reproducibility for key biological resources [23–25].

Methods

<u>Zebrafish Husbandry</u>

This study was performed with the approval of the Institutional Animal Care and Use Committee (IACUC) protocols AC18-014 and AC18-15 at Boise State University. Zebrafish (AB strain) were housed under standard laboratory conditions [26]. Developmental staging was reported as hours post-fertilization (hpf) at 28.5°C. Embryos were raised in egg water (pH 7.2) [26]. CRISPR/Cas9 was used to knockout Col11a1a expression. Full knockout was lethal in the majority of offspring; therefore, a heterozygous fish line was created by outbreeding with wildtype fish. Heterozygous crosses were used in addition to wildtype to validate the antibody. All mutant embryos were humanely euthanized at 72 hpf before nervous system development occurred. No animals were excluded during this study. Potential confounders were not controlled. A total number of 40 animals were used in this study.

Antibody design and development

Antibodies were generated using the peptide sequence NH_2-ck(g)$_9$dvphkdtlqa-COOH conjugated to keyhole limpet hemocyanin. Antibody production was outsourced to Bethyl Laboratories, Inc. According to Bethyl Laboratories, rabbits were immunized, and sera were collected. Sequential bleeds were screened by ELISA against the peptide to determine titer. Antibodies were affinity purified, concentrated, and stored at -20°C upon arrival.

Protein isolation and detection by immunoblot

Wildtype, heterozygotes (Col11a1a$^{+/-}$) and homozygotes (Col11a1a$^{-/-}$) embryos were used for protein isolation and detection by immunoblot. Each experimental group contained 20 embryos for sufficient protein extraction. Embryos were dechorionated using 1 mg/mL pronase at room temperature then rinsed in Ringer's solution. Embryos were treated with ethylenediamine tetraacetic acid (EDTA) and protease/phosphatase inhibitor cocktail (Thermo Fisher Scientific) in Ringer's and passed through a glass pipette to remove the yolk.

Samples were processed as previously described [27] with modification. In brief, samples previously fixed in 4% paraformaldehyde (PFA) were incubated in 2% sodium dodecyl sulfate (SDS) at 95°C for 30 min and 60°C for 2 hours to reverse PFA fixation. The embryos were pelleted by centrifugation for 20 min at 5000 x g and the supernatant was removed. De-yolked embryos were homogenized in SDS sample buffer with a microfuge pestle, boiled, and centrifuged to clarify the extract. Extracted proteins were separated on a 4-12% gradient bis-Tris gel and transferred to polyvinylidene difluoride membranes and blocked for 60 min at room temperature. Membranes were rinsed with

Tween-20 Tris buffered saline (TTBS) 3 x 5 min. Primary antibody was added to the membrane in TTBS with 5% bovine serum albumin and incubated overnight at 4°C with constant rocking. For peptide blocking experiments, the peptide was added to the primary antibody solution and agitated for 1 hour before adding to the membrane. The primary antibody solution was decanted, and unbound antibody was removed by rinsing the membrane with TTBS 3 x 5 min. Secondary antibody conjugated to horseradish peroxidase was added to the membrane and rocked at room temperature for one hour. The secondary antibody was decanted, and the membrane washed 3 x 5 min with TTBS. Enhanced chemiluminescence reagent was added to the membrane and imaged on a FluorChem E Digital Darkroom.

LC-MS/MS-based protein sequence analysis

LC-MS/MS analysis was performed using methods established previously [28] with modifications. Briefly, excised gel pieces were destained in 50% acetonitrile and 50mM NH_4HCO_3, followed by the treatment with dithiothreitol (10 mM) to reduce disulfide bonds and iodoacetamide (55 mM) for alkylation and then digested with proteomics grade trypsin (Thermo Fisher Scientific, Waltham, MA, USA) overnight at 37°C. Peptides were extracted, dried under vacuum, and reconstituted in 5% acetonitrile and 0.1% formic acid. Tryptic peptides were analyzed on a Velos Pro Dual-Pressure Linear Ion Trap mass spectrometer equipped with a nano electrospray ionization source and coupled with an Easy-nLC II nano LC system (Thermo Fisher Scientific, Waltham, MA, USA).

Peptide spectral matching and protein identification were achieved by database search using Sequest HT algorithms in Proteome Discoverer 2.2 (Thermo Fisher

Scientific). Raw spectrum data were searched against the UniProtKB/Swiss-Prot protein database for Zebrafish (downloaded from www.uniprot.org on September 8, 2020). Search parameters included: trypsin, maximum missed cleavage site of two, precursor mass tolerance of 1.5 Da, fragment mass tolerance of 0.8 Da, fixed modification of cysteine carbamidomethylation (+57.021 Da), and variable modification of oxidation/hydroxylation of methionine, proline, and lysine (+15.995Da). Decoy database search was performed to calculate false discovery rate (FDR). Proteins containing two or more peptides with FDR≤0.01were considered positively identified.

Immunofluorescence

Wildtype, heterozygotes (Col11a1a$^{+/-}$) and homozygotes (Col11a1a$^{-/-}$) embryos were used for immunofluorescence analysis. Each experimental group contained 15 embryos. Zebrafish embryos were fixed in 4% PFA and embedded in paraffin prior to sectioning. Samples were cut into 10 micrometer sections. Sections were deparaffinized in xylenes and rehydrated in a graded alcohol series. Sections were rinsed with 0.1% Tween-20 in PBS and Triton X-100 at room temperature. Blocking was performed in 5% goat serum and 2% Tween-20 in PBS for one hour. Primary antibodies were diluted in blocking solution and samples were incubated at 4ºC overnight. Secondary antibody was diluted 1:200 in blocking solution and applied to samples overnight in the dark. ProlongTM Gold antifade mountant with DAPI (Fisher Scientific) was used to mount the coverslip. Samples were imaged on a Zeiss LSM 510 Meta confocal microscope.

Results

<u>Epitope selection</u>

We identified a unique sequence within the zebrafish collagen α1(XI) protein corresponding to the NTD [29–31]. This sequence is encoded by exon 5, preceding the start of the variable region (**Figure 1**).

<u>Immunoblot analysis</u>

We tested the specificity of the antibody against protein extracted from whole zebrafish lysates by immunoblot. The antibody recognized protein bands with apparent molecular weights of 100 kDa and 35 kDa from total lysate collected from embryos at 24 hpf. Collagenase treatment of an ECM extract resulted in the disappearance of the 100 kDa band and a concomitant generation of a protein band with an apparent molecular weight of 35 kDa **Figure 2A**.
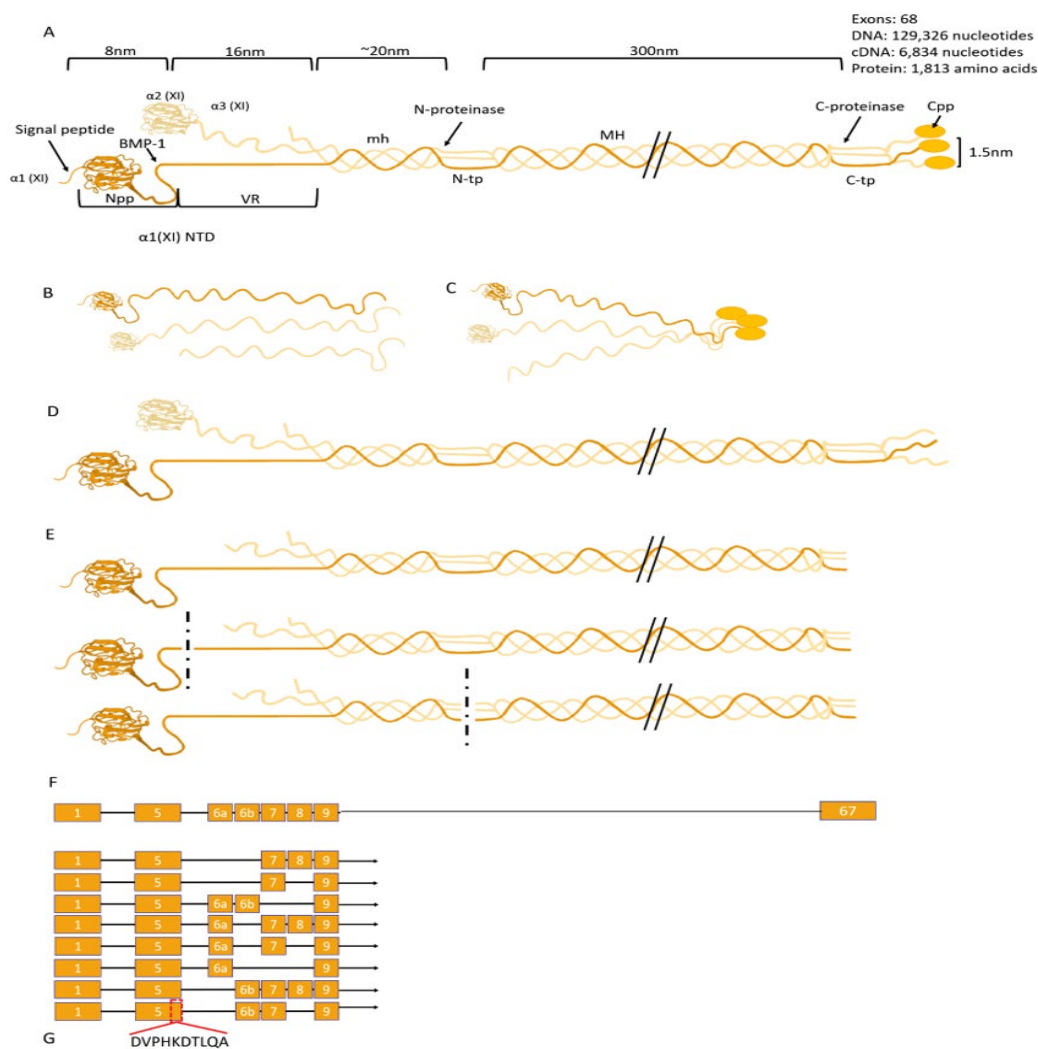
Figure 3.1.   Model of Collagen type XI.
A) Collagen type XI molecule. Structural regions of the type XI collagen molecule are indicated including the signal peptide, amino terminal propeptide, variable region, the minor helix, the amino telopeptide, the major triple helix, the carboxy telopeptide, and the carboxy propeptide. Relative size and dimensions are shown above the molecular model. B) Three alpha chains: α1(XI), α2(XI), and α3(XI) C) Formation of triple helical molecule is initiated at the C-terminus. D) Fully assembled triple helical collagen molecule with carboxy propeptide. E) Potential cleavage events, with carboxy propeptide removed, with amino propeptide removed at the BMP-1 cleavage site (35 kDa), and finally, with the ADAMTS2 cleavage site within the amino telopeptide indicated by the vertical dotted line that would release the major triple helix and generate a fragment containing the amino propeptide and variable region (100kDa). F) Exon structure of Col11a1a, indicating alternatively spliced isoforms. G) Epitope sequence unique to the new antibody. This sequence is encoded by exon 5 which is present in all spliceforms. Abbreviations: amino terminal domain (NTD); amino propeptide domain (Npp); variable region (VR); minor helix (mh); amino telopeptide (N-tp); major triple helix (MH); carboxy telopeptide (C-tp); carboxy propeptide (Cpp).

The antibody recognized the peptide originally used to generate the antibody under the conditions of the immunoblot, as indicated by observed competition by the peptide and abolition of the detection of protein bands at 100 kDa and 35 kDa (**Figure 2A**).

Protein sequence analysis

The protein bands identified by immunoblot were excised from the gel and submitted for mass spectrometry to confirm identity of the proteins by sequencing (**Figure 2**). Mass spectrometry results of the band migrating with an apparent molecular weight of 100 kDa identified peptides from the NTD of Col11a1a. The NTD peptides were also identified in a band with an apparent molecular weight of 35 kDa (**Figure 2B-C**).

Specificity of Col11a1a antibody

To confirm antibody specificity, we tested the antibody on proteins extracted from Col11a1a knockout zebrafish. Immunoblot indicated a lower expression of Col11a1a in heterozygous embryos and no expression in knockout homozygous embryos. Full length and the fragment of Col11a1a was observed in wildtype and heterozygous embryos while knockout embryos displayed no Col11a1a protein expression (**Figure 2D**).
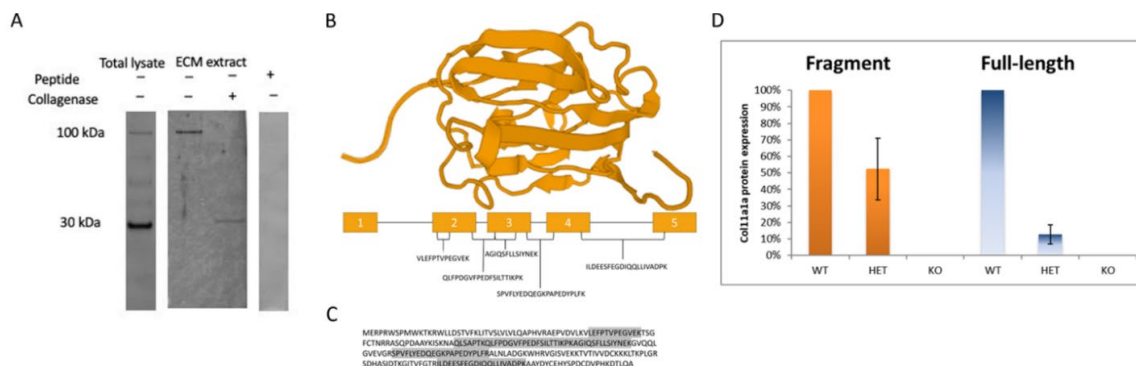
Figure 3.5.   Antibody detection of Col11a1a protein by immunoblot and confirmed by mass spectrometry.

A) The antibody recognized protein bands migrating with apparent molecular weights of 100 and 35 kDa from zebrafish total lysate. Proteins extracted from the ECM contained the 100 kDa that was converted to a 35 kDa band upon treatment with collagenase. In the presence of a large excess of the peptide used as the antigen, the 100 kDa and 35 kDa bands from total lysate are not visible on the immunoblot, supporting competition by the peptide for the antigen binding site on the antibody. B) Structural model of the amino propeptide domain of Col11a1a. Peptides detected by mass spectrometry are indicated in their respective locations of the exons encoding the protein. C) Protein sequence of Col11a1a amino propeptide domain with grey shading indicates the sequence coverage used to confirm the identity of the protein recognized by the new antibody as Col11a1a. D) Quantification of immunoblot band intensity from proteins extracted from wildtype (WT), heterozygotes, and homozygous knockout embryos. The NTD fragment and full-length molecule were quantified by densitometry. Absence of these protein bands from homozygous knockout embryos confirmed specificity of the new antibody. Abbreviations: wildtype (WT); heterozygous (HET); knockout (KO).

Immunohistochemistry

We confirmed that the antibody recognized tissues in which expression of collagen type XI is well established. The antibody specifically labeled cartilage within the jaw and eye structures at 72 hpf (**Figure 3**).
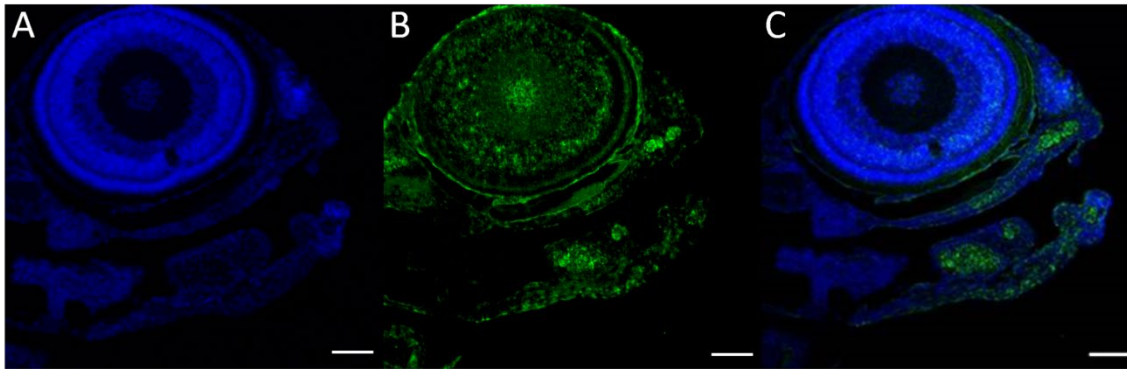
Figure 3.6. Immunohistochemistry demonstrating location of Col11a1a within developing craniofacial region (72 hpf).
Zebrafish embryos were fixed, embedded, and sectioned for immunofluorescence detection of Col11a1a using the new antibody. A) DAPI staining indicates the location of nuclei; B) Col11a1a primary antibody detects Col11a1a in the eye and within the jaw cartilage. C) Merge of panels A and B. Scale bar = 50 µm.

Discussion

Collagens are essential molecules for establishing tissue morphology during embryological development. Our goal was to develop an antibody recognizing Col11a1a of zebrafish. We chose an epitope that was unique to zebrafish Col11a1a within the NTD of Col11a1a that could be used for both immunoblotting and immunohistochemistry. The detection of a protein migrating with an apparent molecular weight of 100 kDa is consistent with a fragment generated by proteolytic cleavage by ADAMTS2 (ADAM (A Disintegrin And Metalloproteinases) Metallopeptidase with Thrombospondin Type 1 Motif 2) within the amino telopeptide [31,32]. The recognition of the 35 kDa protein band is consistent with a released NTD fragment upon collagenase digestion to remove the minor helix or alternatively, proteolytic processing by bone morphogenetic protein-1 (BMP-1) [31,33,34]. Together, these results support the utility of the new antibody to recognize biologically relevant forms of Col11a1a in the zebrafish embryo.

Mass spectrometry results identified peptides unique to Col11a1a in bands identified by the new antibody, supporting future investigations of collagens during

development [35,36]. Important aspects of the molecular processing of procollagens that results in mature collagens [37,38] and the fates of fragments [39] may be enabled by this antibody. Additionally, this antibody may facilitate the localization of collagens in tissues such as skin, bones and ligaments [40–43]. The epitope recognized by the new antibody is unique to zebrafish Col11a1a and the antibody did not recognize other collagen types. Immunoblot analysis of Col11a1a knockouts confirmed specificity of the Col11a1a antibody.

Tissue staining within the eye and craniofacial cartilage of the jaw at 72 hpf is consistent with results from other species [40]. The Col11a1 chondrodystrophic (cho) mouse is characterized by deficiencies in chondrogenesis including in the craniofacial skeleton [40,44]. Human disorders such as type 2 Stickler syndrome due to a mutation in COL11A1, display a smaller jaw, high myopia, and retinal detachment [18,45–47].

Collagen type XI nucleates and limits the diameter of collagen type II fibrils and interacts with non-collagenous molecules. Previous studies demonstrated severe changes in the ECM and collagen networks when Col11a1a was knocked down in zebrafish [1,18]. Additionally, Col11a1 mutations in the cho mouse show disordered chondrocytes and collagen fibrils in the growth plate [40–43].

We have generated a novel tool for monitoring changes in Col11a1a synthesis and localization in zebrafish tissue during embryonic development. We show that the antibody is useful for immunoblot and immunohistochemistry and confirmed the expression in cartilage of the developing skeleton as would be expected for collagen type XI. Future studies will rely on this antibody to investigate zebrafish models for syndromic and nonsyndromic congenital disease and diseases associated with aging.

Limitations

- As expected, additional collagens were found to migrate with apparent molecular weight of approximately 100 kDa specifically, collagen XIIα1, however, this collagen does not contain the peptide epitope and recognition by the antibody is unlikely.

- Classification of homozygous and heterozygous offspring was performed visually based on severity of observed phenotype. It is possible that some more severely affected heterozygous embryos were classified as homozygous knockouts, leading to low levels of Col11a1a present in protein extracts from the homozygous knockout group. However, based on original homozygous embryo data before outcrossing, we feel confident in our ability to distinguish between homozygous knockouts and heterozygous knockdown mutant groups.

Declarations

Ethics Approval and Consent to Participants

This study was performed with the approval of the Institutional Animal Care and Use Committee (IACUC) protocols AC18-014 and AC18-015 at Boise State University.

Consent for Publication

Not applicable.

Availability of Data and Materials

The datasets used and/or analyzed during the current study are available from corresponding author on request.

Competing Interests

The authors declare that they have no competing interests.

Authors' Contributions

Jonathon Reeck and Julia Thom Oxford conceived and designed the approach; Jonathon Reeck prepared the first draft and Makenna Hardy prepared subsequent drafts, figures. Xinxhu Pu carried out mass spectrometry; Cynthia Keller-Peck performed histological embedding and sectioning. All authors approved final edits. All authors have contributed substantially to the work reported.

References

1.   Baas D, Malbouyres M, Haftek-Terreau Z, le Guellec D, Ruggiero F. Craniofacial cartilage morphogenesis requires zebrafish col11a1 activity. Matrix Biology [Internet]. 2009 [cited 2021 Mar 14];28(8):490–502. Available from: https://pubmed.ncbi.nlm.nih.gov/19638309/

2.   Bootorabi F, Manouchehri H, Changizi R, Barker H, Palazzo E, Saltari A, et al. Zebrafish as a model organism for the development of drugs for skin cancer [Internet]. Vol. 18, International Journal of Molecular Sciences. MDPI AG; 2017 [cited 2021 Mar 14]. Available from: /pmc/articles/PMC5536038/

3.   Vacaru AM, Unlu G, Spitzner M, Mione M, Knapik EW, Sadler KC. In vivo cell biology in zebrafish - providing insights into vertebrate development and disease. Journal of Cell Science [Internet]. 2014 Feb 1 [cited 2021 Mar 14];127(3):485–95. Available from: http://zfin.

4.   Rahman Khan F, Sulaiman Alhewairini S. Zebrafish (Danio rerio) as a Model Organism . In: Current Trends in Cancer Management [Internet]. IntechOpen; 2019 [cited 2021 Mar 14]. Available from: www.intechopen.com

5.   Veldman MB, Lin S. Zebrafish as a developmental model organism for pediatric research [Internet]. Vol. 64, Pediatric Research. Nature Publishing Group; 2008 [cited 2021 Mar 14]. p. 470–6. Available from: http://zfin.org/zf_info/zfbook/zfbk.html

6.   Warner LR, Blasick CM, Brown RJ, Oxford JT. Expression, purification, and refolding of recombinant collagen α1(XI) amino terminal domain splice variants. Protein Expression and Purification [Internet]. 2007 Apr [cited 2021 Mar 14];52(2):403–9. Available from: /pmc/articles/PMC2713663/

7.   Truscott RJW, Schey KL, Friedrich MG. Old Proteins in Man: A Field in its Infancy [Internet]. Vol. 41, Trends in Biochemical Sciences. Elsevier Ltd; 2016 [cited 2021 Mar 14]. p. 654–64. Available from: /pmc/articles/PMC5500981/

8.   Warner LR, Brown RJ, Yingst SMC, Oxford JT. Isoform-specific heparan sulfate binding within the amino-terminal noncollagenous domain of collagen α1(XI).

Journal of Biological Chemistry [Internet]. 2006 Dec 22 [cited 2021 Mar 14];281(51):39507–16. Available from: /pmc/articles/PMC2948787/

9. Lodish H, Berk A, Zipursky SL, Matsudaira P, Baltimore D, Darnell J. Collagen: The Fibrous Proteins of the Matrix. Molecular Cell Biology [Internet]. 2000 [cited 2021 Mar 14]; Available from: https://www.ncbi.nlm.nih.gov/books/NBK21582/

10. Exposito JY, Valcourt U, Cluzel C, Lethias C. The fibrillar collagen family [Internet]. Vol. 11, International Journal of Molecular Sciences. Multidisciplinary Digital Publishing Institute (MDPI); 2010 [cited 2021 Mar 14]. p. 407–26. Available from: /pmc/articles/PMC2852846/

11. Bierbaum S, Hintze V, Scharnweber D. 2.8 Artificial extracellular matrices to functionalize biomaterial surfaces. In: Comprehensive Biomaterials II. Elsevier; 2017. p. 147–78.

12. Lee BS, Huang JS, Jayathilaka LP, Lee J, Gupta S. Antibody production with synthetic peptides. In: Methods in Molecular Biology [Internet]. Humana Press Inc.; 2016 [cited 2021 Mar 11]. p. 25–47. Available from: https://pubmed.ncbi.nlm.nih.gov/27515072/

13. Trier N, Hansen P, Houen G. Peptides, antibodies, peptide antibodies and more [Internet]. Vol. 20, International Journal of Molecular Sciences. MDPI AG; 2019 [cited 2021 Mar 11]. Available from: /pmc/articles/PMC6941022/

14. Yoshioka H, Sumiyoshi H, Iyama K-I, Matsuo N. Alternative splicing of collagen genes that express in cartilage. Connective Tissue. 2002;34:157–63.

15. Richards AJ, Snead MP. The influence of pre-mRNA splicing on phenotypic modification in Stickler's syndrome and other type II collagenopathies. In: Eye [Internet]. Nature Publishing Group; 2008 [cited 2021 Mar 11]. p. 1243–50. Available from: www.nature.com/eye

16. Yamauchi M, Sricholpech M. Lysine post-translational modifications of collagen. Essays in Biochemistry [Internet]. 2012 [cited 2021 Mar 11];52(1):113–33. Available from: /pmc/articles/PMC3499978/

17. Toyama BH, Savas JN, Park SK, Harris MS, Ingolia NT, Yates JR, et al. Identification of long-lived proteins reveals exceptional stability of essential cellular structures. Cell [Internet]. 2013 Aug 29 [cited 2021 Mar 11];154(5):971–82. Available from: /pmc/articles/PMC3788602/

18. Hardy MJ, Reeck JC, Fang M, Adams JS, Oxford JT. Col11a1a expression is required for zebrafish development. Journal of Developmental Biology [Internet]. 2020 Sep 1 [cited 2021 Mar 17];8(3). Available from: https://pubmed.ncbi.nlm.nih.gov/32872105/

19. Fang M, Adams JS, Memahhan BL, Brown RJ, Oxford J. The Expression Patterns of Minor Fibrillar Collagens During Development in Zebrafish. Gene Expr Patterns. 2010;

20. Latimer A, Jessen JR. Extracellular matrix assembly and organization during zebrafish gastrulation. Matrix Biology. 2010 Mar 1;29(2):89–96.

21. Eyre D. Collagen of articular cartilage [Internet]. Vol. 4, Arthritis Research. BioMed Central; 2002 [cited 2021 Mar 11]. p. 30–5. Available from: /pmc/articles/PMC128915/

22. Heinegård D, Saxne T. The role of the cartilage matrix in osteoarthritis [Internet]. Vol. 7, Nature Reviews Rheumatology. Nat Rev Rheumatol; 2011 [cited 2021 Mar 11]. p. 50–6. Available from: https://pubmed.ncbi.nlm.nih.gov/21119607/

23. NOT-OD-16-004: NIH & AHRQ Announce Upcoming Changes to Policies, Instructions and Forms for 2016 Grant Applications [Internet]. [cited 2021 Apr 6]. Available from: https://grants.nih.gov/grants/guide/notice-files/NOT-OD-16-004.html

24. NOT-OD-16-011: Implementing Rigor and Transparency in NIH & AHRQ Research Grant Applications [Internet]. [cited 2021 Apr 6]. Available from: https://grants.nih.gov/grants/guide/notice-files/NOT-OD-16-011.html

25. NOT-OD-16-012: Implementing Rigor and Transparency in NIH & AHRQ Career Development Award Applications [Internet]. [cited 2021 Apr 6]. Available from: https://grants.nih.gov/grants/guide/notice-files/NOT-OD-16-012.html

26. Westerfield M. ZFIN: Zebrafish Book: Contents [Internet]. The zebrafish book. A guide for the laboratory use of zebrafish (Danio rerio). 4th ed., Univ. of Oregon Press, Eugene. 1993 [cited 2020 Sep 14]. Available from: https://zfin.org/zf_info/zfbook/zfbk.html

27. Gordon A, Kannan K, Gousset K. A Novel Cell Fixation Method that Greatly Enhances Protein Identification in Microproteomic Studies Using Laser Capture Microdissection and Mass Spectrometry. Proteomics. 2018;18(11).

28. Luo Y, Sinkeviciute D, He Y, Karsdal M, Henrotin Y, Mobasheri A, et al. The minor collagens in articular cartilage [Internet]. Vol. 8, Protein and Cell. Higher Education Press; 2017 [cited 2021 Mar 11]. p. 560–72. Available from: https://pubmed.ncbi.nlm.nih.gov/28213717/

29. Arseni L, Lombardi A, Orioli D. From structure to phenotype: Impact of collagen alterations on human health [Internet]. Vol. 19, International Journal of Molecular Sciences. MDPI AG; 2018 [cited 2021 Mar 16]. Available from: /pmc/articles/PMC5983607/

30. Bekhouche M, Colige A. The procollagen N-proteinases ADAMTS2, 3 and 14 in pathophysiology. Vols. 44–46, Matrix Biology. Elsevier; 2015. p. 46–53.

31. Medeck RJ, Sosa S, Morris N, Oxford JT. BMP-1-mediated proteolytic processing of alternatively spliced isoforms of collagen type XI. Biochemical Journal. 2003 Dec 1;376(2):361–8.

32. Mowbray C, Hammerschmidt M, Whitfield TT. Expression of BMP signalling pathway members in the developing zebrafish inner ear and lateral line. 2001;108:179–84.

33. Nah HD, Swoboda B, Birk DE, Kirsch T. Type IIA procollagen: Expression in developing chicken limb cartilage and human osteoarthritic articular cartilage. Developmental Dynamics. 2001;220(4):307–22.

34. Zhu Y, Mcalinden A, Sandell LJ. Type IIA procollagen in development of the human intervertebral disc: Regulated expression of the NH2-propeptide by enzymic processing reveals a unique developmental pathway. Developmental

Dynamics [Internet]. 2001 Apr 1 [cited 2021 Mar 17];220(4):350–62. Available from: http://doi.wiley.com/10.1002/dvdy.1115

35.   Canty EG, Kadler KE. Procollagen trafficking, processing and fibrillogenesis [Internet]. Vol. 118, Journal of Cell Science. The Company of Biologists Ltd; 2005 [cited 2021 Mar 17]. p. 1341–53. Available from: https://jcs.biologists.org/content/118/7/1341

36.   Ricard-Blum S. The Collagen Family. Cold Spring Harbor Perspectives in Biology [Internet]. 2011 Jan [cited 2021 Mar 17];3(1):1–19. Available from: /pmc/articles/PMC3003457/

37.   Gelse K, Pöschl E, Aigner T. Collagens-structure, function, and biosynthesis. Adv Drug Deliv Rev [Internet]. 2003 [cited 2021 Mar 17];55(12):1531–46. Available from: www.elsevier.com/locate/addr

38.   Trackman PC. Diverse biological functions of extracellular collagen processing enzymes. Journal of Cellular Biochemistry [Internet]. 2005 Dec 1 [cited 2021 Mar 17];96(5):927–37. Available from: /pmc/articles/PMC1352157/

39.   Wu J-J, Weis MA, Kim LS, Eyre DR. Type III Collagen, a Fibril Network Modifier in Articular Cartilage *. Journal of Biological Chemistry. 2010;285(24):18537–44.

40.   Hafez A, Squires R, Pedracini A, Joshi A, Seegmiller RE, Oxford JT. Col11a1 regulates bone microarchitecture during embryonic development. Journal of Developmental Biology [Internet]. 2015 Dec 1 [cited 2021 Mar 17];3(4):158–76. Available from: /pmc/articles/PMC4711924/

41.   Li Y, Lacerda DA, Warman ML, Beier DR, Yoshioka H, Ninomiya Y, et al. A fibrillar collagen gene, Col11a1, is essential for skeletal morphogenesis. Cell [Internet]. 1995 Feb 10 [cited 2021 Mar 16];80(3):423–30. Available from: https://pubmed.ncbi.nlm.nih.gov/7859283/

42.   Seegmiller R, Fraser FC, Sheldon H. A new chondrodystrophic mutant in mice: Electron microscopy of normal and abnormal chondrogenesis. Journal of Cell Biology. 1971 Mar 1;48(3):580–93.

43.   Seegmiller RE, Foster C, Burnham JL. Understanding chondrodysplasia (cho): A comprehensive review of cho as an animal model of birth defects, disorders, and molecular mechanisms [Internet]. Vol. 111, Birth Defects Research. John Wiley and Sons Inc.; 2019 [cited 2021 Mar 16]. p. 237–47. Available from: https://pubmed.ncbi.nlm.nih.gov/30719872/

44.   Lavrin IO, McLean W, Seegmiller RE, Olsen BR, Hay ED. The mechanism of palatal clefting in the Col11a1 mutant mouse. Archives of Oral Biology. 2001 Sep 1;46(9):865–9.

45.   Nixon T, Richards AJ, Lomas A, Abbs S, Vasudevan P, McNinch A, et al. Inherited and de novo biallelic pathogenic variants in COL11A1 result in type 2 Stickler syndrome with severe hearing loss. Molecular Genetics and Genomic Medicine [Internet]. 2020 Sep 1 [cited 2021 Mar 17];8(9):1354. Available from: /pmc/articles/PMC7507023/

46.   Higuchi Y, Hasegawa K, Yamashita M, Tanaka H, Tsukahara H. A novel mutation in the COL2A1 gene in a patient with Stickler syndrome type 1: A case report and review of the literature. Vol. 11, Journal of Medical Case Reports. BioMed Central Ltd.; 2017.

47.   Richards AJ, McNinch A, Martin H, Oakhill K, Rai H, Waller S, et al. Stickler syndrome and the vitreous phenotype: Mutations in COL2A1 and COL11A1. Human Mutation [Internet]. 2010 Jun [cited 2021 Mar 17];31(6). Available from: https://pubmed.ncbi.nlm.nih.gov/20513134/

CHAPTER FOUR: DEVELOPING OTIC SENSORY HAIR CELLS EXPRESS MINOR

FIBRILLAR COLLAGEN COL11A1A IN AN EMBRYONIC ZEBRAFISH MODEL

SYSTEM

Makenna J. Hardy[1,2], Jonathon C. Reeck[1,2], William Bourland[3], Ming Fang[1,3], Julia Oxford[1,2,3,4,*]

[1] Biomolecular Research Center; Boise State University, Boise, ID 83725 USA

[2] Biomolecular Sciences Graduate Program; Boise State University, Boise, ID 83725 USA

[3] Department of Biological Sciences, Boise State University, Boise, ID 83725 USA

[4] Center of Biomedical Research Excellence in Matrix Biology, Boise State University, Boise, ID 83725 USA

[*]Correspondence: joxford@boisestate.edu; Tel: +1-208-426-2395

Abstract

Sensory hair cells are responsible for mechanotransduction in hearing and balance function. Mutations and single nucleotide polymorphisms in the gene encoding Collagen XI alpha one chain (COL11A1) protein can play a role in hearing and balance dysfunction in humans as seen in disorders such as Stickler Type 2 and Marshall Syndrome, and nonsyndromic hearing loss DFNA37. Here, we address the role of the COL11A1 zebrafish orthologue Col11a1a in otic development and structure. *In situ* hybridization, immunofluorescence, and scanning electron microscopy techniques were implemented to observe normal Col11a1a expression. We found that Col11a1a was expressed in the developing otic vesicles by *in situ* hybridization. Col11a1a protein was localized to the sensory hair cells. Knockdown and knockout models of Col11a1a resulted in abnormal numbers of otoliths and shortened kinocilia. This research highlights the importance of Col11a1a in the development and structure of the inner ear as a whole including the hair cells, kinocilia, and otolith formation.

Keywords: collagen, zebrafish, inner ear, balance

1. Introduction

The inner ear is essential to maintaining balance and hearing. The hearing component of the inner ear contains the semicircular canals and the cochlea. Similarly, the semicircular canals, saccule, and utricle contribute to balance maintenance [1–6]. Hair cells are found in the cochlea and along the semicircular canals, saccule, and utricle. Each of these sensory hair bundles consist of rows of actin-containing stereocilia and one microtubule-containing kinocilia [1–4]. Tethering links between stereocilia and the kinocilia allow the cilia to move together, which is sensed by the hair cell, which sends

hearing signals through nerves [7,8]. Dysfunction of hair cells lead to hearing and balance complications.

The molecular basis for a link between hair cell dysfunction and complications with hearing and balance can be the extracellular matrix (ECM) molecule, collagen [9]. Collagen has been characterized in the nervous system including the innervated regions of vertebrates, the spinal cord, and the ear [9,10]. Collagen type XI is an essential minor fibrillar collagen in cartilaginous tissues and provides structure during development by nucleating the fibrillogenesis process and limiting the final diameter of collagen fibers [11–14]. Collagen type XI is found within the fluid of the inner ear and mutations of Collagen type XI alpha 2 chain (COL11A2) have been reported to cause an increase in auditory thresholds, and abnormal structure of the tectorial membrane [15]. However, little is known about the function of Collagen type XI alpha 1 chain (COL11A1) in the ear. According to limited literature, the family member COL11A1 is assumed to be present in the inner ear because of hearing impairment and balance dysfunction that is associated with Stickler syndrome type 2, Marshall syndrome, and nonsyndromic hearing loss deafness autosomal dominant 37 (DFNA37) [1–4,16,17].

Results from this study indicate that Col11a1a is important in the development of the ear and new evidence shows Col11a1a protein localized to hair cells in zebrafish. In the absence of Col11a1a, structure of the ear is altered. Changes that occurred as a result of a decrease in or loss of Col11a1a included the length of kinocilia and stereocilia, and otolith morphology. These results provide new information about Col11a1a in ear development and may provide an explanation for the mechanism of COL11A1 associated hearing loss in humans, whether it is syndromic or nonsyndromic. These results also

indicate new and novel functions for the amino terminal proteolytic fragment of COL11A1 that is not related to chondrodystrophies. Additionally, these results enable a more thorough understanding of the molecular, cellular, anatomical, and physiological mechanisms of Col11a1a in hearing and balance.

2. Materials and Methods

2.1. Zebrafish Husbandry

This study was performed with the approval of the Institutional Animal Care and Use Committee (IACUC) at Boise State University. Zebrafish were raised and housed under standard laboratory conditions at 28.5 °C [18]. Wild-type AB strain were used. Developmental staging the embryos were reported as hours post-fertilized (hpf) at 28.5 °C. Embryos were raised in egg water (pH 7.2) [18]. In embryos raised to older than 24 hpf, 200 μM 1-phenyl-2-thiourea (PTU) was added to the embryo incubation water as previously described in [19].

2.2. In Situ Hybridization

Whole mount *in situ* hybridization (ISH) was performed as previously described [20]. Antisense digoxigenin labeled riboprobes for Col11a1a were synthesized and used. Sequences for the primers to design these probes were published in [20]. Previously published in situ hybridization protocol was used for whole mount sample preparation [21].

2.3. Immunofluorescence and Confocal Microscopy

Custom-made antibody against Col11a1a was generated in rabbits (Bethyl Laboratories). Antibody to acetylated alpha-tubulin was purchased from Thermo Fisher Scientific. The custom antibody was validated and authenticated as published previously

[22]. Alterations to the following protocols [21], were used during immunofluorescence preparation. Samples were fixed in 4% paraformaldehyde (PFA) and then rinsed three times with a solution of 0.1% Tween-20 in PBS. TritonX-100 was used as a permeabilization step where samples are incubated for 1.5 hours at room temperature. Blocking solution was prepared using 5% goat serum and 2% Tween-20 in PBS and samples were incubated for one hour. Further permeabilization was performed by incubating samples in ice cold acetone for eight minutes at -20 °C. Primary antibodies were diluted in blocking solution, and samples were incubated while rocking at 4 °C overnight. Samples were rinsed in blocking solution, and then secondary antibodies were diluted 1:200 in blocking solution. Samples were incubated while rocking overnight in the dark at 4 °C. Samples were imaged on a Zeiss Confocal LSM 510 Meta microscope.

2.4 Antisense Morpholino Oligonucleotide Injection

Antisense morpholino oligonucleotides (AMOs) were designed as previously described [23–25]. AMOs injections resulted in knockdown of protein expression of Col11a1a (Gene Tools, LLC Philomath, OR). The sequence was been detailed in Hardy, et al [23]. and is as follows: 5'-GGGACCACCTTGGCCTCTCCATGGT-3'. As a negative control, a standard control AMO 5'-CCTCTTACCTCAGTTACAATTTATA-3' directed to the gene encoding β-globin in human thalassemia patients was used (Gene Tools #18633993). AMOs were injected at 1.75 nL of 150 ng/µL concentration into the cell cytoplasm. AMO injection effectiveness was confirmed by RT-PCR [23].

2.5. CRISPR/Cas9 Gene Editing

CRISPR/Cas9 probes were used to cause a premature stop codon in Col11a1a as previously described [26]. The target sequences were identified through the CHOPCHOP

webtool [27,28]. Hardy et al, [23], previously described the six best targets for

introducing a stop codon in Col11a1a. In this study, we used guide sequence e201

resulting in a premature stop codon in exon 2 to generate Col11a1a CRISPR/Cas9 mutant

generation shown in Table 1 modified from [23].

Table 4.1.   **CRISPR/Cas9 gene editing constructs.**

Name	Target	Guide Sequence[1]	Forward Primer	Reverse Primer
E201	Exon 2	ATTTAGGTGACACTATA AAGAGCATCACAGCCAGACG GTTTTAGAGCTAGAAATAGCAAG	CTGCTGACATTTTGCATGTCTT	CATTTAAACGCAGCTGAACGTA

[1] Bold nucleotides indicate the coding sequence within the guide sequence.
[2] Insert contains homology arms (lowercase) and the stop codon insert (capitals).
(Hardy et al., 2020)

2.6. Scanning Electron Microscopy

    Previously fixed (4% PFA) embryos were treated with respect to their designated

treatment group (untreated wild-type, hyaluronidase, ethylenediaminetetraacetic acid

(EDTA), and TritonX-100). After treatment, samples were prepared for SEM as

previously described in [7]. The following changes to the protocol were used in order to

compensate for younger samples: samples were fixed in glutaraldehyde and osmium

tetroxide for two hours, the tips were not silver coated, and gold sputter coats were

applied at 60 second intervals for 15 cycles at 0.15 mbar and 10 mA [7]. Samples were

imaged on a Hitachi S-3500N SEM.

2.7. Image Processing

Digital images were processed using Fiji ImageJ [29]. Image processing for use in Figures was done in Inkscape and Photoshop. Images were adjusted in full for brightness and contrast.
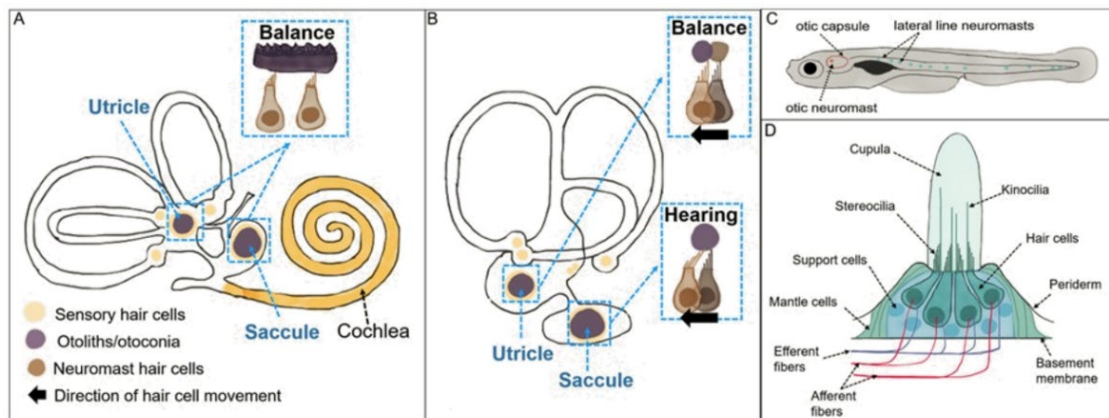

Figure 4.1.   Neurovestibular anatomy and function.
A) Anatomy of human neurovestibular organs responsible for balance. B) Anatomy of zebrafish neurovestibular organs responsible for hearing and balance. The utricle and saccule are structurally and functionally conserved between the two species. C) 5 day post fertilized larval zebrafish displaying the sensory neuromasts along the lateral line and within the otic capsule. D) Anatomy of a zebrafish neuromast showcasing the important cilium showcased in the utricle and saccule in both A and B.

3. Results

3.1. The Zebrafish Inner Ear Counterparts to The Human Inner Ear

Sequencing studies have shown 71% of human genes and 82% of human diseases have one or more zebrafish ortholog [30,31]. Not only do zebrafish have orthologous genes, the structure and function of several organs are also conserved [32]. The zebrafish inner ear is representative of the vertebrate inner ear as shown in [33]. **Figure 1** displays the similar structures between the human and zebrafish inner ear (**Figure 1A-B**). Both vertebrate models have three fluid-filled semicircular canals lined with sensory hair cells.

Two otocania/otoliths, the utricle and the saccule, are present in both models. The human

model has a cochlea which is absent in the zebrafish model. In the zebrafish model the

two otoliths, utricle and saccule, do not perform the same function unlike the human

otocania (**Figure 1A-B**). Zebrafish have sensory hair cells in the inner ear as well as

along the lateral line (**Figure 1C**). These hair cells contain the stereocilia and the

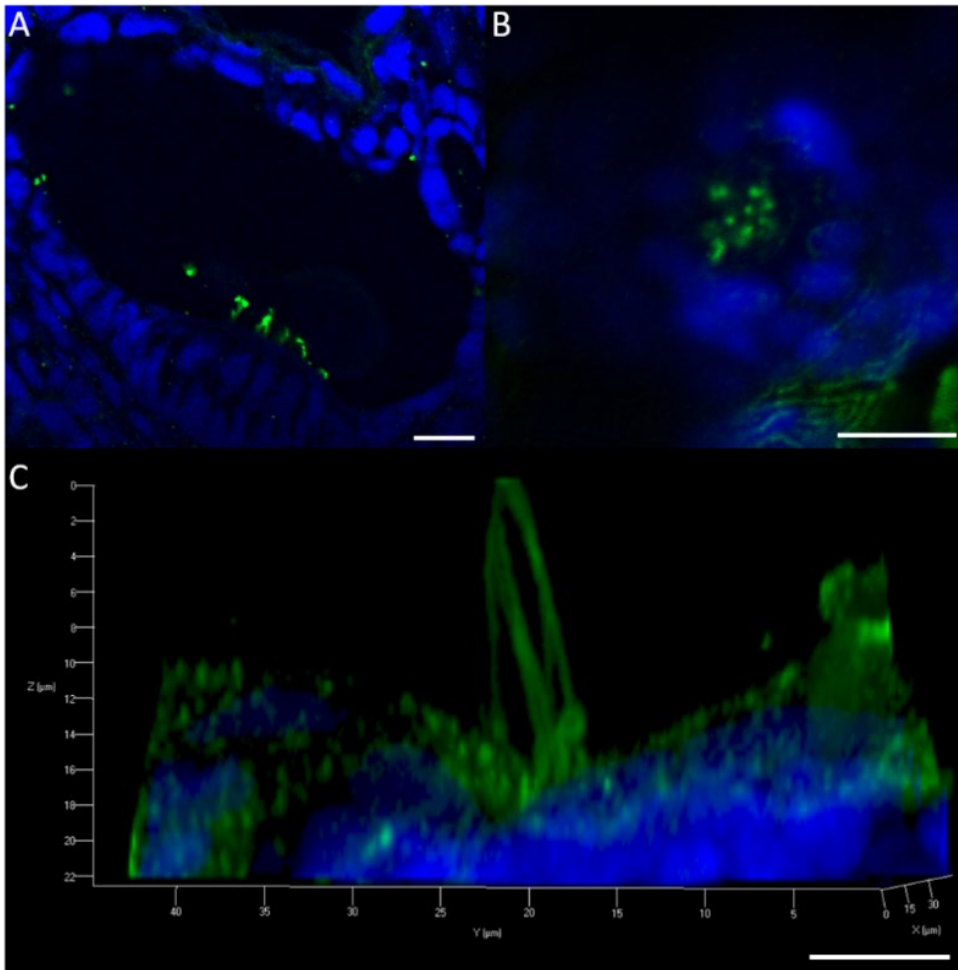kinocilia responsible for balance and hearing sensing (**Figure 1D**).

Figure 4.2.   Inner ear hair cells and neuromasts of embryonic zebrafish.
Immunohistochemistry of 60 hpf embryo sections stained with DAPI (blue) and anti-
acetylated alpha tubulin (green). A) Longitudinal section showing the opening of the
otic vesicle where a series of hair cells are visible in green. B) Section looking down at
a neuromast. The kinocilia are seen in green. C) Cross section of the 3D view of B.
Axes are z, y, and x dimensions respectively measured in µm. Long kinocilia (green)
are seen coming out of the neuromast. Scale bars = 10 µm. n = 10.

3.2 Imaging Structure of Neuromast and Kinocilium of the Hair Cells.

Confocal imaging of paraffin sectioned zebrafish embryos was performed to

visualize neuromasts. Sectioning of the otic vesicle reveals sensory patches containing a

neuromast (**Figure 2A**). Imaging a full neuromast revealed the cell structure of the

neuromast as well as the long kinocilia in the middle (**Figure 2B**). Z-stack confocal

images of the neuromast was used to create a 3D image of the neuromast. A cross section of this 3D image reveals the internal structure of the neuromast including the long kinocilia of the hair cells (**Figure 2C**).

3.3. COL11A1 Ortholog mRNA Expression in the Otic Vesicle.

Col11a1a is present the cartilage of developing vertebrates. Our lab has previously shown that loss of Col11a1a expression resulted in abnormal otic appearance. *In situ* hybridization (ISH) was used to characterize the expression pattern of collagen type XI alpha one chain mRNA orthologue in zebrafish embryos. Zebrafish orthologue Col11a1a mRNA expression was characterized in 72 hpf embryos by ISH riboprobe or a sense probe control. Control probe samples were prepared for comparison (**Figure 3A-B**). Col11a1a riboprobe allowed visualization of Col11a1a mRNA expression around the otic vesicle (**Figure 3C**). Closer observation of the otic vesicle suggested Col11a1a was expressed within the otic vesicle (**Figure 3D**).
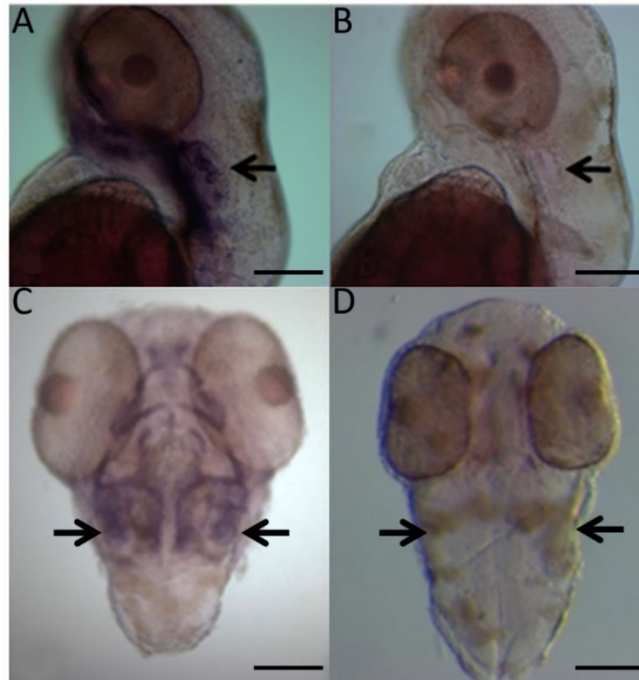
Figure 43.   *In situ* **hybridization of COL11A1 zebrafish ortholog probe Col11a1a.**
A) 24 hour post fertilized (hpf) embryo with Col11a1a probe. B) 24 hpf wild-type
embryo. C) 72 hpf embryo with Col11a1a probe. D) 72 hpf wild-type embryo. Arrows
indicate location of otic vesicles. Scale bar = 200 μm.

3.4. Col11a1a protein was present at 18 hpf and 24 hpf of embryonic otic vesicle

development.

To determine the expression of Col11a1a protein during development, we

performed immunofluorescence (IF) at specific timepoints. We found that expression of

Col11a1a varied throughout different stages of embryonic otic development. Otic vesicle

development observations spanned a 10-hour time frame in fish of age 14 to 24 hpf in

order to characterize expression at placode formation through full otic vesicle

development. Anatomy presented in Figure 1 was used to evaluate the location of

Col11a1a expression. The otic vesicle was observed forming at 14 hpf with no Col11a1a

expression (**Figure 4A**). At 18 hpf, the otic vesicle showed Col11a1a expression (**Figure

4B).** By 24 hpf the otic vesicle was fully formed with Col11a1a expression located along

the opening and the hair cell kinocilia (**Figure 4C**). The observed expression indicated

that Col11a1a was expressed around and within the otic vesicle during mid to late otic

vesicle development.

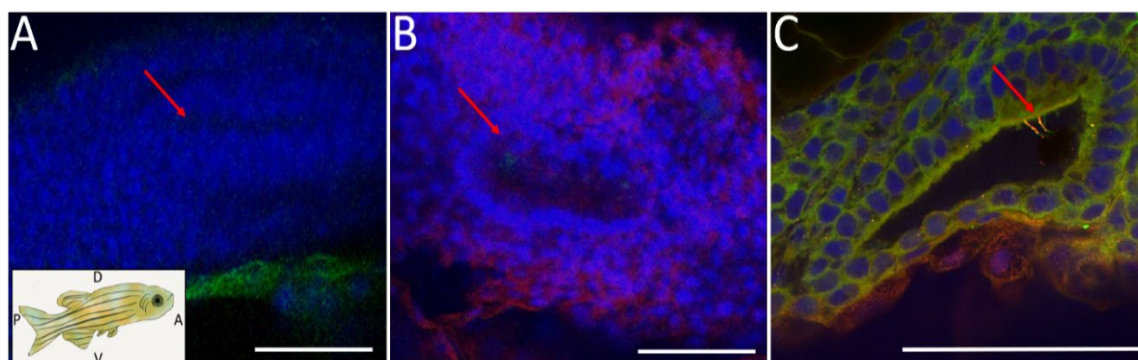3.5. Col11a1a Protein is Present in the Kinocilia of the Otic Vesicle Hair Cells in Early

Development.

**Figure 4.4.   Col11a1a expression in the otic vesicle through embryonic
development.**
Immunofluorescence of otic vesicle development in wild-type embryonic zebrafish over
the course of 10 hours. The fish diagram indicates the orientation of each sample in
panels A, B, and C. Expression of Col11a1a (red), anti-acetylated alpha tubulin (green),
and DAPI (blue) are shown. A) 14 hpf embryo showing no expression of Col11a1a. The
otic vesicle is starting to form as shown in the DAPI channel. Arrow indicates formation
of otic vesicle. B) 18 hpf embryo showing Col11a1a expression around the otic vesicle.
Arrow indicates opening of the otic vesicle. C) 24 hpf embryo has Col11a1a expression
around the otic vesicle as well as within the otic vesicle. Arrow indicates expression of
Col11a1a within the otic vesicle along the neuromast hair cell's kinocilia as stained by
acetylated alpha tubulin. Scale bars are all 50 µm. Abbreviations: P, posterior; A,
anterior; D, dorsal; V, ventral. n=30.

Further analysis of Col11a1a expression around and within the otic vesicle and in

the hair cells was performed to determine the exact localization of the protein. Key

features of the anatomy of a 24 hpf embryos were mapped for reference in analysis of IF

data (**Figure 5A**). Anti-Col11a1a antibody fluorescence indicated Col11a1a protein

within the embryonic zebrafish (**Figure 5B**). Analysis of the otic vesicle and the inner ear

hair cells demonstrated Col11a1a expression along the otic vesicle opening and in the

hair cells (**Error! Reference source not found.C-D**). Col11a1a expression along

kinocilia of the otic hair cells was also observed (**Error! Reference source not**

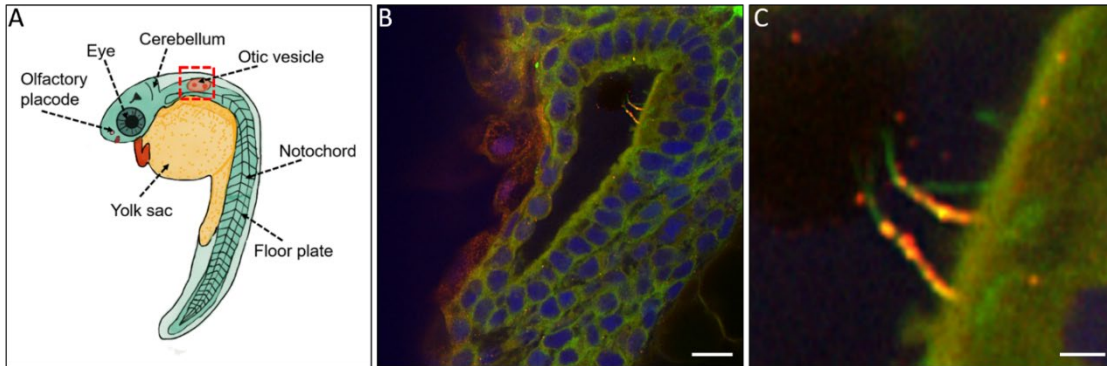**found.D**). This expression suggested Col11a1a is located along the kinocilia.

Figure 4.5.   Localization of Col11a1a in the kinocilia of hair cells in zebrafish otic vesicle.

Immunofluorescence on 24 hpf wild-type whole mount embryos for Col11a1a expression (red), anti-acetylated alpha tubulin (green), and DAPI (blue). A) Diagram of 24 hpf embryo with important landmarks indicated for labeling purposes. Red square indicates location of otic vesicle where we will focus. B) Otic vesicle with Col11a1a expression colocalizing along the opening and kinocilia. C) Close-up of otic neuromast. Col11a1a is shown along the kinocilia attaching to the otolith (black sphere). Scale bars = 10 µm B and 1 µm C. n = 30.

3.6. Col11a1a Protein is Present in the Kinocilia of the Otic Vesicle Hair Cells Later in

Development.

Col11a1a expression along the kinocilia is still observed in later embryonic

development. At later stages in development, Col11a1a expression is more specific. As

shown by **Figure 6,** 60 hpf embryos have less general expression around the otic vesicle

compared to 24 hpf embryos in **Figure 5** (**Figure 6A and Figure 5B**). Expression of

Col11a1a along the kinocilia was detected along several kinocilia in a neuromast (**Figure**

6B). Imaging of a single kinocilium revealed a punctate pattern of Col11a1a expression similar to what is observed at 24 hpf (**Figure 6C and Figure 5C**).
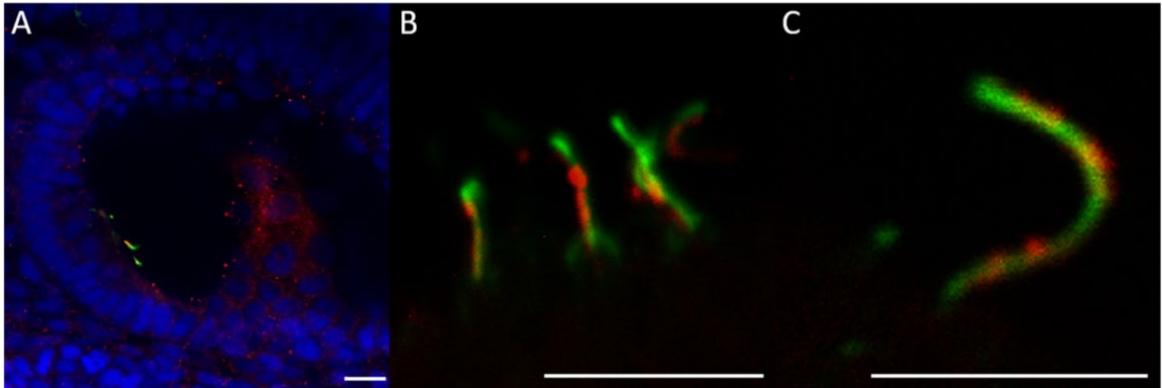

Figure 4.8. Col11a1a in the kinocilia of the inner ear of a 60 hpf zebrafish embryo histological section.

Col11a1a expression (red), anti-acetylated alpha tubulin (green), and DAPI (blue). A) Full view of the inner ear. Minimum Col11a1a (red) expression is seen along the vesicle itself and more contained to the hair cells (green) themselves. B) Close up of patch of hair cells. Kinocilia (green) have Col11a1a (red) expression along them. C) Individual kinocilium. Punctate Col11a1a (red) expression along the kinocilium (green). Scale bars = 10 μm A and B, 5 μm C. n = 10.

3.7. Structurally Abnormal Otic Vesicle in Col11a1a Knockdown Models.

Col11a1a knockdown models were generated to observe the effect on the embryonic otic vesicle. Antisense morpholino generated Col11a1a knockdown morphants (AMO morphants) displayed curved notochord unlike the straight wildtype notochord (**Figure 7A and 7D**). AMO morphant's otic vesicles were abnormally shaped with otolith malformations (**Figure 7E**). Normal wild type zebrafish otic vesicles contain two otoliths: the larger saccule and the smaller utricle. Three small otoliths or one large otolith were observed in AMO morphant embryos with three otoliths being the predominate phenotype (**Figure 7B and 7E**).
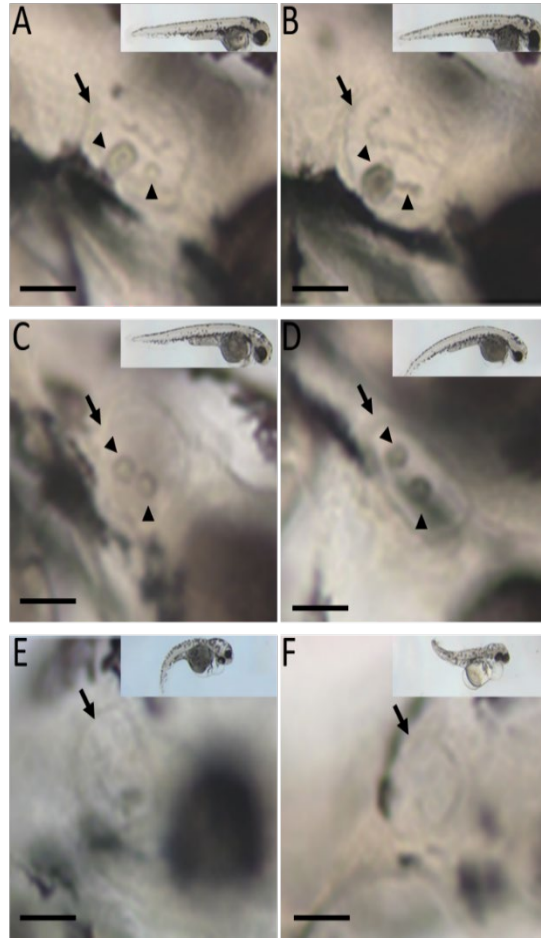
Figure 4.9.   Abnormal otic vesicle of Col11a1 AMO morphant model.
Light microscopy of antisense morpholino oligonucleotide mediated knockdown of Col11a1a embryos at 48 hours post fertilized. Insets show general phenotype of whole embryos as severity in phenotype is observed. Images displayed by increase in severity. A) Wild-type embryo treated with standard AMO injection control. Normal otic vesicle with two otoliths one larger in size. B-F) Increased severity of Col11a1a AMO knockdown embryos. B) Otic vesicle largely unchanged as a whole, but abnormal otolith formation with one large otolith and several smaller fragments. C) Otic vesicle normally shaped with two abnormal otoliths of the same size. D) Abnormal oblong shape of otic vesicle with two abnormal otoliths of the same size. E) Otic vesicle shape is typical with a smaller opening with no otoliths observed. F) Otic vesicle shape is slightly oblong with no otoliths observed. Long arrows indicate location of otic vesicle. Arrowheads indicate otolith location. Scale bars = 50 µm. Each treatment group n = 15.

CRISPR/Cas9 generated Col11a1a knockdown mutants (Figure 8B-C) shared curved notochords preliminarily consistent with AMO morphants (Figure 7C and 7F).

CRISPR/Cas9 homozygous mutants were nonviable so a heterozygous model was created. Homozygous mutants had a disorganized body structure with more severe otic vesicle and otolith malformation (Figure 8C). Heterozygous mutants had a less severe overall phenotype with otolith malformations including two similar sized otoliths, one or absent otoliths, or three or more otoliths (Figure 8B). Phenotypic observation of AMO and CRISPR/Cas9 models compared to wild type suggest that otic vesicle development was influenced by Col11a1a (**Figure 7 and Figure 8**).
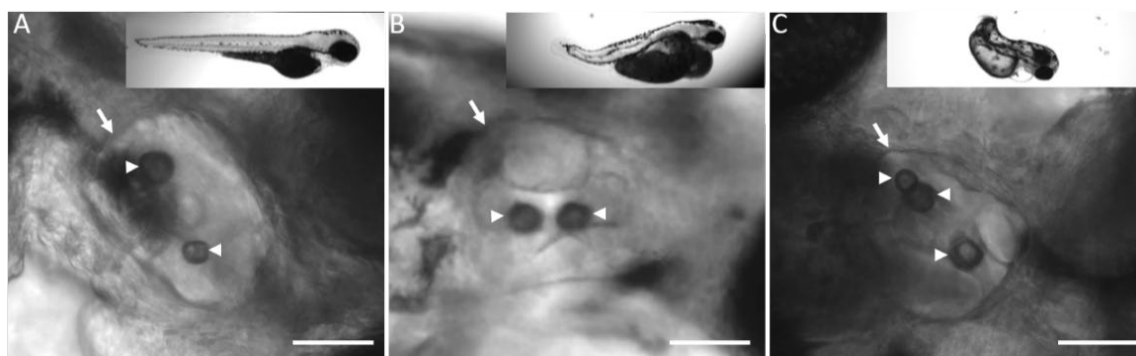

Figure 4.10.   Abnormal otic vesicle of CRISPR/Cas9 mutant models.
Light microscopy of CRISPR/Cas9 Col11a1a knockdown mutant embryos at 48 hours post fertilized. Insets show general phenotype of whole embryos as severity in phenotype is observed. A) Wild-type embryo otic vesicle. Normal otic vesicle with two otoliths one larger in size. B) CRISPR/Cas9 Col11a1a heterozygote knockdout (Col11a1a+/-) embryo otic vesicle. Otic vesicle largely unchanged as a whole, but abnormal otolith formation with two abnormal otoliths of approximately the same size. C) CRISPR/Cas9 Col11a1a homozygote knockout (Col11a1a-/-) embryo. Otic vesicle slightly smaller with minor shape malformation. Abnormal otolith formation with three otoliths all of differing sizes. Long arrows indicate location of otic vesicle. Arrowheads indicate otolith location. Scale bars = 50 μm. Each treatment group n = 20.

3.8. Col11a1a Knockdown Stunts Growth of Cilia in Hair Cells of the Otic Vesicle and Neuromasts.

Scanning electron microscopy (SEM) of 72 hpf wild-type embryos was performed. This timepoint allowed for successful SEM preparation while conserving the structure of the otic vesicle. Imaging revealed normal structure and anatomy (**Figure 9**).

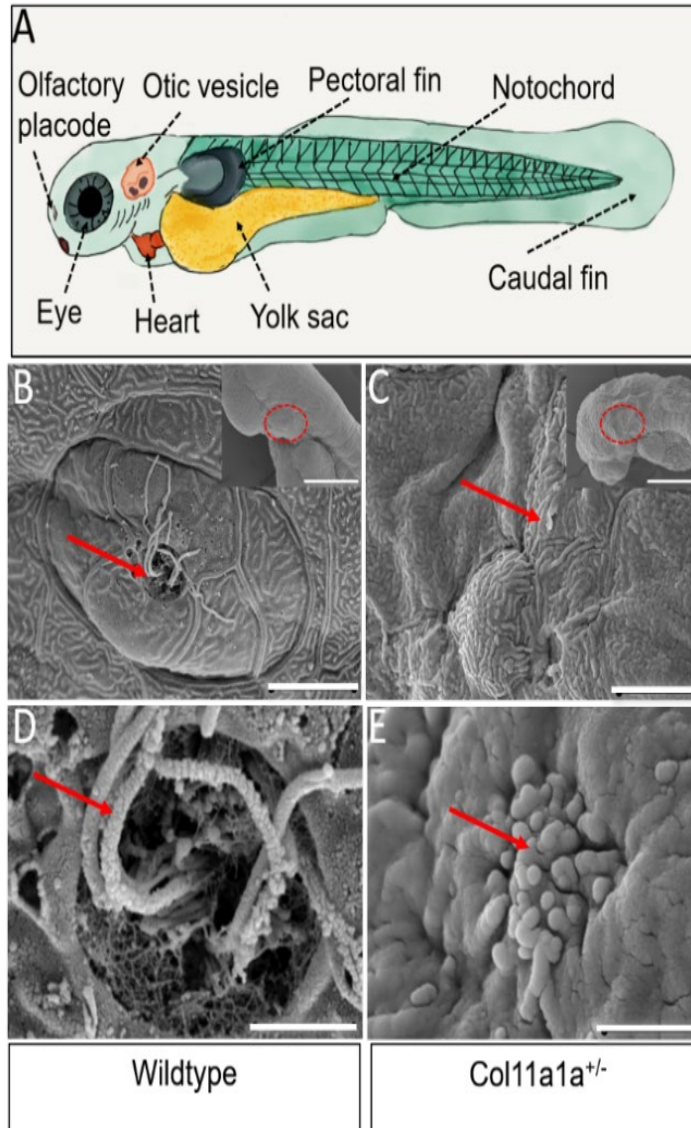In col11a1a knockdown CRISPR/Cas9 mutants, severe phenotypes were observed

(**Figure 9E**).

Figure 4.11. Morphological abnormalities in otic vesicle hair cells and neuromasts in Col11a1+/- embryos.

Scanning electron microscopy of 72 hours post fertilized (hpf) wild-type and heterozygous Col11a1a CRISPR/Cas9, Col11a1a+/- embryos. A) Diagram of 72 hpf embryo indicating important landmarks for referring purposes. B) Close-up of wild-type embryo otic vesicle. Inset shows the upper region of embryo with the otic vesicle location marked by a red circle. Arrow indicating neuromast. C) Close-up of Col11a1a+/- embryo otic vesicle. Inset shows the upper region of embryo with the otic vesicle location marked by a red circle. Arrow indicating neuromast. D) Close-up of wild-type embryo neuromast. Arrow indicating kinocilia. E) Close-up of Col11a1a+/- embryo neuromast. Arrow indicating kinocilia. Scale bars = 200 µm (insets), 10 µm (B-C), 2 µm (D-E). Each treatment group n=10.

Visual differences in the structure, organization, and pattern of the otic vesicle was observed (**Figure 9**). Compared to the wildtype, otic vesicles in the knockdown mutants were irregularly shaped with abnormal patterning along the epithelial lining of the otic vesicle (**Figure 9C**). The mutant vesicle had a smaller opening barely revealing the cilia within (**Figure 9C and 9E**). The cilia were more truncated and clustered together than the wildtype samples (**Figure 9B and 9D**). Among other defects, the Col11a1a mutant suggested Col11a1a expression is involved in the proper structural development of sensory neuromasts and the otic vesicle.

4. Discussion

In this study, we observed the expression of the zebrafish orthologue of COL11A1 during zebrafish otic development. Otic expression of Col11a1a indicates a role for this protein in the inner ear, specifically in the sensory hair cells. The absence of Col11a1a in zebrafish embryos shows abnormal otic structure specifically in respect to the stereocilia and kinocilia of the hair cells. These findings suggest that Col11a1a is involved in proper otic vesicle formation, sensory hair cell development, and stereocilia and kinocilia development

Otic vesicle research is critical balance and hearing research to understand dysfunction in disorders and diseases including but not limited to Stickler and Marshall syndrome. Many molecules are essential to the structure and function of the inner ear and otic vesicle, but the current list does not include COL11A1. Expression of collagen type XI alpha one chain in the otic vesicle was first shown in a report of Col11a1 in mouse tectorial membrane in 2004 [34]. We therefore explored the expression of COL11A1 in the inner ear and the relationship between expression and proper development.

Expression of Col11a1a in zebrafish was observed by in situ hybridization (ISH) and immunofluorescence experiments. ISH data indicated general expression in and around the otic vesicle. The first characterization of expression as observed in the epithelial lining of the otic vesicle in zebrafish embryos during early development. Further analysis by immunofluorescence revealed a punctate-pattern along kinocilia of the sensory hair cells. Knockdown of Col11a1a in zebrafish embryos by both antisense morpholino (AMO) and CRISPR/Cas9 was performed to observe structural defects. AMO morphant knockdowns had abnormal otic vesicle shape and size along with abnormal epithelial lining. Otolith formation was observed to be affected and was indicated by abnormal number of otoliths including no otolith, one large otolith, or three or more otoliths. CRISPR/Cas9 Col11a1a knockout mutants resulted in similar observable structural defects. SEM imaging of mutants allowed higher resolution revealing that the otic opening lacked structure and organization resulting in a smaller opening with shorter, malformed kinocilia. Both these models were global mutations and thus showed global effects that could be causing inner ear defect.

Inner ear dysfunction has been shown in diseases caused by a mutation in COL11A1 which could be due to global effects as well. Therefore, we suggest that these models accurately reflect collagen XI related changes in human ear development. Overall, these experiments demonstrate that Col11a1a is essential in the development of the anatomy of the structures within the inner ear including the otic vesicle and the kinocilia.

5. Conclusions

In summary, we found COL11A1 expression in the developing otic vesicles and sensory hair cells. Knockdown of Col11a1a indicated a correlation between the protein location and otic vesicle formation. Sensory hair cell development was dependent on Col11a1a protein expression. Importantly, we demonstrated that the absence of Col11a1a causes structural dysfunction in kinocilia of the sensory hair cells. These novel findings provide the basis for future studies on direct and indirect influences on otic development and the effects of specific mutations within the COL11A1 gene that are known to cause human diseases. Col11a1a is essential to the proper structure and function of the inner ear and may be key to rescuing the sense of hearing and balance in those individuals who have lost their hearing due to mutations in COL11A1.

Funding

Author Contributions

Makenna Hardy ad Julia Thom Oxford conceived and designed the ap-proach; Makenna Hardy and William Bourland designed and analyzed Scanning Electron Mi-croscopy data; Makenna Hardy, Jonathon Reeck, and Ming Fang collected and analyzed

data; Makenna Hardy designed and prepared Figures; Makenna Hardy prepared the first draft; Makenna Hardy, Jonathon Reeck, William Bourland and Julia Thom Oxford prepared final edits. All authors have contributed substantially to the work.

Institutional Review Board Statement

This study was approved by the Institutional Animal Care and Use Committee under protocol AC18-015.

Data Availability Statement

The data presented in this study are available in this article.

Conflicts of Interest

The authors declare no conflict of interest.

References

1. Acke, F.R.; Swinnen, F.K.; Malfait, F.; Dhooge, I.J. Auditory Phenotype in Stickler Syndrome : Results of Audiometric Analysis in 20 Patients. **2016**, *185*, 3025–3034, doi:10.1007/s00405-016-3896-6.

2. Annunen, S.; Körkkö, J.; Czarny, M.; Warman, M.L.; Brunner, H.G.; Kääriäinen, H.; Mulliken, J.B.; Tranebjærg, L.; Brooks, D.G.; Cox, G.F.; et al. Splicing Mutations of 54-Bp Exons in the COL11A1 Gene Cause Marshall Syndrome, but Other Mutations Cause Overlapping Marshall/Stickler Phenotypes. *American Journal of Human Genetics* **1999**, *65*, 974–983, doi:10.1086/302585.

3. Booth, K.T.; Askew, J.W.; Talebizadeh, Z.; Huygen, P.L.M.; Eudy, J.; Kenyon, J.; Hoover, D.; Hildebrand, M.S.; Smith, K.R.; Bahlo, M.; et al. Splice-Altering Variant in COL11A1 as a Cause of Nonsyndromic Hearing Loss DFNA37. *Genetics in Medicine* **2019**, *21*, 948–954, doi:10.1038/s41436-018-0285-0.

4. Griffith, A.J.; Sprunger, L.K.; Sirko-Osadsa, D.A.; Tiller, G.E.; Meisler, M.H.; Warman, M.L. Marshall Syndrome Associated with a Splicing Defect at the COL11A1 Locus. *American Journal of Human Genetics* **1998**, *62*, 816–823, doi:10.1086/301789.

5. Khalifa, O.; Imtiaz, F.; Allam, R.; Al-hassnan, Z.; Al-hemidan, A.; Al-mane, K.; Abuharb, G.; Balobaid, A.; Sakati, N.; Hyland, J.; et al. A Recessive Form of Marshall Syndrome Is Caused by a Mutation in the COL11A1 Gene. **2012**, 246–248, doi:10.1136/jmedgenet-2012-100783.

6. Vijzelaar, R.; Waller, S.; Errami, A.; Donaldson, A.; Lourenco, T.; Rodrigues, M.; Mcconnell, V.; Fincham, G.; Snead, M.; Richards, A. Deletions within COL11A1 in Type 2 Stickler Syndrome Detected by Multiplex Ligation-Dependent Probe Amplification (MLPA). **2013**, 2–7.

7. Sheets, L.; Kindt, K.S.; Nicolson, T. Presynaptic Cav1.3 Channels Regulate Synaptic Ribbon Size and Are Required for Synaptic Maintenance in Sensory Hair Cells. *Journal of Neuroscience* **2012**, *32*, 17273–17286, doi:10.1523/JNEUROSCI.3005-12.2012.

8.   Kremer, H.; van Wijk, E.; Märker, T.; Wolfrum, U.; Roepman, R. Usher Syndrome: Molecular Links of Pathogenesis, Proteins and Pathways. *Human Molecular Genetics* **2006**, *15*, doi:10.1093/hmg/ddl205.

9.   Meyer Zum Gottesberge, A.M.; Gross, O.; Becker-Lendzian, U.; Massing, T.; Vogel, W.F. Inner Ear Defects and Hearing Loss in Mice Lacking the Collagen Receptor DDR1. *Laboratory Investigation* **2008**, *88*, 27–37, doi:10.1038/labinvest.3700692.

10. Fox, M.A. Novel Roles for Collagens in Wiring the Vertebrate Nervous System. *Current Opinion in Cell Biology* **2008**, *20*, 508–513, doi:10.1016/j.ceb.2008.05.003.

11. Eyre, D.R. Collagens and Cartilage Matrix Homeostasis. In Proceedings of the Clinical Orthopaedics and Related Research; Lippincott Williams and Wilkins, 2004.

12. Fallahi, A.; Kroll, B.; Warner, L.R.; Oxford, R.J.; Irwin, K.M.; Mercer, L.M.; Shadle, S.E.; Oxford, J.T. Structural Model of the Amino Propeptide of Collagen XI A1 Chain with Similarity to the LNS Domains. *Protein Science* **2005**, *14*, 1526–1537, doi:10.1110/ps.051363105.

13. Gregory, K.E.; Oxford, J.T.; Chen, Y.; Gambee, J.E.; Gygi, S.P.; Aebersold, R.; Neame, P.J.; Mechling, D.E.; Bächinger, H.P.; Morris, N.P. Structural Organization of Distinct Domains within the Non-Collagenous N-Terminal Region of Collagen Type XI. *Journal of Biological Chemistry* **2000**, *275*, 11498–11506, doi:10.1074/jbc.275.15.11498.

14. Hansen, U.; Bruckner, P. Macromolecular Specificity of Collagen Fibrillogenesis: Fibrils of Collagens I and XI Contain a Heterotypic Alloyed Core and a Collagen I Sheath. *Journal of Biological Chemistry* **2003**, *278*, 37352–37359, doi:10.1074/jbc.M304325200.

15. Masaki, K.; Gu, J.W.; Ghaffari, R.; Chan, G.; Smith, R.J.H.; Freeman, D.M.; Aranyosi, A.J. Col11a2 Deletion Reveals the Molecular Basis for Tectorial

Membrane Mechanical Anisotropy. *Biophysical Journal* **2009**, *96*, 4717–4724, doi:10.1016/j.bpj.2009.02.056.

16.   Khalifa, O.; Imtiaz, F.; Ramzan, K.; Allam, R.; Faqeih, E.; Abuharb, G.; Balobaid, A.; Sakati, N. Marshall Syndrome : Further Evidence of a Distinct Phenotypic Entity and Report of New Findings. **2014**, 2601–2606, doi:10.1002/ajmg.a.36681.

17.   Richards, A.J.; Fincham, G.S.; McNinch, A.; Hill, D.; Poulson, A. v.; Castle, B.; Lees, M.M.; Moore, A.T.; Scott, J.D.; Snead, M.P. Alternative Splicing Modifies the Effect of Mutations in COL11A1 and Results in Recessive Type 2 Stickler Syndrome with Profound Hearing Loss. *Journal of Medical Genetics* **2013**, *50*, 765–771, doi:10.1136/jmedgenet-2012-101499.

18.   Westerfield, M. ZFIN: Zebrafish Book: Contents Available online: https://zfin.org/zf_info/zfbook/zfbk.html (accessed on 14 September 2020).

19.   Antinucci, P.; Hindges, R. A Crystal-Clear Zebrafish for in Vivo Imaging. *Scientific Reports* **2016**, *6*, doi:10.1038/srep29490.

20.   Fang, M.; Adams, J.S.; McMahan, B.L.; Brown, R.J.; Thom Oxford, J. The Expression Patterns of Minor Collagens during Development in Zebrafish. *Gene Expr Patterns* **2011**, *10*, 315–322, doi:10.1016/j.gep.2010.07.002.The.

21.   Goody, M.F.; Kelly, M.W.; Reynolds, C.J.; Khalil, A.; Crawford, B.D.; Henry, C.A. NAD+ Biosynthesis Ameliorates a Zebrafish Model of Muscular Dystrophy. *PLoS Biology* **2012**, *10*, doi:10.1371/journal.pbio.1001409.

22.   Reeck, J.; Hardy, M.; Pu, X.; Keller-Peck, C.; Oxford, J.T. Authentication of a Novel Antibody to Zebrafish Collagen Type XI Alpha 1 Chain (Col11a1a)J. *BMC Research Notes* **2021**.

23.   Hardy, M.J.; Reeck, J.C.; Fang, M.; Adams, J.S.; Oxford, J.T. Col11a1a Expression Is Required for Zebrafish Development. *Journal of Developmental Biology* **2020**, *8*, doi:10.3390/JDB8030016.

24. Rosen, J.N.; Sweeney, M.F.; Mably, J.D. Microinjection of Zebrafish Embryos to Analyze Gene Function. *Journal of Visualized Experiments* **2009**, doi:10.3791/1115.

25. Yuan, S.; Sun, Z. Microinjection of MRNA and Morpholino Antisense Oligonucleotides in Zebrafish Embryos. *Journal of Visualized Experiments* **2009**, doi:10.3791/1113.

26. Gagnon, J.A.; Valen, E.; Thyme, S.B.; Huang, P.; Ahkmetova, L.; Pauli, A.; Montague, T.G.; Zimmerman, S.; Richter, C.; Schier, A.F. Efficient Mutagenesis by Cas9 Protein-Mediated Oligonucleotide Insertion and Large-Scale Assessment of Single-Guide RNAs. *PLoS ONE* **2014**, *9*, doi:10.1371/journal.pone.0098186.

27. CHOPCHOP Available online: https://chopchop.cbu.uib.no/ (accessed on 19 April 2021).

28. Montague, T.G.; Cruz, J.M.; Gagnon, J.A.; Church, G.M.; Valen, E. CHOPCHOP: A CRISPR/Cas9 and TALEN Web Tool for Genome Editing. *Nucleic Acids Research* **2014**, *42*, doi:10.1093/nar/gku410.

29. Schindelin, J.; Arganda-Carreras, I.; Frise, E.; Kaynig, V.; Longair, M.; Pietzsch, T.; Preibisch, S.; Rueden, C.; Saalfeld, S.; Schmid, B.; et al. Fiji: An Open-Source Platform for Biological-Image Analysis. *Nature Methods* 2012, *9*, 676–682.

30. Howe, K.; Clark, M.D.; Torroja, C.F.; Torrance, J.; Berthelot, C.; Muffato, M.; Collins, J.E.; Humphray, S.; McLaren, K.; Matthews, L.; et al. The Zebrafish Reference Genome Sequence and Its Relationship to the Human Genome. *Nature* **2013**, *496*, 498–503, doi:10.1038/nature12111.

31. Varga, M.; Ralbovszki, D.; Balogh, E.; Hamar, R.; Keszthelyi, M.; Tory, K. Zebrafish Models of Rare Hereditary Pediatric Diseases. *Diseases* **2018**, *6*, 43, doi:10.3390/diseases6020043.

32. Rahman Khan, F.; Sulaiman Alhewairini, S. Zebrafish (Danio rerio) as a Model Organism . In *Current Trends in Cancer Management*; IntechOpen, 2019.

33. Whitfield, T.T.; Granato, M.; van Eeden, F.J.; Schach, U.; Brand, M.; Furutani-Seiki, M.; Haffter, P.; Hammerschmidt, M.; Heisenberg, C.P.; Jiang, Y.J.; et al.

Mutations Affecting Development of the Zebrafish Inner Ear and Lateral Line. *Development* **1996**, *123*, 241–254, doi:10.1242/dev.123.1.241.

34. Shpargel, K.B.; Makishima, T.; Griffith, A.J. Col11a1 and Col11a2 MRNA Expression in the Developing Mouse Cochlea: Implications for the Correlation of Hearing Loss Phenotype with Mutant Type XI Collagen Genotype. *Acta Oto-Laryngologica* **2004**, *124*, 242–248, doi:10.1080/00016480410016162.

APPENDIX A

Other Work During Dissertation

Publications

1) Tanikella AS, **Hardy MJ**, Frahs SM, Cormier AG, Gibbons KD, Fitzpatrick CK, Oxford JT. Emerging Gene-Editing Modalities for Osteoarthritis. Int J Mol Sci. 2020 Aug 22;21(17):6046. doi: 10.3390/ijms21176046. PMID: 32842631; PMCID: PMC7504272.

2) Oxford JT, Reeck JC, **Hardy MJ**. Extracellular Matrix in Development and Disease. Int J Mol Sci. 2019 Jan 8;20(1):205. doi: 10.3390/ijms20010205. PMID: 30626024; PMCID: PMC6337388.

3) Stone RN, Frahs SM, **Hardy MJ**, Fujimoto A, Pu,X, Keller-Peck CR, Oxford JT Decellularized porcine cartilage scaffold; validation of decellularization and evaluation of biomarkers of chondrogenesis, Int J Mol Sci 2021. In press.

4) Hardy MJ, Pu X, Oxford JT. Purification and Isolation of Proteins from Hyaline Cartilage. *Methods in Molecular Biology.* Springer 2021. In preparation.

Poster and Podium Presentations

1) **Hardy M**, Reeck J, Lobato D, Oxford J. COL11A1 in the structure and development of the inner ear. Poster presented at Boise State University Graduate Research Conference. 2017 April; Boise, ID, USA.

2) **Hardy M**, Reeck J, Fang M, Oxford J. COL11A1 knockdown zebrafish model for syndromic and nonsyndromic hearing loss. Annual Scientific and Technology Conference AAS. 2021 March; Presentation.

3) **Hardy M**, Reeck J, Fang M, Oxford J. COL11A1 knockdown zebrafish model for syndromic and nonsyndromic hearing loss. Annual Scientific and Technology Conference American Auditory Society. 2021 March; Poster.

4) **Hardy M**, Reeck J, Fang M, Bourland W, Oxford J. Col11a1a is essential for ear development in zebrafish. Annual Meeting Society for Developmental Biology. 2021 July; Poster.

5) **Hardy M**, Reeck J, Fang M, Bourland W, Oxford J. Col11a1a is essential for inner ear development in a zebrafish model of syndromic and nonsyndromic hearing loss. Idaho INBRE Statewide Research Conference. 2021 July; Presentation.

Awards

1)   Hilda D. Elliot Biomedical Research Award. 2017.

2)   Sigma Xi Grant-in-Aid of Research (GIAR). 2019.